J. O. Halford

THE JOURNAL OF CHEMICAL PHYSICS

VOLUME 11 NUMBER 4

APRIL, 1943

Published by the
AMERICAN INSTITUTE OF PHYSICS
Incorporated
LANCASTER, PA., AND NEW YORK, N. Y.

THE JOURNAL OF CHEMICAL PHYSICS

ADVISORY EDITORIAL BOARD

R. T. BIRGE
A. H. COMPTON
JAMES FRANCK
IRVING LANGMUIR
JOHN T. TATE
HAROLD C. UREY

BOARD OF EDITORS

JOSEPH E. MAYER, *Editor*

Associate Editors

Term ending December 31, 1942.
SIMON FREED
MAURICE L. HUGGINS
J. G. KIRKWOOD
GEORGE SCATCHARD
J. H. VAN VLECK

Term ending December 31, 1944
CHARLES O. BECKMAN
BRYCE L. CRAWFORD, JR.
P. DEBYE
DAVID HARKER
FRANK H. WESTHEIMER

Term ending December 31, 1946
L. O. BROCKWAY
RONALD W. GURNEY
KENNETH S. PITZER
ALFRED L. SKLAR
E. W. R. STRACIE
HUGH S. TAYLOR

THE JOURNAL OF CHEMICAL PHYSICS is published monthly by the American Institute of Physics. Its purpose is to bridge a gap between journals of physics and journals of chemistry. The artificial boundary between physics and chemistry has now been in actual fact completely eliminated and a large and active group is engaged in research which is as much the one as the other. It is to this group that the Journal is rendering its principal service and makes its greatest appeal, both as a prompt and efficient medium for publication of research and as a convenient and carefully edited assemblage of pertinent information.

Manuscripts for publication should be submitted to Joseph E. Mayer, Havemeyer Hall, Columbia University, New York, New York.

Proof and all correspondence concerning papers in the process of publication should be addressed to the Publications Manager, American Institute of Physics, 175 Fifth Avenue, New York, New York.

Subscriptions and orders for single copies should be addressed to Prince and Lemon Streets, Lancaster, Pennsylvania, or to the American Institute of Physics, 175 Fifth Avenue, New York, New York.

Changes of address should be addressed to the Publications Manager.

Entered as second-class matter December 1, 1932, at the Post Office at Lancaster, Pa., under the Act of August 24, 1912. Acceptance for mailing at special rate of postage, provided for in the Act of February 28, 1925, embodied in paragraph 4, Section 538, P. L. & R., authorized January 4, 1933.

Subscription Price

The United States and Possessions, Canada and Mexico $10.00
Elsewhere 11.00

Back Numbers

Complete set: Vol 1, 1933—Vol 10, 1942 ..... $100.00
Yearly rate: $11.00.
Single copies: $1.00 each.

The Journal of Chemical Physics is published monthly at Prince and Lemon Streets, Lancaster, Pennsylvania.

THE JOURNAL
OF
CHEMICAL PHYSICS

VOLUME 11, NUMBER 4 APRIL, 1943

Average $H-H_2$ Repulsive Potential from Collision Cross Section Measurements*

I. AMDUR
Research Laboratory of Physical Chemistry, Massachusetts Institute of Technology, Cambridge, Massachusetts
(Received December 9, 1942)

The average repulsive potential between a hydrogen atom and a hydrogen molecule has been computed from experimental values of elastic collision cross sections for fast hydrogen atoms (with energies of 200 to 800 electron volts) scattered in room temperature molecular hydrogen. It was possible to solve the classical theory scattering equations explicitly for the repulsive potential by proper analytical representation of the experimental cross section values as a function of the relative kinetic energy of the scattering system. The potential function so obtained predicts total collision cross sections within the experimental error and has the form $V(r)=A\exp(-ar^2)+B\exp(-br^2)$ where r, the distance between the mass points representing the hydrogen atom and the hydrogen molecule, extends, in the present case, from 0.28 to 0.70A. For r in A units, $A=0.846\times10^{-10}$ erg, $a=24.9\text{A}^{-2}$, $B=0.211\times10^{-10}$ erg and $b=2.40\text{A}^{-2}$.

THE repulsive potential between two helium atoms at interaction distances of 0.55 to 1.05A has been estimated[1] from measured values of total collision cross sections of high velocity helium atoms elastically scattered by room temperature helium. Since experimental values are available[2] for total collision cross sections of high velocity hydrogen atoms scattered by room temperature hydrogen, it should be possible to estimate the average repulsive potential between a hydrogen atom and a hydrogen molecule at the separation distances involved in the scattering, 0.28 to 0.70A.

The original curve of $H-H_2$ cross sections as a function of the hydrogen atom energy indicated the presence of some inelastic scattering for beam particle energies between 500 and 700 volts. Since only elastic collision cross sections can be used in the present calculation, it is necessary to draw the best smooth curve through the original experimental points in order to read off the appropriate elastic collision cross sections in the range 500–700 volts. The values so obtained are listed in Table I where the original experimental values which show the effects of inelastic scattering at 600 and 700 volts appear in parentheses.

TABLE I. Total elastic collision cross sections for high velocity hydrogen atoms scattered by room temperature hydrogen.

Voltage, V	Cross section, S_Θ (10^{-16} cm^2)		Percent error (±)
200	1.455	(1.455)	3.5
300	0.618	(0.618)	5.7
400	0.410	(0.410)	2.4
500	0.310	(0.310)	1.8
600	0.268	(0.302)	1.1
700	0.243	(0.250)	1.9
800	0.230	(0.230)	4.2

* Contribution No. 470 from the Research Laboratory of Physical Chemistry, Massachusetts Institute of Technology. Presented before the Division of Physical and Inorganic Chemistry of the American Chemical Society at the Buffalo Meeting, September 8, 1942.

[1] I. Amdur and H. Pearlman, J. Chem. Phys. **9**, 503 (1941).

[2] I. Amdur and H. Pearlman, J. Chem. Phys. **8**, 7 (1940).

The estimated percent errors are those originally recorded for the values in parentheses and shall be taken to represent the probable reproducibility of the total elastic collision cross sections, since only the 600-volt value shows appreciable correction for inelastic scattering.

It has been shown[2] that the elastic scattering of the high velocity hydrogen atoms may be treated by classical methods since the average relative angular aperture of the detecting system,

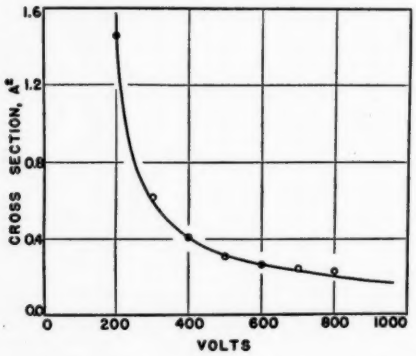

FIG. 1. Analytical representation of total elastic collision cross section as a function of beam particle energy.

3.37° (2.25° in apparatus coordinates) far exceeds the maximum relative angular aperture, 1.15° to 1.72°, required for detection of effects due to quantum theory diffraction.[3]

The general equations and method of procedure for estimating repulsive potentials of the form $V(r)=A\exp(-ar^n)$ have been discussed in connection with the calculations for helium.[1] The reduced mass μ and the relative angle of scattering Θ appearing in the equations are equal, in the present case, to two-thirds the mass of the beam particle and to three-halves the angular deflection of the beam particle with respect to the beam axis, respectively.

Attempts to reproduce the tabulated cross sections by variation of the constants, A, a, and n, in the general potential $V(r)=A\exp(-ar^n)$ were unsuccessful. Accordingly, the potential $V(r)=A\exp(-ar^n)+B\exp(-br^n)$ was investigated. For $n=2$, the relative angle of scattering is given in closed form by

$$\Theta=\frac{2r_0}{\mu v^2}\int_{r_0}^{\infty}\frac{[V(r_0)-V(r)]rdr}{(r^2-r_0^2)^{\frac{1}{2}}}=\frac{2(a\pi)^{\frac{1}{2}}r_0A}{\mu v^2}\times\exp(-ar_0^2)+\frac{2(b\pi)^{\frac{1}{2}}r_0B}{\mu v^2}\exp(-br_0^2),\quad(1)$$

where r_0 is the distance of closest approach of the beam particle to the scatterer and v, the relative initial velocity of the colliding system. Equation (1) assumes that the beam particle and the scatterer are mass points in a spherically symmetrical force field.

It is possible to express r_0 in terms of the collision cross section S_Θ since, for a given voltage and average angular aperture,

$$S_\Theta=\pi\left[1-\frac{V(r_0)}{\frac{1}{2}\mu v^2}\right]r_0^2=\pi b_\Theta^2,$$

where b_Θ is the impact parameter defined by the above equation. From attempts to find a satisfactory single term potential function, it is estimated that $[1-V(r_0)/\frac{1}{2}\mu v^2]$ will have a value between 0.96 and 0.94 for voltages between 200

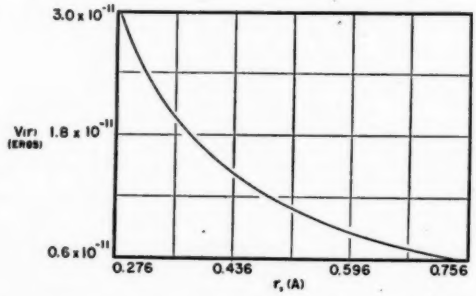

FIG. 2. Average repulsive potential between a hydrogen atom and a hydrogen molecule considered as mass points.

and 800 volts, so that to a first approximation

$$S_\Theta=0.95\pi r_0^2.$$

The accuracy of this approximation can be determined after the potential function has been found, by computing values of $[1-V(r_0)/\frac{1}{2}\mu v^2]$ for the r_0 distances of interest. Since Θ is equal to 0.0589 radian, Eq. (1) reduces to

$$\mu v^2=34.8a^{\frac{1}{2}}AS_\Theta^{\frac{1}{2}}\exp(-0.335aS_\Theta)+34.8b^{\frac{1}{2}}BS_\Theta^{\frac{1}{2}}\exp(-0.335bS_\Theta).\quad(2)$$

[3] H. S. W. Massey and C. B. O. Mohr, Proc. Roy. Soc. **A141**, 434 (1933).

If, then, it is possible to represent the relative kinetic energy of the system, $\frac{1}{2}\mu v^2$, as a function of the total collision cross section, within the estimated error, by an equation of the form

$$\mu v^2/S_\Theta^{\frac{1}{2}}=A' \exp(-a'S_\Theta)+B' \exp(-b'S_\Theta), \quad (3)$$

the problem of finding a satisfactory repulsive potential is solved since the constants A, B, a, and b in the two-term potential function may be directly computed from the numerical values of A', B', a', and b' of Eq. (3).

It was possible by graphical methods to evaluate the constants of Eq. (3) and thus to represent analytically within the average estimated error of ± 2.8 percent, the elastic cross sections of Table I by the equation

$$\frac{4Ve}{3S_\Theta^{\frac{1}{2}}}=\frac{\mu v^2}{S_\Theta^{\frac{1}{2}}}=[146 \exp(-8.25S_\Theta) + 11.3 \exp(-0.795S_\Theta)]\times\frac{10^{-10}\text{ erg}}{\text{A}}, \quad (4)$$

where e is the charge on the electron.

Figure 1 shows that the individual S_Θ values scatter well about the smooth curve represented by Eq. (4).

Comparison of Eqs. (2) and (4) yields directly values for the constants A, B, a, and b so that the first approximation to the desired potential energy function is

$$V(r)=[0.846 \exp(-24.6r^2) + 0.211 \exp(-2.37r^2)]\times 10^{-10}\text{ erg}. \quad (5)$$

If the S_Θ values of Table I are divided by 0.95π a series of first approximation r_0^2 values are obtained for substitution into Eq. (5). From the $V(r_0)$ values so obtained it is found that $[1-V(r_0)/\frac{1}{2}\mu v^2]$ varies between 0.969 and 0.958 so that the second approximation to the general expression for S_Θ becomes

$$S_\Theta=0.963\pi r_0^2$$

and the corresponding improved expression for $V(r)$

$$V(r)=[0.846 \exp(-24.9r^2) + 0.211 \exp(-2.40r^2)]\times 10^{-10}\text{ erg}. \quad (6)$$

Further approximations produce insignificant improvement so that Eq. (6), which is represented graphically in Fig. 2, is the final repulsive potential energy function derivable from the experimental collision cross sections.

The Vibration-Rotation Energies of the Linear X-Y-Z Type Molecule

ALVIN H. NIELSEN
Department of Physics, University of Tennessee, Knoxville, Tennessee
(Received January 29, 1943)

The vibration-rotation energies of the linear X–Y–Z type molecule are derived according to a method suggested by Professor Harald H. Nielsen in a recent paper. By the proper substitutions the energy expressions are reduced to the ones appropriate for the XY_2 type molecule, and a comparison with the work of Professor D. M. Dennison is effected.

I. INTRODUCTION

IN a recent paper[1] Harald H. Nielsen showed that the vibration-rotation energies of a molecule composed of N atoms could be expressed to second order of approximation in perfectly general terms. Following his suggestion that it would be simpler to arrive at the energies of a particular model by the general method than to derive them independently, a solution of the linear X–Y–Z type, of which HCN and COS are examples, is given here.

The proper modifications are made to transform these energy expressions to the XY_2 type and these are compared with similar expressions given by Dennison[2] for this type of molecule.

II. THE NORMAL COORDINATES

In Fig. 1 is given a diagram of the linear X–Y–Z type molecule. The coordinate system is fixed in the molecule with the origin at the center of gravity of the system. The particles are numbered from left to right. In the positional coordinates x_i, y_i, z_i the kinetic energy of vibration is

$$2T=\sum_{i=1}^{3} m_i(\dot{x}_i^2+\dot{y}_i^2+\dot{z}_i^2).$$

The condition that the center of gravity of the system remain at rest in these coordinates is

$$\sum_{i=1}^{3} m_i\alpha_i=0$$

(where α_i takes the values x, y, z) and the condition that to zero order the internal angular momentum is zero may be written

$$\sum_{i=1}^{3} m_i(\alpha_i^0\delta\beta_i-\beta_i^0\delta\alpha_i)=0$$

(α and β taking values x, y, z but $\alpha\neq\beta$). The superscript $(^0)$ indicates the equilibrium value of the coordinates.

As intermediate coordinates in the determination of the normal coordinates let

$$\begin{aligned} 3\sigma x/2\Sigma &= x_2-(m_1x_1+m_3x_3)/2m_2,\\ 3\sigma y/2\Sigma &= y_2-(m_1y_1+m_3y_3)/2m_2,\\ 3\sigma z/2\Sigma &= z_2-(m_1z_1+m_3z_3)/2m_2,\\ q &= z_1-z_3. \end{aligned} \tag{1}$$

The coordinates x_i, y_i, z_i can be expressed in

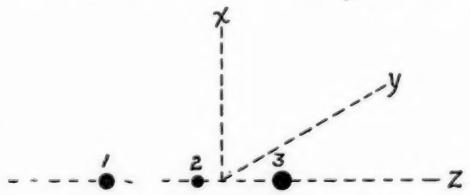

FIG. 1. The coordinate system of the linear X–Y–Z type molecule.

terms of x, y, z, and q as follows:

$$\begin{aligned} x_1&=-m_2\sigma(z_2^0-z_3^0)x/m_1\Sigma(z_1^0-z_3^0),\\ x_2&=\sigma x/\Sigma,\\ x_3&=-m_2\sigma(z_1^0-z_2^0)x/m_1\Sigma(z_1^0-z_3^0),\\ y_1&=-m_2\sigma(z_2^0-z_3^0)y/m_1\Sigma(z_1^0-z_3^0),\\ y_2&=\sigma y/\Sigma,\\ y_3&=-m_2\sigma(z_1^0-z_2^0)y/m_1\Sigma(z_1^0-z_3^0),\\ z_1&=-m_2z/\Sigma+m_3q/\sigma,\\ z_2&=\sigma z/\Sigma,\\ z_3&=-m_2z/\Sigma-m_1q/\sigma, \end{aligned} \tag{2}$$

[1] Harald H. Nielsen, Phys. Rev. **60**, 794 (1941).
[2] D. M. Dennison, Rev. Mod. Phys. **12**, 175 (1940).

where

$$\sigma=m_1+m_3, \quad \sum=m_1+m_2+m_3.$$

The kinetic energy may now be written in these coordinates

$$2T=\mu_1\dot{q}^2+\mu_2(\dot{x}^2+\dot{y}^2)+\mu_3\dot{z}^2$$

where

$$\mu_1=m_1m_3/\sigma, \quad \mu_2=m_2\sigma^2I^e_{xx}/m_1m_3\sum(z_1^0-z_3^0), \quad \mu_3=m_2\sigma/\sum. \tag{3}$$

In the displacement coordinates the potential energy is

$$2V=K_1Q_1^2+K_2Q_2^2+K_3Q_3^2+2K_{12}Q_1Q_2 +2K_{13}Q_1Q_3+2K_{23}Q_2Q_3+K_4(x^2+y^2). \tag{4}$$

Let $Q_1=z_2-z_1$, $Q_2=z_3-z_2$, $Q_3=z_3-z_1$. Making these substitutions into (4) and utilizing the relations (2), the potential energy may be written

$$2V=\mathfrak{K}_1q^2+\mathfrak{K}_3z^2+2\mathfrak{K}_4zq+K_4(x^2+y^2)$$

in which

$$\begin{aligned}\mathfrak{K}_1&=(K_1m_3^2/\sigma^2+K_2m_1^2/\sigma^2+K_3 +2K_{12}m_1m_3/\sigma^2+2K_{13}m_3/\sigma+2K_{23}m_1/\sigma),\\ \mathfrak{K}_3&=(K_1+K_2-2K_{12}),\\ \mathfrak{K}_4&=(-K_1m_3/\sigma+K_2m_1/\sigma -K_{12}(m_1-m_3)/\sigma-K_{13}+K_{23}).\end{aligned} \tag{5}$$

Now let $(\mu_1)^{\frac{1}{2}}q=q_1'$, $(\mu_2)^{\frac{1}{2}}x=q_{21}$, $(\mu_2)^{\frac{1}{2}}y=q_{22}$, $(\mu_3)^{\frac{1}{2}}z=q_3'$. In these coordinates the kinetic and potential energies become

$$\begin{aligned}2T&=\dot{q}_1'^2+(\dot{q}_{21}^2+\dot{q}_{22}^2)+\dot{q}_3'^2,\\ 2V&=k_1'q_1'^2+k_2'(q_{21}^2+q_{22}^2)+k_3'q_3'^2+2k_4'q_1'q_3',\end{aligned} \tag{6}$$

where

$$k_1'=\mathfrak{K}_1/\mu_1, \quad k_2'=K_4/\mu_2, \quad k_3'=\mathfrak{K}_3/\mu_3, \quad k_4'=\mathfrak{K}_4/(\mu_1\mu_3)^{\frac{1}{2}}.$$

If $q_1'=q_1\sin\gamma+q_3\cos\gamma$ and $q_3'=-q_1\cos\gamma+q_3\sin\gamma$ are substituted into (6) and $\sin\gamma=(\frac{1}{2})^{\frac{1}{2}}\{1+[(k_1'-k_3')^2/(4k_4'^2+(k_1'-k_3')^2]\}^{\frac{1}{2}}$ the cross product in $q_1'q_3'$ vanishes and q_1, q_{21}, q_{22}, q_3 are the normal coordinates. The resulting form for the kinetic and potential energies is

$$\begin{aligned}2T&=\dot{q}_1^2+(\dot{q}_{21}^2+\dot{q}_{22}^2)+\dot{q}_3^2,\\ 2V&=k_1q_1^2+k_2(q_{21}^2+q_{22}^2)+k_3q_3^2,\end{aligned}$$

in which

$$\begin{aligned}k_1&=k_1'\sin^2\gamma+k_3'\cos^2\gamma-2k_4'\sin\gamma\cos\gamma,\\ k_2&=k_2',\\ k_3&=k_1'\cos^2\gamma+k_3'\sin^2\gamma+2k_4'\sin\gamma\cos\gamma.\end{aligned} \tag{7}$$

The displacement coordinates can be expressed as linear combinations of the normal coordinates as follows:

$$x_i=\sum l_{is\sigma}q_{s\sigma}, \quad y_i=\sum m_{is\sigma}q_{s\sigma}, \quad z_i=\sum n_{is\sigma}q_{s\sigma},$$

where i is summed over the particles, s is summed over the frequencies, and σ takes the values 1, or 1,2 depending on whether or not the frequency is a degenerate one. An example of these summations is $x_i=l_{i11}q_{11}+l_{i21}q_{21}+l_{i22}q_{22}+l_{i31}q_{31}$. The only coefficients having values other than zero are

$$\begin{aligned}l_{121}&=m_{122}=-[m_2m_3(z_2^0-z_3^0)^2/m_1\sum I^e_{xx}]^{\frac{1}{2}},\\ l_{221}&=m_{222}=[m_1m_3(z_1^0-z_3^0)^2/m_2\sum I^e_{xx}]^{\frac{1}{2}},\\ l_{321}&=m_{322}=-[m_1m_2(z_1^0-z_2^0)^2/m_3\sum I^e_{xx}]^{\frac{1}{2}},\\ n_{111}&=[(m_2/\sigma\sum)^{\frac{1}{2}}\cos\gamma+(m_3/\sigma m_1)^{\frac{1}{2}}\sin\gamma],\\ n_{131}&=-[(m_2/\sigma\sum)^{\frac{1}{2}}\sin\gamma-(m_3/\sigma m_1)^{\frac{1}{2}}\cos\gamma],\\ n_{211}&=-(\sigma/m_2\sum)^{\frac{1}{2}}\cos\gamma,\\ n_{231}&=(\sigma/m_2\sum)^{\frac{1}{2}}\sin\gamma,\\ n_{311}&=[(m_2/\sigma\sum)^{\frac{1}{2}}\cos\gamma-(m_1/\sigma m_3)^{\frac{1}{2}}\sin\gamma],\\ n_{331}&=-[(m_2/\sigma\sum)^{\frac{1}{2}}\sin\gamma+(m_1/\sigma m_3)^{\frac{1}{2}}\cos\gamma].\end{aligned} \tag{8}$$

With the aid of the Eqs. (8) the coefficients $a_{s\sigma}$ and $A_{s\sigma s''\sigma''}$ occurring in the expressions for the instantaneous moments of inertia $I'_{xx}=I'_{yy}$ may be determined. The values of these coefficients follow:

$$\begin{aligned}a_{11}&=-2(I^e_{xx})^{\frac{1}{2}}\xi_{2231}, \quad a_{21}=a_{22}=0, \quad a_{31}=2(I^e_{xx})^{\frac{1}{2}}\xi_{2211},\\ A_{1111}&=1-\xi_{2211}^2, \quad A_{2121}=A_{2222}=0, \quad A_{3131}=1-\xi_{2231}^2,\end{aligned} \tag{9}$$

where

$$\begin{aligned}\xi_{2211}&=\{(m_1m_3/\sigma I^e_{xx})^{\frac{1}{2}}(z_1^0-z_3^0)\cos\gamma +(m_2\sum/\sigma I^e_{xx})^{\frac{1}{2}}z_2^0\sin\gamma\},\\ \xi_{2231}&=\{-(m_1m_3/\sigma I^e_{xx})^{\frac{1}{2}}(z_1^0-z_3^0)\sin\gamma +(m_2\sum/\sigma I^e_{xx})^{\frac{1}{2}}z_2^0\cos\gamma\}.\end{aligned}$$

In the normal coordinates the first- and second-

order potential energy expression may be written

$$V_1=k_{111}q_1^3+k_{113}q_1^2q_3+k_{122}q_1\rho^2+k_{133}q_1q_3^2+k_{223}\rho^2q_3+k_{333}q_3^3,$$

$$V_2=k_{1111}q_1^4+k_{1113}q_1^3q_3+k_{1122}q_1^2\rho^2+k_{1133}q_1^2q_3^2+k_{1333}q_1q_3^3+k_{2222}\rho^4+k_{2233}\rho^2q_3^2+k_{3333}q_3^4 \quad (10)$$

in which

$$\rho^2=(q_{21}^2+q_{22}^2).$$

With the constants derived the explicit expressions for H_0, H_1 and H_2 may now easily be written.

III. THE VIBRATION-ROTATION ENERGY EXPRESSIONS

The vibration-rotation energies may be conveniently written as

$$(E/hc)=(E_{\text{vib}}/hc)+(E_{\text{rot}}/hc),$$

where $(E_{\text{vib}}/hc)=$

$$(E_0/hc)+\omega_1(v_1+\tfrac{1}{2})+\omega_2(v_2+1)+\omega_3(v_3+\tfrac{1}{2})+x_{11}(v_1+\tfrac{1}{2})^2+x_{22}(v_2+1)^2+x_{33}(v_3+\tfrac{1}{2})^2+(x_{12}+x_{21})(v_1+\tfrac{1}{2})(v_2+1)+(x_{13}+x_{31})(v_1+\tfrac{1}{2})(v_3+\tfrac{1}{2})+(x_{23}+x_{32})(v_2+1)(v_3+\tfrac{1}{2})+x_{l_2l_2}l_2^2, \quad (11)$$

where

$$x_{11}=(h/32\pi^4c^3\omega_1^2)\{3k_{1111}-15k_{111}^2/8\pi^2c^2\omega_1^2-k_{113}^2/4\pi^2c^2\omega_3^2+k_{113}^2/8\pi^2c^2(4\omega_1^2-\omega_3^2)\},$$

$$x_{22}=(h/32\pi^4c^3\omega_2^2)\{3k_{2222}-k_{122}^2/4\pi^2c^2\omega_1^2-k_{223}^2/4\pi^2c^2\omega_3^2+k_{122}^2/8\pi^2c^2(4\omega_2^2-\omega_1^2)+k_{223}^2/8\pi^2c^2(4\omega_2^2-\omega_3^2)\},$$

$$x_{33}=(h/32\pi^4c^3\omega_3^2)\{3k_{3333}-15k_{333}^2/8\pi^2c^2\omega_3^2-k_{133}^2/4\pi^2c^2\omega_1^2+k_{133}^2/8\pi^2c^2(4\omega_3^2-\omega_1^2)\},$$

$$x_{12}=(h/32\pi^4c^3\omega_1\omega_2)\{k_{1122}-6k_{111}k_{122}/4\pi^2c^2\omega_1^2-k_{113}k_{223}/4\pi^2c^2\omega_3^2+4\pi^2c^2(\omega_2^2/I_{xx}^e)\xi_{2211}\},$$

$$x_{21}=(h/32\pi^4c^3\omega_1\omega_2)\{k_{1122}-k_{223}k_{113}/4\pi^2c^2\omega_3^2-k_{122}^2/\pi^2c^2(4\omega_2^2-\omega_1^2)+4\pi^2c^2(\omega_1^2/I_{xx}^e)\xi_{2211}\}, \quad (11)$$

$$x_{13}=(h/32\pi^4c^3\omega_1\omega_3)\{k_{1133}-6k_{111}k_{133}/4\pi^2c^2\omega_1^2-k_{113}^2/\pi^2c^2(4\omega_1^2-\omega_3^2)\},$$

$$x_{31}=(h/32\pi^4c^3\omega_1\omega_3)\{k_{1133}-6k_{333}k_{113}/4\pi^2c^2\omega_3^2-k_{133}^2/\pi^2c^2(4\omega_3^2-\omega_1^2)\},$$

$$x_{23}=(h/32\pi^4c^3\omega_2\omega_3)\{k_{2233}-k_{122}k_{133}/4\pi^2c^2\omega_1^2-k_{223}^2/\pi^2c^2(4\omega_2^2-\omega_3^2)+4\pi^2c^2(\omega_3^2/I_{xx}^e)\xi_{2231}\},$$

$$x_{32}=(h/32\pi^4c^3\omega_2\omega_3)\{k_{2233}-6k_{333}k_{223}/4\pi^2c^2\omega_3^2-k_{133}k_{122}/4\pi^2c^2\omega_1^2+4\pi^2c^2(\omega_2^2/I_{xx}^e)\xi_{2231}\},$$

$$x_{l_2l_2}=(-h/32\pi^4c^3\omega_2^2)\{k_{2222}+k_{122}^2/8\pi^2c^2(4\omega_2^2-\omega_1^2)+k_{223}^2/8\pi^2c^2(4\omega_2^2-\omega_3^2)\},$$

and

$$(E_{\text{rot}}/hc)=[J(J+1)-l^2]B_v-[J(J+1)-l^2]^2D \quad (12)$$

in which

$$B_v=B_e-(v_1+\tfrac{1}{2})\alpha_1-(v_2+1)\alpha_2-(v_3+\tfrac{1}{2})\alpha_3,$$

$$B_e=h/8\pi^2cI_{xx}^e,$$

$$\alpha_1=B_e(h/4\pi^2c\omega_1I_{xx}^e)\{1-4\xi_{2211}^2\omega_1^2/(\omega_1^2-\omega_2^2)-4\xi_{2231}^2+6(I_{xx}^e)^{\frac{1}{2}}\xi_{2231}k_{111}/4\pi^2c^2\omega_1^2+2(I_{xx}^e)^{\frac{1}{2}}\xi_{2211}k_{113}/4\pi^2c^2\omega_3^2\},$$

$$\alpha_2=B_e(h/8\pi^2c\omega_2I_{xx}^e)\{-4(I_{xx}^e)^{\frac{1}{2}}\xi_{2211}k_{223}/4\pi^2c^2\omega_3^2+4(I_{xx}^e)^{\frac{1}{2}}\xi_{2231}k_{122}/4\pi^2c^2\omega_1^2-(3\omega_2^2+\omega_1^2)\xi_{2211}^2/(\omega_2^2-\omega_1^2)-(3\omega_2^2+\omega_3^2)\xi_{2231}^2/(\omega_2^2-\omega_3^2)\}, \quad (13)$$

$$\alpha_3=B_e(h/4\pi^2c\omega_3I_{xx}^e)\{1-4\xi_{2231}^2\omega_3^2/(\omega_3^2-\omega_2^2)-4\xi_{2211}^2-6(I_{xx}^e)^{\frac{1}{2}}\xi_{2211}k_{333}/4\pi^2c^2\omega_3^2+2(I_{xx}^e)^{\frac{1}{2}}\xi_{2231}k_{133}/4\pi^2c^2\omega_1^2\},$$

$$D=(h^3/128\pi^6c^3(I_{xx}^e)^3)\{\xi_{2211}^2/\omega_3^2+\xi_{2231}^2/\omega_1^2\},$$

$$l=l_2.$$

IV. REDUCTION TO THE XY_2 TYPE MODEL

The accuracy of the above expressions may be tested by reducing them to the energies for the XY_2 type model and effecting a comparison with

these results[2] which are well known to be correct. The following simplifications may be made:

$$\begin{aligned}
&m_1=m_3,\quad z_1^0=-z_3^0,\quad z_2^0=0,\quad \sin\gamma=1,\\
&\cos\gamma=0,\quad K_1=K_2,\quad K_{13}=K_{23},\\
&\mathfrak{K}_1=\mu_1 k_1'=0,\quad \xi_{2211}=0,\quad \xi_{2231}=-1,\\
&a_{11}=-2(I_{xx}^e)^{\frac{1}{2}},\quad a_{21}=a_{22}=a_{31}=0,\\
&A_{1111}=1,\quad A_{3131}=A_{2121}=A_{2222}=0,\\
&k_{113}=k_{223}=k_{333}=0.
\end{aligned}\tag{14}$$

When these substitutions are made in (11) and (13), these expressions reduce to

$$\begin{aligned}
x_{11}&=(h/32\pi^4c^3\omega_1^2)\{3k_{1111}-15k_{111}^2/8\pi^2c^2\omega_1^2\},\\
x_{22}&=(h/32\pi^4c^3\omega_2^2)\{3k_{2222}\\
&\quad -k_{122}^2(8\omega_2^2-3\omega_1^2)/8\pi^2c^2\omega_1^2(4\omega_2^2-\omega_1^2)\},\\
x_{33}&=(h/32\pi^4c^3\omega_3^2)\{3k_{3333}\\
&\quad -k_{133}^2(8\omega_3^2-3\omega_1^2)/8\pi^2c^2\omega_1^2(4\omega_3^2-\omega_1^2)\},\\
x_{12}&=(h/32\pi^4c^3\omega_1\omega_2)\\
&\quad\times\{k_{1122}-6k_{111}k_{122}/4\pi^2c^2\omega_1^2\},\\
x_{21}&=(h/32\pi^4c^3\omega_1\omega_2)\\
&\quad\times\{k_{1122}-k_{122}^2/\pi^2c^2(4\omega_2^2-\omega_1^2)\},\\
x_{13}&=(h/32\pi^4c^3\omega_1\omega_3)\\
&\quad\times\{k_{1133}-6k_{111}k_{133}/4\pi^2c^2\omega_1^2\},\\
x_{31}&=(h/32\pi^4c^3\omega_1\omega_3)\\
&\quad\times\{k_{1133}-k_{133}^2/\pi^2c^2(4\omega_3^2-\omega_1^2)\},\\
x_{23}&=(h/32\pi^4c^3\omega_2\omega_3)\\
&\quad\times\{k_{2233}-k_{122}k_{133}/4\pi^2c^2\omega_1^2\\
&\quad\quad +4\pi^2c^2(\omega_3^2/I_{xx}^e)\},\\
x_{32}&=(h/32\pi^4c^3\omega_2\omega_3)\\
&\quad\times\{k_{2233}-k_{122}k_{133}/4\pi^2c^2\omega_1^2\\
&\quad\quad +4\pi^2c^2(\omega_2^2/I_{xx}^e)\},\\
x_{l_2l_2}&=(-h/32\pi^4c^3\omega_2^2)\\
&\quad\times\{k_{2222}+k_{122}^2/8\pi^2c^2(4\omega_2^2-\omega_1^2)\},
\end{aligned}\tag{15}$$

$$\begin{aligned}
\alpha_1&=-B_e(h/4\pi^2c\omega_1I_{xx}^e)\\
&\quad\times\{3+6(I_{xx}^e)^{\frac{1}{2}}k_{111}/4\pi^2c^2\omega_1^2\},\\
\alpha_2&=-B_e(h/8\pi^2c\omega_2I_{xx}^e)\\
&\quad\times\{+4(I_{xx}^e)^{\frac{1}{2}}k_{122}/4\pi^2c^2\omega_1^2)\\
&\quad\quad +(3\omega_2^2+\omega_3^2)/(\omega_2^2-\omega_3^2)\},\\
\alpha_3&=-B_e(h/4\pi^2c\omega_3I_{xx}^e)\\
&\quad\times\{2(I_{xx}^e)^{\frac{1}{2}}k_{133}/4\pi^2c^2\omega_1^2\\
&\quad\quad +(3\omega_3^2+\omega_2^2)/(\omega_3^2-\omega_2^2)\},\\
D&=h^3/128\pi^6c^3(I_{xx}^e)^3\omega_1^2,\\
B_e&=h/8\pi^2cI_{xx}^e,\\
B_v&=B_e-(v_1+\tfrac{1}{2})\alpha_1-(v_2+1)\alpha_3-(v_3+\tfrac{1}{2})\alpha_3.
\end{aligned}$$

When it is observed that the relation between Dennison's coordinates σ, ρ, ζ and those given in this discussion, q_1, ρ, q_3, is

$$\sigma=2\pi c\omega_1^{\frac{1}{2}}q_1/(hc)^{\frac{1}{2}},\quad \rho=2\pi c\omega_2^{\frac{1}{2}}\rho/(hc)^{\frac{1}{2}},\quad \zeta=2\pi c\omega_3^{\frac{1}{2}}q_3/(hc)^{\frac{1}{2}}$$

it can easily be shown that the constants $(a\cdots i)$ in his V_1 and V_2 take the following values in terms of $k_{ss's''}$ and $k_{sss's''}$:

$$\begin{aligned}
a&=k_{111}(hc)^{\frac{1}{2}}/8\pi^3c^3\omega_1^{\frac{1}{2}}, & e&=k_{2222}h/16\pi^4c^3\omega_2^2,\\
b&=k_{122}(hc)^{\frac{1}{2}}/8\pi^3c^3\omega_1^{\frac{1}{2}}\omega_2, & f&=k_{3333}h/16\pi^4c^3\omega_3^2,\\
c&=k_{133}(hc)^{\frac{1}{2}}/8\pi^3c^3\omega_1^{\frac{1}{2}}\omega_3, & g&=k_{1122}h/16\pi^4c^3\omega_1\omega_2,\\
d&=k_{1111}h/16\pi^4c^3\omega_1^2, & h&=k_{1133}h/16\pi^4c^3\omega_1\omega_3,\\
& & i&=k_{2233}h/16\pi^4c^3\omega_2\omega_3.
\end{aligned}$$

The substitution of these constants into Eqs. (15) cause them to reduce exactly to the constants x_{ii} given by Dennison.[3]

The author expresses his gratitude to Professor Harald H. Nielsen, of the Ohio State University, who suggested the problem and with whom valuable discussions were held during its solution.

[3] An exception may be noted in that Dennison has neglected to calculate the term D due to centrifugal stretching of the molecules. It should also be noted that the term l^2B_e occurring in Dennison's x_{ll} has here been included in the E_{rot}.

The Quenching of Cadmium Resonance Radiation (3261A) by Hydrocarbons and Other Gases*

E. W. R. STEACIE AND D. J. LEROY
Division of Chemistry, National Research Laboratories, Ottawa, Canada

(Received February 10, 1943)

An investigation has been made of the quenching of cadmium resonance radiation (3261A) by a number of hydrocarbons and other gases. The following values of the quenching cross sections were obtained (in $cm^2 \times 10^{16}$):

H_2	3.54	1-C_4H_8	35.2	C_2H_6	ca. 0.02
D_2	1.80	2-C_4H_8	30.6	C_3H_8	
NH_3	0.052	C_6H_6	28.4	n-C_4H_{10}	
C_2H_4	24.9	C_2H_2	22.0	iso-C_4H_{10}	
C_3H_6	29.1	cyclopropane	0.71		

A few rough measurements have also been made with λ2288.

INTRODUCTION

IN the last few years we have investigated a series of cadmium and zinc photosensitized reactions of hydrocarbons,[1-4] using the cadmium resonance lines 3261A and 2288A, and the zinc lines 3076A and 2139A. For a proper interpretation of the results obtained it is desirable to have information on the quenching of these lines by the gases employed. Since such data do not exist, it was decided to investigate the quenching of cadmium and zinc resonance radiation by a number of gases. The present paper is primarily concerned with the quenching of the 3261A cadmium line (Cd 5^3P_1 − Cd 5^1S_0).

The only previous work on the quenching of λ3261 is that of Bates,[5] Bender,[6] and Lipson and Mitchell.[7] Bates and Bender made purely qualitative observations of the quenching by hydrogen. Lipson and Mitchell made a quantitative investigation with a number of gases and found the following quenching cross sections:

H_2	0.67×10^{-16} cm²	NH_3	0.041×10^{-16} cm²
D_2	0.19	N_2	0.021
CO	0.14	CH_4	0.012.

EXPERIMENTAL

The experimental method was in principle the same as that used by Lipson and Mitchell. Two quartz cells were employed, one of which contained cadmium vapor alone, while the other contained a foreign gas as well. A beam of λ3261 was sent through both cells, and the resonance radiation emitted at right angles to the incident beam was photographed. The intensities of the resonance radiation from the two cells were then compared by photographic photometry.

The experiments were performed in such a way that the light path through the cadmium vapor was a minimum, the pressure of cadmium vapor was very low, and the pressure of the foreign gas was as low as possible. Under these conditions the Stern-Volmer equation holds, and the quenching cross sections can be calculated from the relation[8]

$$\sigma_Q^2 = \frac{1}{Q\cdot p} \Big/ 2666.6\tau\left[\frac{2\pi N}{kT}\left(\frac{1}{M_1}+\frac{1}{M_2}\right)\right]^{\frac{1}{2}}$$

where σ_Q^2 is the quenching collision cross section in cm², Q is the quenching, i.e. the ratio of the resonance radiation emitted in the presence of a foreign gas to that which would be emitted in its absence, $1/(Q\cdot p)$ is the slope of the curve obtained by plotting $1/Q$ against the pressure of the foreign gas in mm, τ is the mean life of the 5^3P_1 state of cadmium, which was taken to be

* Contribution No. 1104 from the National Research Laboratories, Ottawa, Canada.

[1] E. W. R. Steacie, D. J. LeRoy and R. Potvin, J. Chem. Phys. **9**, 306 (1941).

[2] E. W. R. Steacie, Annals N. Y. Acad. Sci. **41**, 187 (1941).

[3] E. W. R. Steacie and D. J. LeRoy, J. Chem. Phys. **10**, 22 (1942).

[4] H. Habeeb, D. J. LeRoy and E. W. R. Steacie, J. Chem. Phys. **10**, 261 (1942).

[5] J. R. Bates, Proc. Nat. Acad. Sci. **14**, 849 (1928).

[6] P. Bender, Phys. Rev. **36**, 1535 (1930).

[7] H. C. Lipson and A. C. G. Mitchell, Phys. Rev. **48**, 625 (1935).

[8] A. C. G. Mitchell and M. Zemansky, *Resonance Radiation and Excited Atoms* (The Macmillan Co., New York, 1934).

2.5×10^{-6} sec.,[8] N is Avogadro's number, k is the gas constant per molecule, and M_1 and M_2 are the molecular weights of the colliding particles.

The Light Source

The source of cadmium resonance radiation was of a type which has been previously described.[3] The emitting part of the lamp was made of fused quartz. To the ends of this, through graded seals, were attached Pyrex electrode chambers containing "coated" iron electrodes. The lamp contained a small piece of cadmium and was filled with neon at a pressure of 3 mm at room temperature. It was operated from a sign transformer at 120 milliamperes. The lamp, including the electrode chambers, was contained in an electric furnace at 280°C, the radiation emerging through a fused quartz window.

The radiation from the lamp consisted mainly of the resonance lines at 2288 and 3261A. The intensity of these lines was very high, and the output of the lamp was unusually steady, the maximum variation being less than 5 percent over long periods of time.

The Optical System

The radiation from the lamp passed through a slit, and through a Corex D plate which removed λ2288 completely, and was then focused into a convergent beam by two quartz lenses. The beam then passed a shutter and entered the furnace containing the resonance cells through a quartz window. The resonance cells were situated one above the other, and the image of the source gave a narrow line which was long enough to cover both cells. Opposite each cell was a slit which allowed a narrow pencil of radiation to enter the cell.

The fluorescent radiation was taken off at right angles to the incident beam through another slit. The incident and emergent slits were situated as close as possible to a common edge of the resonance cells in order to provide the shortest possible light path through cadmium vapor, and thus diminish effects due to imprisonment.

The beams emerging from the cells passed out of the furnace through a quartz window and entered the camera where they were focused on an Eastman 40 plate. The method of photometry, etc. will be described later.

The Resonance Cells, etc.

The resonance cells were made of fused quartz, with two polished windows about 2 cm in diameter meeting at a common edge. For the dual purpose of maintaining uniformity of temperature, and the elimination of scattered light, the cells were mounted above one another in a metal box with heavy walls, provided with slits for the incident and fluorescent beams. The cells were of the usual "light-trap" type.

Short side tubes of wide bore (14 mm) passed out from each cell into holes in a single large brass block. Each side tube contained small pieces of cadmium. The wide, short tubes permitted rapid diffusion of the vapor, and the brass block kept the vapor pressure of cadmium the same in both cells.

A further side tube from each cell led through a graded quartz-to-Pyrex seal to a magnetic cut-off to prevent diffusion of cadmium vapor to the cold tubing outside the furnace. The tubing on the far side of the cut-off passed out of the furnace and was connected through a stopcock with a vacuum system consisting of pumps, McLeod gauges, gas reservoirs, etc.

The whole system up to the far side of the magnetic cut-offs was contained in an electric furnace. The distribution of the heating elements in the furnace was such that the brass block was colder than the rest of the system, and its temperature could be independently controlled. The windows of the resonance cells were kept at a slightly higher temperature than the rest of the system to prevent the condensation on them of cadmium vapor. Five thermocouples in various parts of the system, and independent electrical circuits for the various heating elements enabled the temperature to be accurately controlled to within 1° throughout the furnace, and to within 0.5° or better for the brass block containing the side tubes with the cadmium supply.

The reason for the somewhat elaborate temperature control system is that the main source of error in the measurements arises from variations in the cadmium vapor pressure. The intensity of the fluorescent radiation is very sensitive to such variations, and the function of the

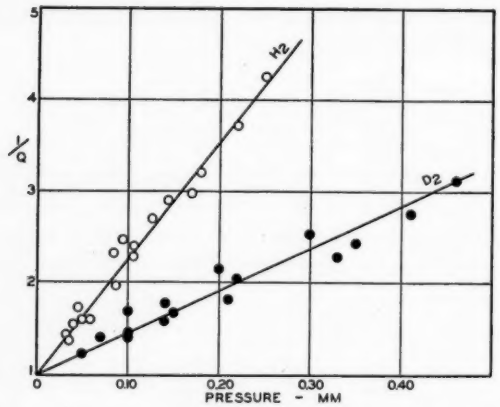

FIG. 1. Quenching of λ3261 by hydrogen and deuterium.

comparison cell is much more to compensate for fluctuations in cadmium vapor pressure than for fluctuations in the incident light intensity. By maintaining the cadmium supplies for the two cells at the same temperature equality of vapor pressure is achieved in principle. However, in operation one cell contains a foreign gas and the other does not. If the fluctuations in the temperature of the cadmium supply are large, or if the tubing leading from it to the cells is long and narrow, diffusion of cadmium vapor will be much slower in the cell containing the foreign gas and this may give rise to large errors. For this reason the fluctuations in temperature were reduced as much as possible, and the connecting tubing was short and wide.

Experimental Procedure

The procedure in carrying out an experiment was as follows. Both cells were evacuated to at least 10^{-4} mm. They were then closed off and allowed to stand for an hour or more to ensure cadmium vapor pressure equilibrium. The shutter between the lamp and the cells was then opened, and exposures of various lengths of time, from about 10 sec. to 100 sec., were made with the camera. These served as calibration marks on the plate. Trial exposures made with calibrated screens showed that the failure of the reciprocity law was appreciable (about 4 times the normal experimental error), and a correction for this failure was therefore made when translating plate blackenings into intensities.

After the calibration marks had been put on the plates, the gas under investigation was added to one cell, its pressure measured with a McLeod gauge, and the system was then shut off and allowed to stand for about an hour. During this time the shutter between the lamp and the cell was kept closed to avoid possible photochemical reactions of the added gas. The radiation from the cells was then photographed again, the pressure of the added gas was altered, and the system was shut off and allowed to stand again. In this way a series of 4 or 5 pressures were investigated in a single experiment.

The plate was then developed and the blackenings determined with a microphotometer. The light source was very steady and the fluctuations in intensity were negligible over the short period of time required for the calibration exposures. Over the long period required for a whole experiment some fluctuations occurred, but these were compensated for by comparing the blackening of the spot from the cell containing the foreign gas with the blackening from the evacuated cell. By means of the calibration marks blackenings were translated into intensities, and the value of $1/Q$ determined by dividing the intensity of the

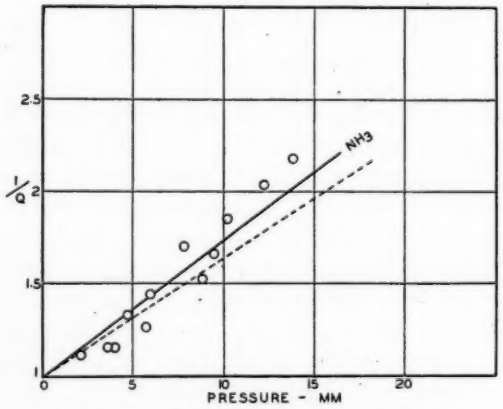

FIG. 2. Quenching of λ3261 by ammonia.

fluorescence in the absence of a foreign gas by that in the presence of a foreign gas.

Materials

The quenching efficiencies of the gases investigated varied widely. In the case of substances such as the olefins which quenched very strongly the presence of traces of impurities could have no appreciable effect on the results. The paraffins, however, quench only very slightly, and it was

therefore of great importance to free them as far as possible from traces of gases which quench strongly.

Hydrogen was taken from a commercial cylinder of "pure" gas and passed over platinized asbestos at 600°C, and through a liquid-air trap. In some experiments it was stored over phosphorus pentoxide and in others it was not. A number of preparations gave identical results. Further, a sample taken direct from the cylinder differed only slightly from the purified samples.

Deuterium was obtained in a cylinder from the Stuart Oxygen Company, and was stated to be at least 99.5 percent D_2. It was purified by the procedure used for hydrogen.

Ammonia was taken from a cylinder and purified by an extended series of bulb-to-bulb distillations. Ammonia taken directly from the cylinder gave almost identical results.

Ethylene was obtained in cylinders from the Ohio Chemical and Manufacturing Company, and was stated to be 99.5 percent C_2H_4. It was purified by distillation in a still of the Podbielniak type.

Propylene was also 99.5 percent grade, and was fractionated similarly.

Butene-1 and butene-2 were prepared by the methods given by Kistiakowsky, Ruhoff, Smith and Vaughan.[9] The resulting gases were fractionated in the Podbielniak column.

Cyclopropane was Ohio 99.5 percent grade. Since propylene was a possible impurity and quenches much more strongly than cyclopropane, the purification procedure was designed mainly for its removal. Cyclopropane from the cylinder was shaken for 24 hours with alkaline permanganate solution, and was then distilled at a high reflux ratio in the column. A further sample was taken directly from the cylinder and was merely given a bulb-to-bulb distillation. This gave results identical with those from the preceding sample, and it may therefore be concluded that no significant amount of strongly quenching impurity was present.

TABLE I. The quenching of λ3261.

Gas	Slope of quenching curve mm^{-1}	Quenching cross section $cm \times 10^{16}$
H_2	12.65	3.54
D_2	4.60	1.80
NH_3	0.072	0.052
C_2H_4	26.3	24.9
C_3H_6	26.5	29.1
1-C_4H_8	29.0	35.2
2-C_4H_8	25.0	30.6
C_6H_6	20.9	28.4
C_2H_2	24.0	22.0
cyclopropane	0.64	0.71
C_2H_6	(0.025)	(0.024)
C_3H_8	(0.011)	(0.012)
n-C_4H_{10}	(0.052)	(0.064)
iso-C_4H_{10}	(0.037)	(0.046)

[9] G. B. Kistiakowsky, J. R. Ruhoff, H. A. Smith, and W. E. Vaughan, J. Am. Chem. Soc. **57**, 876 (1935).

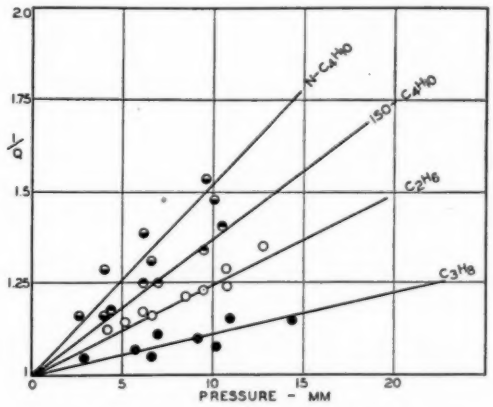

FIG. 3. Quenching of λ3261 by the paraffins.

Benzene of American Chemical Standard grade was used without purification other than outgassing. It quenched so strongly that impurities could have no appreciable effect on the results.

Acetylene also quenched very strongly, and hence a bulb-to-bulb distillation of the commercial product was a sufficient purification.

Ethane proved to have a quenching efficiency only about 1/1000 that of ethylene, which is one of the most likely impurities. Hence, assuming the experimental error to be 5 percent, it is necessary to reduce the amount of ethylene in the ethane to 1/20,000. Ohio cylinder ethane which had previously been given a Podbielniak distillation was saturated with bromine vapor and passed slowly through a vessel illuminated with a 1000-watt photo-flood lamp. The gas was then passed through a 40 percent potassium hydroxide solution, a dry-ice trap to remove water, and the ethane was collected in a liquid-air trap. The ethane was then again distilled through the column.

Propane from a cylinder of 99.9 percent grade was given a treatment similar to that used for

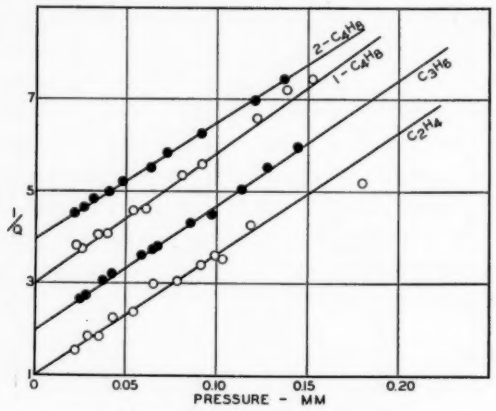

FIG. 4. Quenching of λ3261 by the olefins.

ethane. Since the relatively high boiling point made it more difficult to remove water, the gas was stored in a reservoir over phosphorus pentoxide.

n- and iso-butane of 99 percent grade were treated as described for propane.

RESULTS

Preliminary experiments with hydrogen and a number of other gases showed that the quenching curve was independent of the intensity of the incident radiation: this was reduced by a factor of about 10 for these experiments by introducing a thin soft glass plate into the light path. The results were also shown to be independent of the position of the entering slit, which was moved from its normal grazing position to a distance of about 2 mm from the common edge of the cell. This indicates that imprisonment of resonance radiation is not affecting the results. This was confirmed by experiments in which the cadmium vapor pressure was varied over a wide range. In these experiments the results were shown to be independent of the temperature of the cadmium supply over the range 170° to 240°C, corresponding to cadmium vapor pressures from 4×10^{-5} to 2×10^{-3} mm.

The final results were obtained with the resonance cells at a temperature of 213°C and the cadmium supply at 180°C, corresponding to a cadmium vapor pressure of 9×10^{-5} mm. It was possible to work with this very low vapor pressure of cadmium on account of the very high intensity of the source.

The results obtained are shown in the form of plots of $1/Q$ against pressure in Figs. 1 to 6. In some cases the origin has been shifted vertically to avoid overlapping of the curves. The slopes of the lines in these diagrams and the quenching cross sections calculated from Eq. (1) are given in Table I.

DISCUSSION

The only previous work with which the above results can be compared is that of Lipson and Mitchell on hydrogen, deuterium and ammonia. Their results are compared with ours in Table II. The agreement in the case of ammonia is as good as could be expected. The heavy line in Fig. 2 represents our results, the dotted line those of Lipson and Mitchell. There is, however, a very large discrepancy in the case of hydrogen and deuterium. In an attempt to discover the cause of this a large number of experiments were made with hydrogen under various conditions. As mentioned previously, the results were independent of cadmium pressure, the length of the light path in the vapor and of the intensity. We therefore feel confident that our results are not affected by errors due to imprisonment of radiation.

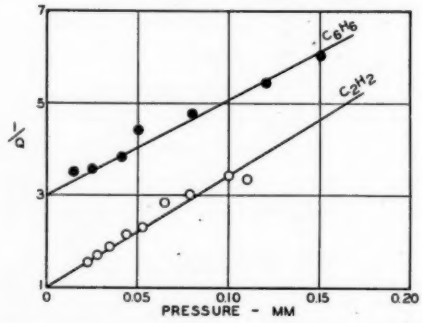

FIG. 5. Quenching of λ3261 by benzene and acetylene.

In some experiments a spectrograph was substituted for the camera and long exposures were made. These showed no detectable radiation other than λ3261, and thus prove that errors were not introduced by scattered visible light, or by effects concerned with other transitions involving the 5^3P_1 level, i.e. by λλ3404, 3466, and 3613.

A number of runs were made with different samples of hydrogen. Tank hydrogen gave results only slightly different from those with the puri-

fied gas. Further, the addition of water vapor or oxygen in quantities much larger than the possible amounts present as an impurity caused a change in the quenching far too small to account for the discrepancy. It appears impossible to account for the difference in the results on the basis of an impurity. The greatest "quenching efficiency," i.e. slope of the $1/Q-p$ curve, which we have found is 29.0 for butene-1. If we assumed that the true value for hydrogen is 2.45 as found by Lipson and Mitchell, and that our value of 12.65 is due to the presence of butene in the hydrogen, it would be necessary to assume that 40 percent of butene was present as an impurity. To account for the result on the basis of any reasonable amount of impurity, say even the extremely unlikely amount of 2 percent, would necessitate a substance with an efficiency 20 times greater than butene-1, i.e. with a quenching cross section of about 700×10^{-16} cm^2. To say the least this is extremely unlikely, especially since such an impurity would have to possess a low enough molecular weight to be volatile at liquid-air temperatures.

The only way in which our technique differed appreciably from that of Lipson and Mitchell was in the source of λ3261. They used a cadmium-hydrogen discharge, while we used a cadmium-neon source. This difference might possibly furnish an explanation of the discrepancy. The cadmium-hydrogen discharge contains, in addition to λ3261, cadmium hydride bands of considerable intensity. Since the quenching process presumably involves the formation of CdH,[10] it is possible to have resonance emission of the CdH bands from the quenching cell. If this were the case in Lipson and Mitchell's investigation, some of the excited atoms quenched by forming CdH would subsequently emit CdH bands, and the result would be an apparent quenching efficiency much less than the true value. The values obtained for hydrogen, and for deuterium since the CdH and CdD bands would largely overlap, would be low, while those for substances which do not form CdH in the quenching process, such as ammonia, would not be affected. However, it seemed unlikely that such a large discrepancy could arise from this cause, and after correspondence with Professor Mitchell it was decided to reinvestigate the quenching with a lamp of the type used by Lipson and Mitchell.

TABLE II. Quenching cross section, cm$^2\times10^{16}$.

Gas	Lipson and Mitchell	Present paper
H_2	0.67	3.54
D_2	0.19	1.80
NH_3	0.041	0.052

[10] L. O. Olsen, J. Chem. Phys. **6**, 307 (1938).

A lamp of the general type described by Ellett[11] was therefore constructed. This consisted of a quartz tube connected through graded seals to Pyrex electrode chambers containing large cylindrical aluminium electrodes. Hydrogen flowed into the lamp through a saturator containing a liquid cadmium-tin alloy, heated by an electric furnace, passed through the lamp, and was then pumped away by a diffusion pump. The lamp was operated at 5000 volts and about 0.5 amp. This source gave λ3261 relatively weakly, as compared with a cadmium-neon lamp, but gave the CdH bands, especially those at λ4310 and λ4500 with good intensity. As before, the radiation from the lamp passed through a Corex D filter.

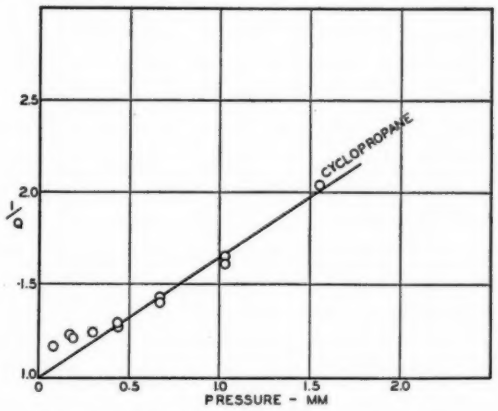

FIG. 6. Quenching of λ3261 by cyclopropane.

The results obtained were not as reproducible as those with the previous source, since fluctuations in lamp intensity were considerably greater than before. However, they showed conclusively that no appreciable difference was caused by the change in the source. In other words the quenching values obtained were in complete agreement with our previous values with the cadmium-neon source.

[11] A. Ellett, J. Opt. Soc. Am. **10**, 427 (1924).

As a further check, experiments were made with the cadmium-hydrogen lamp in which a chlorine filter was placed in the fluorescent beam emerging from the quenching cells. The filter was such that λ3261 would be completely absorbed, but λλ4310 and 4500 would be fairly largely transmitted. Any fluorescent emission of these bands could thus be easily detected. Long exposures were made, but only negligible amounts of CdH fluorescence were observed. It may thus be concluded that no large error could have been introduced into Lipson and Mitchell's experiments on account of fluorescence by cadmium hydride.

The discrepancy between the two investigations in the case of hydrogen and deuterium thus remains unexplained. We have, however, considerable confidence in our results since (a) all pertinent conditions were varied over wide ranges, (b) the cadmium vapor pressures employed were so low that imprisonment effects cannot have been of importance, (c) a much lower quenching cross section for hydrogen and cadmium as compared with hydrogen and mercury would be rather surprising since the energy balance for

$$Cd(5^3P_1)+H_2=CdH+H$$

is almost exact, and (d) there is some theoretical support for the higher value.[12]

Accuracy of Results

The percentage accuracy of the results for substances which quench strongly is of the order of 5 percent, and is much greater than that for substances which quench only slightly. Further, in the case of substances which quench very slightly the requirements as far as purity is concerned become impossibly exacting. As a result the values given for the paraffins in Table I cannot be considered to be more than an upper limit to the quenching cross sections. Certainly the relative order of the quenching for the paraffins cannot be relied on. Actually it is probably easier to remove propylene from propane than any other olefin from the corresponding paraffin, since ethylene is less reactive than the other olefins and the higher boiling butenes are more difficult to handle. The low value obtained for propane probably means merely that it was the purest of the paraffins used.

[12] K. J. Laidler, J. Chem. Phys. **10**, 34, 43 (1942).

TABLE III. Comparison of results with cadmium, mercury, and sodium.

Gas	Quenching cross section, $cm^2 \times 10^{16}$		
	$Cd(5^3P_1)$	$Hg(6^3P_1)$	$Na(3^2P)$[d]
H_2	3.54	8.60[b]	7.4
CH_4	0.012[a]	0.085[b]	0.11
C_2H_6	0.024	0.59[b]	0.17
C_3H_8	0.012	2.32[b]	0.2
"butane"	0.46, 0.64	5.88[b]	0.3
C_2H_4	24.9	48[c]	44.0
C_3H_6	29.1	—	52.0
C_4H_8-1	35.2	—	58.0
C_4H_8-2	30.6	—	58.0
C_6H_6	28.4	59.9[b]	75.0

[a] See reference 7 in text.
[b] See reference 8 in text.
[c] E. W. R. Steacie, Can. J. Research **B18**, 44 (1940).
[d] R. G. W. Norrish and W. MacF. Smith, Proc. Roy. Soc. **A176**, 295 (1940).

Comparison with Mercury and Sodium

The values of the quenching cross sections for 5^3P_1 cadmium atoms obtained here are compared in Table III, wherever the data exist, with corresponding values for $Hg(6^3P_1)$ and $Na(^2P)$ atoms.

In a general way it will be seen that a parallelism exists among the results for the three substances. Thus hydrogen has a rather large quenching cross section in all three cases, the olefins quench very strongly, and the paraffins are relatively inefficient. In the case of the paraffins, however, there is a definite difference between the results for mercury and those for the other two metals. Thus with sodium and cadmium all paraffins quench very poorly. With mercury the lower paraffins quench equally poorly, but there is a steady rise in cross section with increasing molecular weight. Actually, no special precautions were taken to free the paraffins from olefin impurities in the investigation with mercury.[13] Since propane and butane would be much harder to free from olefins by a simple bulb-to-bulb distillation, the results for these gases may well be too high. However, in view of the fact that Bates found a cross section for heptane much too large to be accounted for on the basis of an impurity, it seems certain that there is a real and large increase in the quenching cross sections with increasing molecular weight.

The mechanism of the quenching of sodium, mercury, and cadmium has recently been dis-

[13] J. R. Bates, J. Am. Chem. Soc. **52**, 3825 (1930); **54**, 569 (1932).

cussed theoretically by Laidler[12] from the standpoint of potential energy surfaces. It appears certain in the case of hydrogen that quenching of sodium is of a physical nature, while that of cadmium involves the formation of CdH. In the case of mercury there is spectroscopic evidence against the formation of HgH in the quenching process.[10] However, Laidler suggests that in reality the quenching act involves the formation of HgH, but that this possesses sufficient excess energy to dissociate and does so immediately.

In the case of the paraffins a similar mechanism appears to hold. It is certain from photochemical evidence[2] that the quenching of $Cd(5^3P_1)$ by paraffins involves the process

$$Cd(5^3P_1)+RH=CdH+R,$$

since the evidence is overwhelmingly in favor of a C−H bond split in the primary process, and the excitation energy of the 5^3P_1 state is insufficient to permit the reaction

$$Cd(5^3P_1)+RH=Cd(5^1S_0)+R+H.$$

It seems likely that quenching of $Hg(6^3P_1)$ proceeds by the same mechanism. From this point of view it is difficult to see why the cross sections of the paraffins increase with increasing molecular weight for mercury but not for cadmium.

The very large quenching cross sections of all the olefins must mean that the quenching phenomenon is associated with the double bond. This leads to an interesting photochemical result.[14] It has been found that the cadmium photosensitized reactions of ethane and propane proceed readily, the primary step involving the formation of CdH and an alkyl radical. The strength of the C−H bond in the paraffins is certainly higher than the 87 kcal. excitation energy of the cadmium atom, so that the above reaction is possible only because of the 15 kcal. heat of formation of CdH. In the case of ethylene the quenching apparently involves the double bond, and practically no photosensitized reaction occurs. With propylene it might be expected that reaction would occur by the mechanism

$$Cd(5^3P_1)+CH_3CH=CH_2$$
$$=CdH+CH_2CH=CH_2$$
$$\text{etc.}$$

[14] D. J. LeRoy and E. W. R. Steacie, J. Chem. Phys. 10, 683 (1942).

analogous to the reaction with propane. Actually, virtually no photosensitized reaction occurred. Apparently quenching occurs again at the double bond by a mere transfer of energy. The 87 kcal. thus received is then incapable of causing reaction since even if it is transferred internally to a C−H bond it is insufficient to rupture it. The photosensitization experiments thus provide a very clean-cut example of the difference between the two quenching mechanisms.

Quenching of λ2288

For comparison with the above results and for photochemical reasons it would be of considerable interest to have data on the quenching of the lower cadmium resonance line λ2288. This is, however, very difficult to investigate. The 5^1P_1 state has a life of only 2×10^{-9} sec., i.e. about 1200 times less than that of the 5^3P_1 state. Hence, other things being equal, the actual quenching will be 1200 times smaller for a given value of σ_Q^2. Appreciable quenching will thus only be obtained at high foreign gas pressures where pressure broadening will introduce large errors, or at relatively high cadmium vapor pressures where imprisonment will come into play.

In order to avoid imprisonment effects, it is necessary to work at low cadmium vapor pressures since the absorption coefficient of the line is very large. A few experiments were made with hydrogen and with ethylene at cadmium vapor pressures corresponding to temperatures from 245°C to 170°C. The apparent quenching fell off with the cadmium vapor pressure throughout the whole range. All that may be concluded from the results is that the quenching cross sections for ethylene and hydrogen are not greater than those with λ3261, and are probably somewhat less.

In order to obtain relative values which might be of some use, at least for photochemical purposes, a few measurements were made under comparable conditions for C_2H_4, C_3H_8, and H_2 at 245°C. If it is assumed that imprisonment effects will be identical in all three cases, the quenching cross sections for the three gases are roughly in the ratio

$$C_2H_4 : H_2 : C_3H_8=1 : 1 : 3.$$

The Transference Numbers of Potassium Bromide in Aqueous Solution at 25°C

A. G. KEENAN AND A. R. GORDON
Chemistry Department, University of Toronto, Toronto, Canada

(Received January 14, 1943)

The transference numbers for aqueous solutions of potassium bromide at 25°C have been determined by the moving boundary method. Cells with cadmium bromide and lithium bromide as cation indicators and with potassium iodate as anion indicator were employed. The measurements are more difficult than with potassium and sodium chlorides; with sheared junctions, a thorough investigation of the effect of indicator concentration is necessary for each solution studied, and the same is true with both sheared and autogenic boundaries of the effect of current density. The results differ slightly from those previously reported by Longsworth, but are consistent with the known value of t_+^0. Potassium bromide also differs from the alkali chlorides and acetates in that the Longsworth function $t_+^{0'}$ is not linear in the concentration, thus precluding an independent extrapolation of the transference data.

THIS research was originally undertaken to provide for potassium bromide transference numbers covering a range of temperature analogous to those reported from this laboratory for potassium chloride[1] and sodium chloride.[2] In this way it was hoped to obtain from the recently reported conductances[3] for this salt an additional check on the limiting ionic mobilities.[4] The work has, however, been much interrupted, and moreover it has become evident that unlike the alkali chlorides and acetates,[5] potassium bromide does not permit an unambiguous extrapolation of the transference data *per se*. We therefore report briefly our results for 25° since these differ somewhat from the existing transference numbers for this salt reported in the literature.

The experimental technique[1,2] and the method of preparation of the potassium bromide solutions[3] have already been adequately described. Autogenic cation boundaries with cadmium bromide as indicator (Cell II), sheared anion boundaries with potassium iodate as indicator (III), and falling cation boundaries with lithium bromide as indicator (IV) were employed. It was found that while autogenic boundaries were satisfactory up to 0.07 N, at 0.10 N it was impossible to obtain reproducible results; thus, while at the lower concentrations the values of t_+ for a run showed no progression as the boundary moved up the tube, and were within experimental error independent of the current used,[6] at tenth normal this was no longer the case. This behavior was apparently associated with the appearance of a heavy syrupy liquid layer above the cadmium anode, and no current density which still gave a visible boundary was sufficiently low to prevent its appearance. It was for this reason that falling LiBr boundaries were used for this solution. As is well known, such falling boundaries require careful adjustment of indicator concentration within narrow limits, but if this condition obtains, the resulting transference numbers are highly reproducible.[7]

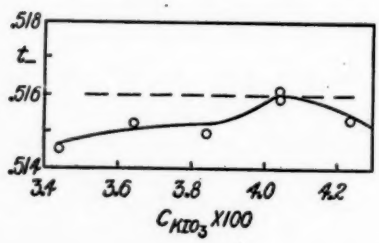

FIG. 1.

[1] R. W. Allgood, D. J. LeRoy, and A. R. Gordon, J. Chem. Phys. **8**, 418 (1940).
[2] R. W. Allgood and A. R. Gordon, J. Chem. Phys. **10**, 124 (1942).
[3] H. E. Gunning and A. R. Gordon, J. Chem. Phys. **11**, 18 (1943).
[4] H. E. Gunning and A. R. Gordon, J. Chem. Phys. **10**, 126 (1942).
[5] D. J. LeRoy and A. R. Gordon, J. Chem. Phys. **6**, 398 (1938), **7**, 314 (1939).

[6] For example, the first and third entries at 0.07 N in Table I were run at 1.6 ma, while the second and fourth were run at 1.2 and 0.4 ma, respectively.
[7] The lithium bromide concentration used to obtain the entries in Table I was 0.069 normal; the first two entries were run at 2.3 ma and the third at 1.6. At lower indicator concentrations, e.g., at 0.065 N, the measured t_+ is low and tends to increase as the boundary moves down the

The measurements on anion boundaries with potassium iodate as indicator also lead to a rather surprising result. With potassium chloride solutions, MacInnes and Longsworth[8] found (and measurements in this laboratory[1] confirmed them) that the measured t_- was independent of indicator concentration within wide limits. In contrast, Fig. 1 shows the effect of indicator concentration for KBr/KIO_3 boundaries at 0.05 N; in all the experiments, the current was the same (1.6 ma) and it is apparent that only at

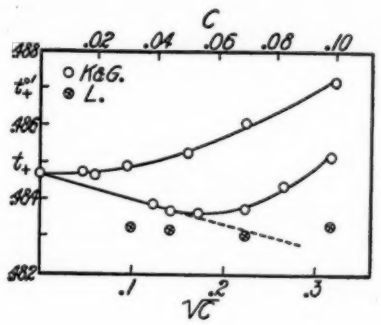

FIG. 2.

$C_{KIO_3}=0.0405$ N does t_- equal $1-t_+$ (indicated by the dotted line in the figure). Moreover, it is only for this indicator concentration that the observed t_- is independent of the current—a run at 0.95 ma giving $t_-=0.5162$. The results for 0.03 N were similar to those indicated in the figure, while for 0.07 and 0.10 N we were unable at any indicator concentration to obtain anion transference numbers independent of the current.

It would therefore seem that with potassium bromide absence of progression in the measured transference number as the boundary moves is not of itself conclusive evidence as to the reliability of the result. We therefore suggest, as a routine precaution in future investigations of other electrolytes, that the effect of changing the current and (with sheared junctions) of changing the indicator concentration should be studied for each solution, and that where possible both t_+ and t_- should be measured.

The results are given in Table I as a function of the concentration in moles per liter; the solvent and volume corrections[8] are listed in the fourth column. The latter[9] is given by $-C\Delta V/1000$ where

Cell II	$\Delta V=-\frac{1}{2}V_{Cd}+\frac{1}{2}\bar{V}_{CdBr_2}-t_+\cdot\bar{V}_{KBr}$
Cell III	$\Delta V=+\frac{1}{2}V_{Cd}-\frac{1}{2}\bar{V}_{CdBr_2}+t_+\cdot\bar{V}_{KBr}$
Cell IV	$\Delta V=V_{Ag}-V_{AgBr}+t_+\cdot\bar{V}_{KBr}$

since in both cells II and III the cadmium anode forms the closed side of the cell, while in Cell IV the silver-silver bromide cathode is the closed

TABLE I.

Cell	C	$t_\pm$ obs.	Sol.+Vol. Corr.	$t_\pm$	t_+
II	0.014980	0.4835	+0.0004	0.4839	
II	.015057	.4834	+0.0004	.4838	0.4839
II	.019892	.4835	+0.0003	.4838	
II	.020169	.4833	+0.0003	.4836	0.4837
III	.029026	.5160	+0.0001	.5161	
III	.029933	.5164	+0.0001	.5165	
II	.029981	.4834	+0.0003	.4837	0.4837
II	.030081	.4835	+0.0003	.4838	
III	.049864	.5161	−0.0001	.5160	
III	.049970	.5163	−0.0001	.5162	
III	.049970	.5162	−0.0001	.5161	
II	.050168	.4834	+0.0003	.4837	0.4839
II	.050120	.4837	+0.0003	.4840	
II	.050120	.4836	+0.0003	.4939	
II	.050436	.4834	+0.0003	.4837	
II	.070293	.4842	+0.0004	.4846	
II	.069961	.4842	+0.0004	.4846	
II	.070136	.4838	+0.0004	.4842	0.4844
II	.070249	.4840	+0.0004	.4844	
IV	.099807	.4849	+0.0003	.4852	
IV	.099893	.4849	+0.0003	.4852	0.4852
IV	.099692	.4849	+0.0003	.4852	

tube; at higher indicator concentrations, there is no progression in the apparent t_+ but its value is again low. For both higher and lower indicator concentrations, the transference number depends on the current used. See also reference 13.

[8] D. J. MacInnes and L. G. Longsworth, Chem. Rev. **11**, 171 (1932).

[9] The volume correction for Cell III*a* of refreence 1 (p. 420) is incorrectly stated; ΔV is given by $V_{Ag}-V_{AgCl}+t_+\cdot\bar{V}_{KCl}$. This has the effect of making the volume corrections for the three strongest solutions at 25° which employed this cell +0.0001, so that the resulting t_- in the sixth column of Table I are 0.5099, 0.5101, and 0.5098 instead of 0.5098, 0.5100, and 0.5097 as printed.

TABLE II.

C	0.0005	0.001	0.002	0.005	0.010
t_+	0.4846	0.4845	0.4844	0.4843	0.4841
C	0.02	0.03	0.05	0.07	0.10
t_+	0.4838	0.4837	0.4838	0.4843	0.4852

TABLE III.

C	0	0.0005	0.001	0.002	0.005	0.010
$(\lambda^+)_{KBr}$	(73.52)	72.50	72.08	71.52	70.46	69.35
$(\lambda^+)_{KCl}$	73.52	72.48	72.06	71.48	70.40	69.27

side. To a close enough approximation, the volume corrections are given by $+0.004_1C$, -0.004_1C, and $+0.002_6C$ for cells II, III, and IV, respectively. The results are shown as a function of the square root of the concentration on the lower curve of Fig. 2, which also gives the previously reported data of Longsworth.[10] It is at once apparent that the difference between his results and ours is somewhat greater than the apparent precision of the experiments. This is disturbing in view of the excellent agreement between the results obtained in this laboratory for potassium and sodium chlorides and his 25° data for the two salts, and correspondence with Dr. Longsworth, to whom we wish to express our thanks, has failed to explain the discrepancy.

There is however some independent evidence. The limiting conductance[11] for potassium bromide, obtained by two entirely independent methods,[3,12] is 151.67; from this and the known limiting mobility of potassium ion[4] *viz.*, 73.52, t_+^0 is 0.4847, to which our transference data have been extrapolated. A glance at the figure will show the difficulty of extrapolating Longsworth's numbers to this value whereas ours for the lower concentrations actually lie on the theoretical limiting slope,[10] indicated by the dotted line in the figure; while we regard this as fortuitous, it nevertheless permits a reasonable extrapolation. Secondly, our result for 0.1 N is in good agreement with the earlier value reported by MacInnes and Smith[13] for this concentration *viz.*, 0.485. Finally, it might be added that the transference numbers reported here, when used in conjunction with e.m.f. measurements on cells with transference, lead to values of the activity and osmotic coefficients for potassium bromide solutions which by isopiestic comparison are in excellent agreement with the now well-established thermodynamic data for potassium and sodium chloride solutions.[14]

The upper curve in Fig. 2 shows the Longsworth function[1,2] $t_+^{0\prime}$, computed from our data, as a function of the concentration (indicated on the upper scale of the figure). This method of plotting has proven extremely useful with potassium and sodium chlorides and the corresponding acetates, but here the plot is definitely curved and thus does not give a satisfactory extrapolation to infinite dilution.

Table II gives t_+ for round values of C, corresponding to the continuous curves of Fig. 2, while Table III gives $(\lambda^+)_{KBr}$, obtained from Table II and the conductances.[3] The table also gives for comparison $(\lambda^+)_{KCl}$ obtained from Tables V and VI of reference 4. It is apparent that with increasing concentration there are deviations from the rule of independent ionic mobilities comparable with those found for chloride ion with potassium and sodium as cations (see Table VI of reference 4). There is however one difference; the anion chloride had the greater mobility with sodium, the slower cation, while here the cation potassium has the greater mobility with bromide, the faster anion. Whether this is of general significance or not, can only be settled by further experiment.

[10] L. G. Longsworth, J. Am. Chem. Soc. **57**, 1185 (1935).

[11] There is an obvious misprint in Table II of reference 3; the first three lines of the table should be labeled ϑ, σ and Λ_0.

[12] Grinnell Jones and C. F. Bickford, J. Am. Chem. Soc. **56**, 602 (1934).

[13] D. A. MacInnes and E. R. Smith, J. Am. Chem. Soc. **45**, 2246 (1923).

[14] A. S. Brown and D. A. MacInnes, J. Am. Chem. Soc. **57**, 1356 (1935); T. Shedlovsky and D. A. MacInnes, J. Am. Chem. Soc. **59**, 503 (1937); W. J. Hornibrook, G. J. Janz, and A. R. Gordon, J. Am. Chem. Soc. **64**, 513 (1942); G. J. Janz and A. R. Gordon, J. Am. Chem. Soc. **65**, 218 (1943).

The Influence of Hindered Molecular Rotation on the Dielectric Constants of Water, Alcohols, and Other Polar Liquids

GERALD OSTER AND JOHN G. KIRKWOOD
Baker Laboratory, Cornell University, Ithaca, New York
(Received January 7, 1943)

The theory of dielectric polarization of polar liquids is used to calculate the dielectric constants of water and some alcohols. Quasi-rigid coordination models, based upon x-ray structural investigations, are employed in the calculation of a function g which measures the orientational correlation between neighbors in the liquid. It is pointed out that the correlation function g is closely related to the thermodynamic "abnormality" of polar liquids.

INTRODUCTION

In an earlier article a general theory of the dielectric polarization of polar liquids was formulated.[1] The role of hindered molecular rotation was clarified and it was shown how correlation in the orientation of neighboring molecules might augment or diminish the contributions of the individual molecular dipoles to the dielectric constant of a liquid.

In the present article, we shall discuss some applications of the theory to water, the aliphatic alcohols, and certain other hydrogen bonded liquids. On the basis of simplified but reasonable models of the local structure maintained by each molecule in its environment by hydrogen bonding with its neighbors, we are able to calculate the dielectric constants of these liquids with some degree of success. Due to strong orientational correlation, the effect of the individual molecular dipoles is greatly enhanced. This circumstance makes it possible for water and the alcohols to have dielectric constants considerably greater than those of certain other polar liquids the molecules of which possess dipole moments of comparable magnitude.

According to our theory of dielectric polarization, the dielectric constant ϵ of a liquid is related to the polarization P_0 by the equation

$$(\epsilon-1)/3=[3\epsilon/(2\epsilon+1)]P_0/v \qquad (1)$$
$$P_0=(4\pi N/3)[\alpha+(\boldsymbol{\mu}\cdot\bar{\boldsymbol{\mu}}/3kT)],$$

where v is the molal volume, α the optical polarizability, N Avogadro's number, and kT the product of Boltzmann's constant and the absolute temperature. In the scalar product $\boldsymbol{\mu}\cdot\bar{\boldsymbol{\mu}}$, $\boldsymbol{\mu}$ is the molecular dipole moment and $\bar{\boldsymbol{\mu}}$ is the sum of the molecular dipole moment and the average electric moment induced by the molecule in its environment by hindering the rotation of its neighbors relative to itself. When P_0/v is large compared with unity, Eq. (1) may be simplified to

$$\epsilon-1=(9/2)(P_0/v) \qquad (2)$$

and the dielectric constant becomes proportional to the density of the liquid.

WATER

If the orienting effect of a water molecule is assumed to extend only to its first shell of neighbors and if the region of exclusion of the first coordination shell is roughly spherical, the product $\boldsymbol{\mu}\cdot\bar{\boldsymbol{\mu}}$ may be expressed in the form

$$\boldsymbol{\mu}\cdot\bar{\boldsymbol{\mu}}=g\mu^2,$$
$$g=1+z(\cos\gamma)_{Av}, \qquad (3)$$

where z is the average number of neighbors in the first coordination shell. The coordination number z may be estimated from the area under the first peak of the radial distribution function of the liquid. These approximations will be employed in the calculation of the dielectric constant of water.

We shall assume water to be approximately tetrahedrally coordinated in accordance with the Bernal-Fowler model.[2] A directed hydrogen bond about which there is free rotation but no bending is assumed to exist between neighboring molecules. The bond is assumed to be directed along

[1] J. G. Kirkwood, J. Chem. Phys. **7**, 911 (1939); L. Onsager, J. Am. Chem. Soc. **58**, 1486 (1936).

[2] J. D. Bernal and R. H. Fowler, J. Chem. Phys. **1**, 515 (1933).

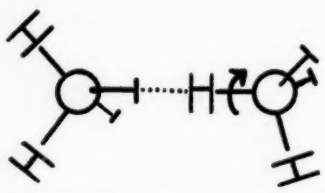

FIG. 1. Hydrogen bonding in water. Free rotation is assumed about the hydrogen bond between adjacent water molecules. The short dashes indicate regions of negative charge and are in a plane perpendicular to the H—O—H plane.

the O—H bond of the one molecule toward the oxygen atom of the second molecule passing through the concentration of negative charge due to one of the non-bonding $2p$ electrons of the latter, as exhibited in Fig. 1. With this quasi-rigid model of the local structure, we calculate

$$(\cos\gamma)_{Av}=\cos^2\frac{\theta}{2},\quad g=1+z\cos^2\frac{\theta}{2},\qquad(4)$$

where θ is the $\mathrm{O}\langle^{\mathrm{H}}_{\mathrm{H}}$ bond angle in the water molecule, which we take to be 105°, the best spectroscopic value. The dipole moment μ of a water molecule in the liquid differs from its moment μ_0 in the vapor due to induction of an additional moment by the dipole field of its neighbors. If α is the polarizability of the water molecule, we have approximately

$$\mu=\mu_0\Big/\left[1-\left(2\alpha z\cos^2\frac{\theta}{2}\Big/a^3\right)\right],\qquad(5)$$

where a is the distance between neighbors.

We are now able to estimate the dielectric constant of water with the aid of Eqs. (2), (4), and (5). The coordination number z and the intermolecular distance a are available from the x-ray scattering data of Morgan and Warren.[3] In the temperature range, 0°C to 83°C, the average coordination numbers are non-integral, lying between 4 and 5. Although non-integral coordination numbers exceeding 4 are not entirely consistent with our simplified model of the neighbor structure, we shall nevertheless employ them in the calculation. This is equivalent to approximating $(\cos\gamma)_{Av}$ by $\cos^2\theta/2$ for small deviations from the tetrahedrally coordinated structure.

In Table I the theoretical values of the dielectric constant of liquid water are compared with the experimental values of Wyman.[4] The agreement between the theoretical and experimental values of the dielectric constant is remarkably close at 25°C. At 83°C, the values differ by about 13 percent. In view of the obvious limitations of the model of local structure upon which the theoretical values are based, the agreement may be considered satisfactory.

We remark that the experimental values of g decrease with increasing temperature whereas the theoretical values increase. This trend is in accord with failures of the simple model which might be expected. A partial destruction of the tetrahedrally coordinated structure would naturally tend to decrease the correlation in orientation of neighbors and thus diminish $(\cos\gamma)_{Av}$. Bending of the hydrogen bond would have the same effect and would be expected to be more pronounced the higher the temperature.

ALIPHATIC ALCOHOLS

The structure of the liquid alcohols has been extensively investigated by the x-ray scattering technique.[5] These investigations have led to the conclusion that the average coordination number of a molecule is 2. It has therefore been suggested that the molecules are arranged in chains by means of hydrogen bonds.

TABLE I. The dielectric constant of liquid water.

t(°C)	v	z	a(A)	g(obs.)	g(calc.)	ϵ(obs.)	ϵ(calc.)
0	18.02	4.4	2.90	2.75	2.63	88.0	84.2
25	18.07	4.5	2.92	2.68	2.67	78.5	78.2
62	18.34	4.9	3.00	2.56	2.82	66.1	72.5
83	18.58	4.9	3.05	2.49	2.82	59.9	67.5

$\theta=105°$; $\alpha=1.5\mathrm{A}^3$ (constant over temperature range); $\mu_0=1.88\times10^{-18}$ e.s.u.

Cole[6] has discussed the application of the present theory to the liquid alcohols, which we wish to elaborate here. We shall assume that each

[3] J. Morgan and B. E. Warren, J. Chem. Phys. **6**, 666 (1938).

[4] J. Wyman, Jr., Phys. Rev. **35**, 623 (1930).

[5] W. H. Zachariasen, J. Chem. Phys. **3**, 158 (1935); G. G. Harvey, J. Chem. Phys. **7**, 878 (1939); Pierce and MacMellan, J. Am. Chem. Soc. **60**, 779 (1938). See also L. Pauling, *Nature of the Chemical Bond* (Cornell University Press, Ithaca, 1940), second edition, p. 305.

[6] R. H. Cole, J. Chem. Phys. **9**, 251 (1941).

alcohol molecule is a member of an infinite chain and is correlated in orientation only with members of its own chain. We shall further suppose that the average configuration of a specified chain, due to curling up by internal rotation, is approximately spherical. Directed hydrogen bonds of the type existing in water are assumed to link each alcohol molecule with its two nearest neighbors in the chain, as exhibited in Fig. 2. Free rotation around the hydrogen bonds is allowed, but bending is excluded.

For chainwise coordination, the factor g becomes

$$g=1+2\sum_{n=1}^{\infty}(\cos\gamma_n)_{Av}, \tag{6}$$

where γ_n is the angle between the dipole moments of a molecule and a chain neighbor separated from it by n bonds. On the basis of our assumptions concerning the hydrogen bond, we may calculate[7]

$$(\cos\gamma_n)_{Av}=f\left(\cos^2\frac{\theta}{2}\right)^n,$$
$$f=\frac{(\mu_H+\mu_R)(\mu_H+\mu_R\cos\theta)}{[\mu_H^2+\mu_R^2+2\mu_R\mu_H\cos\theta]}, \tag{7}$$

where μ_H and μ_R are the components of the dipole moment of the alcohol molecule ROH along the O−H and O−R bonds, respectively, and θ is the bond angle, taken to be 105°. For the infinite chain we obtain by summation of the series resulting from the substitution of Eq. (7) into Eq. (6)

$$g=1+2f\cot^2(\theta/2). \tag{8}$$

TABLE II. Dielectric constants of the normal alcohols at 20°C.

	v	n	g(obs.)	g(calc.)	ϵ(obs.)	ϵ(calc.)
Methyl alcohol	40.4	1.33	2.94	2.57	32.8	29.2
Ethyl alcohol	58.3	1.36	3.04	2.57	24.6	21.3
n-Propyl alcohol	75.5	1.38	3.07	2.57	19.5	17.3
n-Butyl alcohol	91.5	1.40	3.21	2.57	18.0	14.6
n-Amyl alcohol	108.0	1.41	3.43	2.57	15.8	12.8

$\theta=105°$; $\mu=1.70\cdot10^{-18}$; $\mu_R=0.7\cdot10^{-18}$; $\mu_H=1.6\cdot10^{-18}$.

In order to estimate f, we use the bond dipole moments which have been assigned to methyl alcohol in the vapor phase.[8] In order to estimate the ratio of liquid dipole moment μ to the vapor dipole moment μ_0, we employ Onsager's[9] sphere formula

$$\mu=\frac{2\epsilon+1}{2\epsilon+n^2}\,\frac{n^2+2}{3}\mu_0, \tag{9}$$

where n is the optical refractive index. The use

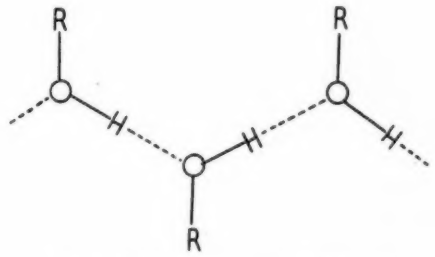

FIG. 2. Hydrogen bonding in alcohol.

of Eq. (9) in the liquid alcohols is somewhat questionable, since the model on which it is based scarcely applies. However, it serves for a rough estimate of the induction effect from neighbors on the dipole moment of a given molecule, and a detailed calculation of the dipole field from chain neighbors is more complicated than the limitations of our idealized coordination model justifies.

In Table II the theoretical values of the dielectric constants of several of the normal aliphatic alcohols are compared with the observed dielectric constants.[10] The agreement with experiment is not as good as in the case of water. It is, however, remarkably good in view of the limitations of the assumed model of local structure. The fact that the experimental value of g exceeds the theoretical value suggests that there is a residual correlation in the orientations of molecules in different chains. It will be observed that the experimental correlation parameter increases with increasing chain length in the case of the normal alcohols.

[7] Fuoss and Kirkwood, J. Am. Chem. Soc. **63**, 390 (1941).

[8] Eucken and Meyer, Physik. Zeits. **30**, 397 (1929).

[9] L. Onsager, J. Am. Chem. Soc. **58**, 1486 (1936).

[10] Dielectric constants and dipole moments values mainly from P. Debye and Sack, *Tables Annuelles de Constantes et Donnees Numeriques*, Volume XI, Booklet 2 (1937); Volume XII, Booklet 32 (1939). Refractive indices and densities from *International Critical Tables*.

TABLE III. Correlation parameter of ethyl alcohol as a function of temperature.

t(°C)	g(observed)
−90	3.33
−30	3.24
20	3.03
70	2.84

TABLE IV. Influence of organic radical on the correlation parameter of an alcohol ROH at 20°C.

	g(observed)
Secondary butyl alcohol	2.83
Tertiary butyl alcohol	2.38
Isobutyl alcohol	3.36
Benzyl alcohol	2.08

The correlation parameter g differs very little for the several alcohols. It is interesting to examine the effect of temperature and the effect of the organic radical on this parameter. In Table III the experimental value of g for ethyl alcohol is presented as a function of temperature. As one would expect, g decreases with increasing temperature. In Table IV, the effect of the organic radical on the correlation parameter of the alcohols is exhibited. Here there does not appear to be any striking regularity in the manner in which the organic radical influences orientational correlation. It is, of course, reasonable that g should be low for tertiary butyl alcohol, since steric interference with hydrogen bond formation is likely.

OTHER POLAR LIQUIDS

The correlation parameter g is a useful index to the degree of hindered rotation in a liquid. Polar liquids possessing values of g differing appreciably from unity form a class which is frequently, although perhaps unfortunately, designated as the class of associated liquids. Polar liquids with a value of g near unity fall into the class of normal liquids. As a basis for classification of liquids according to their thermodynamic behavior, it appears that the correlation parameter g is more significant than the molecular dipole moment.

TABLE V. Correlation parameters of several polar liquids.

	t(°C)	$\mu_0 \cdot 10^{18}$	ϵ(observed)	g(observed)
Hydrogen cyanide	20	2.80	116	4.1
Hydrogen fluoride	0	(1.8)*	83.6	3.1
Hydrogen peroxide	0	2.13	91	2.8
Ammonia	15	1.48	17.8	1.3
Ethyl ether	20	1.15	4.4	1.7
Acetone	20	2.85	21.5	1.1
Nitrobenzene	20	3.90	36.1	1.1
Ethyl bromide	20	1.80	9.4	1.1
Pyridine	20	2.20	12.5	0.9
Benzonitrile	25	3.90	25.2	0.8

* Estimate by L. Pauling, *Nature of the Chemical Bond*, p. 292.

Orientational correlation is determined not by the molecular dipole moment alone, but also by the location of the permanent charge distribution in the interior of a polar molecule. When the charge distribution is exposed, as in the molecules of hydrogen bonded liquids, neighbors can assume relative configurations in which there is very strong interaction. When the charge distribution is shielded, as in nitrobenzene, such configurations are excluded by intermolecular repulsive forces, and orientational correlation is not great.

In Table V, the correlation parameter is presented for a series of polar liquids. No attempt will be made at the present time to interpret g on the basis of specific structural models, although this offers interesting possibilities in several instances. For a more comprehensive survey of the data for other liquids, the reader is referred to an article by J. N. Wilson.[11]

[11] J. N. Wilson, Chem. Rev. **25**, 377 (1939).

Diffraction of X-Rays by Sodium Stearate at Room Temperature*

JAMES W. McBAIN, ALEXANDER DE BRETTEVILLE, JR., AND SYDNEY ROSS
Department of Chemistry, Stanford University, Stanford University, California

(Received June 22, 1942)

The alpha-form of sodium stearate, originally reported by Thiessen and Stauff, and of which a sample was made available to us, has been re-examined and the data found to be in general conformity with those of the previous investigation. Re-examination of their monoclinic beta-form of sodium stearate, obtained by heating the rhombic form above 54°C, yields a different set of data. A new, more stable, monoclinic form of sodium stearate has been examined and designated as the gamma-form.

EVER since 1923 when the x-ray study of soap systems was begun at Bristol University,[1] it has been recognized that this approach gives invaluable information. Such work has become more urgent since in the last few years it has been found that every soap exists in a large number of forms, only some of which are typically crystalline or liquid crystalline. Even isotropic solutions in water show spacings corresponding to lamellar micelles.[2] Nearly two dozen papers dealing with the x-ray examination of soap systems have now appeared, coming from many laboratories.

As a preliminary to an extensive investigation of soap systems by means of x-ray diffraction, being carried out at Stanford University, it was necessary to review the material already published. Of this the paper by Thiessen and Stauff[3] on crystalline forms of sodium stearate and sodium palmitate at room temperature has gone furthest towards presenting a complete x-ray analysis of these substances. This valuable and important paper is marred by a number of numerical errors, so that significant revision is here suggested.[4] The present paper contains further data on the alpha- and two monoclinic forms of sodium stearate, beta- and gamma-. By courtesy of Dr. J. Stauff of Berlin the authors were able to obtain, through Dr. Vold, a sample of the alpha-sodium stearate actually used in the first investigation, so that there is no doubt but that the present paper deals with some of the very same specimen that was examined by Thiessen and Stauff.

MATERIALS

Two samples of alpha-sodium stearate were available, one (*A*) originating from Kahlbaum purified by Dr. J. Stauff in Berlin, and the other (*B*) prepared by Dr. R. D. Vold in this laboratory from Eastman stearic acid No. 402. The alpha-crystals are obtained by slow crystallization from 1 percent solution in 95 percent ethyl alcohol and subsequent drying in air. The monoclinic beta-form was obtained from the alpha-form in both cases by heating the latter above 54°C. On cooling, no trace of the original alpha-form was to be found.

The new γ-monoclinic form was prepared by merely melting and cooling the soap. Stearate prepared from stearic acid Kahlbaum[5] and from Eastman stearic acid No. 402 was employed.

METHOD

The radiation was supplied by a copper-target, water-cooled x-ray tube made by Mr. J. F. Lee and purchased through a grant from the Cyrus M. Warren Fund of the American Academy of Arts and Sciences. The tube was operated at 28 kv, with a current of 28 ma. The radiation was filtered through nickel foil to make it es-

* This manuscript was first completed for publication on November 6, 1940; cf. reference 6.

[1] S. H. Piper and E. N. Grindley, Proc. Phys. Soc. London **35**, 269 (1923).

[2] K. Hess and J. Gundermann, Ber. **70**, 1800 (1937); Hess, Kiessig, and Philippoff, Naturwiss. **26**, 184 (1938); Hess, Philippoff, and Kiessig, Kolloid Zeits. **88**, 40 (1939); J. Stauff, Naturwiss. **27**, 213 (1939); H. Kiessig and W. Philippoff, *ibid.* 594 (1939).

[3] P. A. Thiessen and J. Stauff, Zeits. f. physik. Chemie **A176**, 397 (1936).

[4] They themselves have published a subsequent note, Zeits. f. physik. Chemie **A177**, 398 (1936), correcting a very few of the numerical errors and admitting that their published analysis of the monoclinic form is no longer in complete agreement with all the measurements, including new and improved but unpublished data.

[5] McBain, Vold, and Frick, J. Phys. Chem. **44**, 1014 (1940).

TABLE I. Comparison of x-ray diffraction lines for alpha-sodium stearate.

Results of Thiessen and Stauff, from rotation photographs				Results of present investigation, from powder photographs					
hkl	$\sin^2\theta$ calc.*	$\sin^2\theta$ obs.	Int.	*hkl*	$\sin^2\theta$ calc.	*d/n* A	$\sin^2\theta$ (*A*)	$\sin^2\theta$ (*B*)	Int.
002	0.00089	0.00085	m.	002	0.00087	26.1	0.00093	0.00089	m.
003	0.00200	0.00199	s.	003	0.00197	17.4	0.00187	0.00201	m.
004	0.00355	0.00360	m.	004	0.00349	13.0	0.00344	0.00347	w.
005	0.00555	0.00553	s.	005	0.00546	10.4	0.00567	0.00547	w.
007	0.0109	0.0108	m.						
008	0.0142	0.0140	w.						
009	0.0180	0.0184	w.						
110	0.0161	0.0159	v.w.						
150	0.1826	0.0198	v.w.						
020	0.0277	0.0278	v.s.	020	0.0279	4.60	0.0280	0.0279	v.s.
023	0.0297	0.0299	w.	023	0.0299	4.55	0.0305	0.0305	v.w.
200	0.0366	0.0365	v.s.	200	0.0368	4.01	0.0371	0.0369	v.s.
120	0.0369	0.0370	m.	120	0.0371	3.99			
203	0.0386	0.0386	m.						
123	0.0389	0.0386	v.w.						
205	0.0422	0.0422	w.						
125	0.0425	0.0420	v.w.						
				210	0.0438	3.67	0.0440	0.0438	v.s.
210	0.0436	0.0474	v.s.	207	0.0475	3.53		0.0468	v.w.
207	0.0475	0.0481	v.w.						
213	0.0456	0.0493	m.	215	0.0492	3.47	0.0508	0.0509	m.
215	0.0491	0.0529	w.	216	0.0516	3.39			
217	0.0545	0.0580	v.w.						
220	0.0644	0.0642	s.	220	0.0647	3.02	0.0643	0.0644	s.
223	0.0664	0.0699	w.						
130	0.0716	0.0718	w.	130	0.0720	2.87	0.0723	0.0721	w.
225	0.0699	0.0736	v.w.						
310	0.0894	0.0829	m.	229	0.0824	2.67		0.0824	v.w.
				310	0.0897	2.56	0.0912	0.0900	w.
				312	0.0906	2.55			
				315	0.0952	2.49		0.0941	w.
230	0.0991	0.0985	s.	230	0.0995	2.44	0.0995	0.0997	s.
233	0.1011	0.1010	w.						
235	0.1046	0.1040	w.						
320	0.110	0.107	m.						
323	0.112	0.109	v.w.	323	0.113	2.28			
237	0.1099	0.1102	v.w.	237	0.110	2.32	0.111	0.110	w.
040	0.111	0.111	m.	040	0.112	2.30			
325	0.116	0.117	v.v.w.	325	0.116	2.26		0.116	w.
239	0.1171	0.1175	v.w.	239	0.117	2.25			
043	0.1130	0.1213	w.						
140	0.1201	0.1215	v.w.						
410	0.1535	0.135	m.	145	0.126	2.16	0.125	0.125	v.w.
240	0.1476	0.1480	m.	240	0.148	2.00	0.149	0.148	v.w.
				410	0.154	1.96	0.155	0.154	m.
420	0.174	0.176	m.	420	0.175	1.84	0.177	0.175	w.
430	0.209	0.202	w.	430	0.210	1.68	0.206	0.206	v.v.w.
				447	0.269	1.48	0.271	0.268	w.
				543	0.343	1.32	0.345	0.341	v.w.
				620	0.359	1.28	0.362	0.369	v.w.
				630	0.394	1.22		0.397	v.w.

* Many of these values are corrected to their own equation as published by them, although their equation does not completely accord with the data for the unit cell from which it was deduced. It will be noted that the recalculated data in many cases no longer fit the observed data.

sentially monochromatic. A circular camera of 57.2-mm radius[5a] was used to obtain the short spacings and a flat plateholder at distances up to 250 mm to resolve the long spacings. The data were scrutinized to ensure that no tungsten or Cu $K\beta$ lines were included in the tables.

[5a] A. de Bretteville, Jr., Rev. Sci. Inst. **13**, 481 (1942).

ALPHA-FORM OF SODIUM STEARATE

Both samples of the alpha-sodium stearate as observed by us in 1940[6] gave x-ray diffraction lines that agreed in position with each other and

[6] A. de Bretteville, Jr., Ph.D. thesis, Stanford University, 1941; obtainable in bibliofilm from the U. S. Department of Agriculture.

TABLE II. Comparison of x-ray diffraction lines for beta-monoclinic sodium stearate.

Results of Thiessen and Stauff, from rotation photographs				Results of present investigation, from powder photographs					
hkl	$\sin^2\theta$ calc.*	$\sin^2\theta$ obs.**	Int.	*hkl*	$\sin^2\theta$ calc.	d/n A	$\sin^2\theta$ (*A*)	$\sin^2\theta$ (*B*)	Int.
002	0.00111	0.00112	m.	002	0.00109	23.3	0.00103	0.00119	s.
003	0.00251	0.00246	s.	003	0.00245	15.5	0.00253	0.00238	v.s.
004	0.00446	0.00383	m.	004	0.00435	11.7	0.00462	0.00436	w.
005	0.00697	0.00696	s.	005	0.00679	9.32	0.00690	0.00705	m.
006	0.0100	0.0103	w.						
007	0.0137	0.0130	m.	007	0.0133	6.66	0.0131	0.0136	w.
110	0.0333	0.0335	v.s.	110	0.0321‡	4.29	0.0331	0.0334	v.s.
200	0.0496	0.0498	v.s.	200	0.0393	3.88	0.0393	0.0392	v.s.
203	0.0418	0.0520	w.						
				$20\bar{4}$	0.0553	3.27		0.0540	v.w.
				210	0.0616	3.09	0.0600	0.0588	w.
				$21\bar{4}$	0.0775	2.76	0.0761	0.0774	w.
020	0.0835	0.0851	s.	020	0.0891	2.57		0.0894	v.v.w.
205	0.0393	0.0975	v.w.						
206	0.0390								
310	0.132	0.131	w.	310	0.111	2.31	0.112	0.112	w.
400	0.198	0.192	s.						
				$40\bar{5}$	0.193	1.75	0.189	0.189	v.w.
220	0.133	0.212	m.						
				330	0.289	1.43	0.273	0.289	v.w.
				$33\bar{3}$	0.304	1.39	0.309		v.w.
				$33\bar{5}$	0.317	1.36	0.317	0.313	v.w.
040	0.334	0.346	m.						
023	0.0860	0.888	w.						
024	0.0879								

* These values are corrected by us according to their revised equation, $1/d^2=0.0209h^2+0.0352k^2+0.00047l^2-0.0029hl$, to agree with their unit cell dimensions.
** As tabulated by Thiessen and Stauff.
‡ In other photographs this value has been observed as 0.0324, and as low as 0.031.

with the positions reported by Thiessen and Stauff.[3] Because of certain arithmetical errors in the published results it is deemed advisable to print a table of indices in which the $\sin^2\theta$ values calculated from their equation are corrected. The first three columns of Table I reprint the data of Thiessen and Stauff with these corrections. The last five columns report the data obtained by the present authors and a suggested table of indices, some of which differ from those assigned by Thiessen and Stauff. Although these changes are based solely on powder diagrams, they provide in general a better agreement between calculated and observed values, until a more advanced technique has been applied. The equation used to calculate the $\sin^2\theta$ values for the powder photographs is based on the mean of three experimental values, including that of Thiessen and Stauff, for the 200 plane, the 020 plane and the 00*l* planes. The equation is

$$\sin^2\theta=0.009194h^2+0.006974k^2+0.0002184l^2.$$

The column headed (*A*) gives the experimentally determined values of $\sin^2\theta$ for the sample obtained from Dr. Stauff, and that headed (*B*) gives the values for the sample obtained from Dr. Vold. We have not suggested indices for lines not obtained from these two powder photographs.

The dimensions of the unit cell, as reported by Thiessen and Stauff, are $a=8.04$A, $b=9.12$A, and $c=51.77$A. Their equation yields $a=8.04$A, $b=9.24$A, and $c=51.6$A. The calculated density for exactly eight molecules in the unit cell is 1.057. The density measured by them by immersion in xylene was 1.0361. The mean values used in obtaining our equation are $a=8.03\pm0.03$A, $b=9.22\pm0.02$A, and $c=52.1\pm0.3$A. The calculated density is then 1.052.

THE BETA-MONOCLINIC FORM OF SODIUM STEARATE

In a supplementary note[4] to their original paper, Thiessen and Stauff revised the monoclinic equation for sodium stearate, but still based it on their previously published dimensions of the unit cell. When either equation is used to test the suggested indices for the observed spacings they are found to be inconsistent with their tables, and, accordingly, a new investiga-

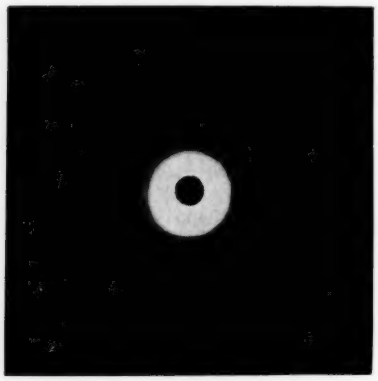

FIG. 1. Long spacings of the γ-form of monoclinic sodium stearate; flat plate 125 mm from sample.

FIG. 2. Powder photograph of the γ-form of monoclinic sodium stearate; flat plate 45 mm from sample.

tion of their beta-monoclinic form was required. This was undertaken on the two samples that were available, one (*A*) obtained from the alpha-form prepared by Thiessen and Stauff and the other (*B*) from the alpha-form prepared by Dr. Vold. In both cases the beta-monoclinic form was prepared from the alpha by heating the latter somewhat above 54°C.

The most significant revision of the data for the beta-monoclinic form concerns the directly observed position of one of the two very strongest lines. This line, indexed by Thiessen and Stauff as 200, is recorded as $\sin^2\theta=0.0498$, whereas we fail to observe any diffraction effect at that position. Instead we obtain a very strong line at $\sin^2\theta=0.0393$, not reported by them. Those two lines are matched by virtue of their intensities, and also by measurement of their actual photograph (Fig. 12), and we conclude* that the real position of the 200 diffraction effect is at $\sin^2\theta=0.0393$.

We have made use of Thiessen and Stauff's oscillation photograph, Fig. 12, in assigning indices. On inspection Fig. 12 exhibits imperfect orientation in the sample. Not all spots seen on the equator have $h0l$ indices; because they can be traced by a continuous line, of constant $\sin\theta$, to more intense spots on the first layer.

* The interesting suggestion has been made to us that possibly their Fig. 12 was obtained by Fe $K\alpha$ radiation at a crystal to plate distance of 37.8 mm, and that, therefore, their beta-form was not that here found. However, if so, the strongest line in Fig. 12 finds no place in their table, and the results would not agree with the values given by Thiessen and Stauff for the dimensions of the unit cell; nor would the results agree with our data. If taken as we assume with Cu $K\alpha$ radiation their Fig. 12 agrees with our data.

Conversely, some of the spots appearing on the first layer are similarly traced to more intense ones on the equator.

Table II presents the data of Thiessen and Stauff for the beta-form of monoclinic sodium stearate, together with the result of the present investigation.

Our equation for the beta-monoclinic form is

$$\sin^2\theta=0.009824h^2+0.02227k^2+0.0002717l^2-0.001454hl.$$

The monoclinic angle β can be derived from the ratio of the measured value of $c\sin\beta$ to the theoretical length 52.4A for the double molecule

TABLE III. Powder diffraction data for the new gamma-form of monoclinic sodium stearate, prepared by melting and allowing to cool.

$\sin^2\theta$ (Kahlbaum)	d/n A	Int.	$\sin^2\theta$ (Eastman)	d/n A	Int.
0.000333	42.2	v.s.		($n=1$)	
0.00119	22.3	m.	0.00125	21.8 ($n=2$)	s.
0.00274	14.7	s.	0.00266	14.9 ($n=3$)	v.s.
			0.00436	11.7 ($n=4$)	w.
0.00765	8.80	m.	0.00728	9.02($n=5$)	m.
			0.0120	7.03($n=6$)	v.w.
0.0142	6.46	w.		($n=7$)	
0.0266	4.72	v.w.	0.0262	4.74	w.
0.0288	4.54	s.	0.0286	4.54	s.
0.0334	4.21	v.w.	0.0333	4.21	w.
0.0371	4.00	v.v.s.	0.0366	4.02	s.
			0.0392	3.88	s.
0.0524	3.36	v.w.	0.0515	3.39	v.w.
0.0594	3.16	v.w.	0.0577	3.20	v.w.
0.0699	2.91	m.	0.0697	2.91	m.
			0.0732	2.84	m.
0.102	2.41	v.v.w.			
0.112	2.30	v.w.	0.112	2.30	w.
0.118	2.24	v.w.	0.121	2.21	w.
0.187	1.78	v.w.	0.188	1.77	v.w.
0.204	1.70	v.w.	0.202	1.71	v.w.
0.275	1.47	v.w.	0.270	1.48	v.v.w.
0.383	1.24	v.v.w.			

of sodium stearate,[7] or the experimentally observed value for the alpha-form, 52.1A, giving β equal to 63°. Thiessen and Stauff found 62.4°, by the method of Brill and Meyer.

Hence we have the following values: $a \sin \beta = 7.77$A; $a = 8.7$A; $b = 5.1$A; $c \sin \beta = 46.6$A; $\beta = 63°$; $\epsilon = b/(a \sin \beta) = 0.66$; density $= 0.99$ for four molecules in the unit cell. ϵ has an average value of 0.64 for a large number of paraffin chain compounds. According to molecular models, this is the approximate proportion of the cross section of a hydrocarbon chain; the zig-zag presumably lies in the a-c plane of the crystal. The spacing b, taken here as 5.16 ± 0.11A, appears slightly variable as we have found with other still unpublished photographs; likewise the layer lines in Thiessen and Stauff's photograph are irregular.

A NEW, MORE STABLE, MONOCLINIC GAMMA-FORM OF SODIUM STEARATE[8]

Kahlbaum sodium stearate, when melted and allowed to cool ("cast") was found to be distinctly different from the beta-monoclinic form. The long spacing is 44.6A (Fig. 1), as compared with 46.6A for beta-monoclinic and 52.1A for alpha-sodium stearate. Likewise the side spacings are distinctive, as appears from Table III and Fig. 2.

The new gamma-form resembles in long spacings the "b" form of stearic acid found by Francis, Piper, and Malkin,[9] $c \sin \beta = 44.0$A, also observed by Muller as 43.8A, whereas the beta-monoclinic form of sodium stearate is like their "a" form of stearic acid 46.6A. The polymorph corresponding to their "c" form, 39.5–40A, remains to be found, although we may have observed it with a sample of thallous palmitate given us by Dr. A. S. C. Lawrence; and there may be yet other forms.[10]

[7] L. Pauling, *Nature of the Chemical Bond* (Cornell University Press, Ithaca, 1940).

[8] Cf. the subsequent note by A. de Bretteville, Jr., and J. W. McBain, Science **96**, 470 (1942).

[9] Francis, Piper, and Malkin, Proc. Roy. Soc. **A128**, 214 (1930).

[10] Cf. the tabulation by L. H. Germer and K.-H. Stork, J. Chem. Phys. **6**, 280 (1938), Table V.

APRIL, 1943 JOURNAL OF CHEMICAL PHYSICS VOLUME 11

Detection of an Intermediate Step in the Autoxidation of Hydroquinone. Aerial Fogging of Photographic Emulsions*

T. H. JAMES
Research Laboratory, Eastman Kodak Company, Rochester, New York

(Received January 13, 1943)

Alkaline hydroquinone solutions, oxidized in the presence of a suitable photographic material, exert a fogging action upon that material. The fogging action is due to some transitory intermediate in the oxidation process. Various possibilities are considered, and the conclusion is reached that the peroxide radical, HO_2, is the fogging agent. The aerial fogging action of a number of essentially different developing agents is explained on the common basis of this intermediate.

INTRODUCTION

OXIDATION processes which do not involve direct addition of oxygen probably take place in steps of single electron transfer.[1–3] Thus, the first step in the reaction between hydroquinone and oxygen should be

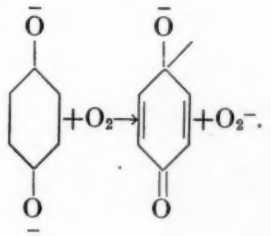

* Communication No. 901 from the Kodak Research Laboratories.

[1] P. A. Schaffer, J. Phys. Chem. **40**, 1021 (1936).

[2] J. Weiss, Naturwiss. **23**, 64 (1935).

[3] L. Michaelis, An. Rev. Biochem. **7**, 1 (1938).

The important participation of the semiquinone in the autoxidation of durohydroquinone has been demonstrated by kinetic methods.[4] The semiquinone reacts more rapidly with oxygen than the hydroquinone. This reaction likewise should yield the peroxide radical, O_2^- (or HO_2). However, the radical has not been detected kinetically in either the oxidation of hydroquinone or durohydroquinone.

FIG. 1. "Collar effect."

It is well known that the oxidation of alkaline hydroquinone solutions in the presence of a suitable photographic emulsion can produce fog.[5–8] This phenomenon has been attributed to chemiluminescence[7] and to the action of hydrogen peroxide.[8] Neither suggestion has been confirmed.

The purpose of the present paper is to show that neither chemiluminescence nor hydrogen peroxide can account for aerial fog. The fog must be due to the action of a transient intermediate formed during the oxidation of the developing agent. This transient substance is probably the peroxide radical, HO_2, since only this radical or a compound of similar character possesses the necessary properties.

EXPERIMENTAL

A modification of Fuchs' experimental technique[7] was employed. The film was immersed for 40 seconds in the solution under examination. The film was then removed and suspended in air for the desired time (usually 9 minutes). It was then bathed for 15 seconds in a one percent acetic acid stop-bath, washed in running water for 5 minutes, and developed for 4 minutes in a standard elon-hydroquinone developer. This procedure at least partially separated fog formation from development effects. Experiment showed that the initial time of immersion was not critical, and could vary from 20 seconds to 1 minute without producing noticeably divergent results. The aerial fog before final "development" was usually invisible or of very low density. Normal fog produced during the experiment was corrected by means of a blank in which aerial fog was suppressed by the addition of phenosafranin to the solution. The validity of this correction was checked by experiments carried out in the absence of oxygen. The normal fog in most cases was quite low, seldom exceeding 0.05.

In additional experiments, the film was allowed to stand quietly for some specified time partly immersed in the test solution. It was then removed and processed as before. Aerial fog showed up in the form of a dense "collar" at the air-liquid interface. An example is shown in Fig. 1.

The standard solution used for the production of aerial fog contained $0.05M$ hydroquinone, $0.10M$ sodium sulfite, $0.10M$ sodium carbonate, and $0.005M$ potassium bromide. When the effect of variation in concentration of one component was studied, all other concentrations and pH were maintained essentially constant. All solutions and air were at 25°C.

The Chemiluminescence Theory

Fuchs had established that aerial fog was connected in some way with the oxygen oxida-

[4] T. H. James and A. Weissberger, J. Am. Chem. Soc. **60**, 98 (1938).
[5] J. I. Crabtree, Am. Ann. Phot. for 1919, p. 20.
[6] M. L. Dundon and J. I. Crabtree, Brit. J. Phot. **71**, 701, 719 (1924).
[7] E. Fuchs, Phot. Ind. **22**, 27, 56 (1924).
[8] C. E. K. Mees, *Theory of the Photographic Process* (The Macmillan Company, New York, New York, 1942), p. 458.

tion of the developing agent. He had shown further that none of the then known oxidation products could account for the effect, and that partially oxidized solutions did not possess enhanced fogging activity. Lenard and Wolf[9] had observed a chemiluminescence during the aerial oxidation of pyrogallol, and Trautz[10] had observed chemiluminescence during oxidation by hydrogen peroxide of certain other developing agents in alkaline solution. Fuchs accordingly attributed aerial fog to the photographic action of chemiluminescence. He was totally unable, however, to obtain aerial fog when the plate was protected by an intermediate quartz sheet from direct contact with the oxidizing developer.

In the present investigation, aerial fog densities up to 0.5 were obtained by 5 minutes' aeration in the absence of copper, and densities greater than 3.0 were obtained in the presence of copper. No trace of chemiluminescence was observed in any case, although the eyes of the observer were well accommodated to faint light. Film suspended at 5 mm above the surface of the oxidizing solutions for several hours showed no fog. Moreover, in experiments on the production of fog "collars" (cf. Fig. 1), the film was immersed at various angles of interface. The line of demarcation of density consistently coincided sharply with the line of wetting of the film. No fog was obtained beyond the portion of the film wetted by the oxidizing solution.

In general, the more sensitive an emulsion is to light action, the more prone it is to aerial fog. This fact was used as an argument in favor of the chemiluminescence theory. There are, however, exceptions to the rule. Emulsion "*B*," described in a previous paper[11] on fog formation, differs essentially from the motion picture positive material in that it was ripened in the presence of a sulfur sensitizer to the point of appreciable ripening fog formation. A standard motion picture positive material, "*D*," was obtained which gave almost identical threshold sensitivity. Figure 2 gives comparative sensitometric curves for $2\frac{1}{2}$ minutes' development in the standard developer. The basic fog of 0.08 obtained with emulsion "*B*" has been subtracted from the total densities. The fifteenth step was the last visible with each emulsion. Control tests showed no significant difference in the reciprocity failure of the two emulsions. However, the standard hydroquinone solution yielded aerial fog of 0.20 on emulsion "*D*," and none on "*B*." A copper-containing solution yielded a collar-fog density of 2.25 on "*D*," and 0.07 on "*B*." Evidently, the correlation between aerial fog and light sensitivity fails badly with this pair of emulsions.

Further evidence advanced as favoring the chemiluminescence theory lay in the fact that certain desensitizers decreased or eliminated aerial fog. However, these same desensitizers decrease or eliminate the purely chemical fog produced by very dilute (*ca.* $10^{-6}M$) solutions of sodium stannite.

An apparently genuine case of chemiluminescence fog was reported by Benton.[12] This was produced on a hypersensitive panchromatic material being developed in a pyrogallol solution. It is interesting to note the differences between this and typical aerial fog. The chemiluminescence was clearly visible to the operator. The fog was formed on film totally immersed in the solution. Finally, the fog was formed in a developer which completely fails to give aerial

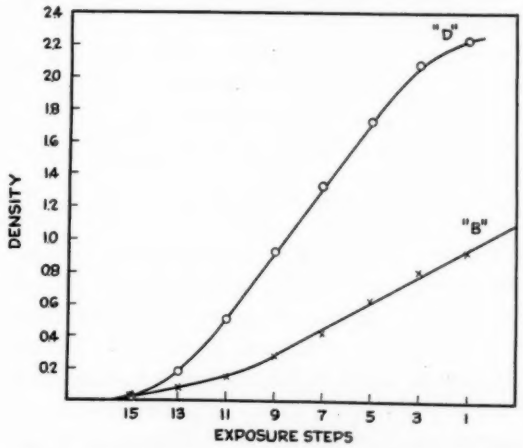

FIG. 2. Sensitometric curves for normal and special emulsions. Dev. time, $2\frac{1}{2}$ minutes at 25°C. Basic Fog: "*B*"=0.08; "*D*"=0.01. Last visible step: the 15th.

[9] Ph. Lenard and M. Wolf, Wied. Ann. **34**, 918 (1888); Eder's Phot. Mitteil., p. 344 (1887).

[10] M. Trautz, Zeits. f. physik. Chemie **53**, 1 (1905); M. Trautz and P. Schorigin, Zeits. f. wiss. Phot. **3**, 121 (1905).

[11] T. H. James, J. Frank. Inst. **234**, 371 (1942).

[12] W. A. Benton, Brit. J. Phot. **86**, 223 (1939).

fog under normal test conditions (in the absence of copper).

Hydrogen Peroxide

Elimination of chemiluminescence as the cause of aerial fog throws the burden upon some chemical entity produced during or as a product of the oxidation process. None of the stable or semi-stable products formed during the oxidation of hydroquinone-sulfite solutions produces significant fog. Hydrogen peroxide, which has a very transitory existence in such solutions,[13] is known to attack normal emulsions, but no direct comparison has been made between hydrogen peroxide fog and aerial fog.

Experiments were carried out in which fog produced by various concentrations of hydrogen peroxide was directly comparable with aerial fog produced in the same length of time and at the same *p*H. A second standard motion picture positive emulsion, "*C*," was employed.[11] Bromide and carbonate, but no sulfite, were added to the peroxide. Figure 3 gives the results for one set of experiments. In order to obtain hydrogen peroxide fog equal in intensity to the aerial fog, a hydrogen peroxide concentration equivalent to almost half of the entire hydroquinone content of the standard test solution is required. Since hydrogen peroxide cannot be detected after the addition of excess sodium sulfite to a hydrogen peroxide solution, and hence the two react together very rapidly, it becomes evident that hydrogen peroxide cannot be responsible for the observed aerial fog. Indeed, the addition of small amounts of copper salt to the hydroquinone solution will increase the aerial fog markedly beyond that given by the simple curve in Fig. 3.

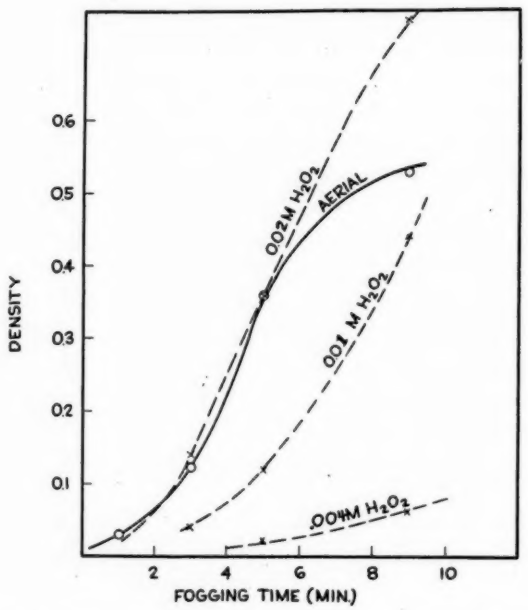

FIG. 3. Comparison of aerial fog and hydrogen peroxide fog.

The Free Radicals

We have established that neither chemiluminescence nor molecular hydrogen peroxide can account for aerial fog. Two possible intermediates of radical character must be considered: (1) the semiquinone, and (2) the peroxide radical, HO_2.

The semiquinone radical is probably capable of producing fog.[14] However, this radical cannot completely account for the phenomenon of aerial fog. In a durohydroquinone developer, for example, aerial fog is decreased by the addition of sodium sulfite. The sulfite does not inhibit the oxygen oxidation of durohydroquinone, and there is no evidence that it reacts with the semiquinone at a kinetically significant rate. Moreover, aerial fog is not restricted to developing agents which can form semiquinones. For example, aerial fog of roughly the same amount was obtained both with the standard hydroquinone test solution and with a ferro-oxalate developer. Considerable aerial fog was obtained also with an ammoniacal cuprous solution. Neither of the latter solutions forms a semiquinone.

The formation of aerial fog can best be accounted for by a reaction of the transitory peroxide radical. Like hydrogen peroxide itself, this radical possesses both oxidizing and reducing properties, and could readily form free silver by reaction with silver bromide.

Three factors would largely control the rate of formation of aerial fog: (1) the rate of formation of the peroxide radical; (2) the relative rates at which the radical reacts with silver bromide and with oxidizable bodies in the immediate vicinity; and (3) the formation in the developer of oxidation products which more or less tend to offset

[13] T. H. James, J. M. Snell, and A. Weissberger, J. Am. Chem. Soc. **60**, 2084 (1938).
[14] T. H. James, J. Phys. Chem. **45**, 223 (1941).

the fogging action of the radical. All factors may vary with the composition of the fogging solution and the nature of the developing agent whose oxidation gives rise to the fog.

Pyrogallol furnishes an extreme example of the importance of the third factor. Solutions containing this agent are notably free from aerial fogging action. The pyrogallol even protects solutions of other developing agents. Thus, the addition of 0.001*M* pyrogallol to a 0.05*M* hydroquinone solution which originally gave an aerial fog density of 0.53 reduced the fog to 0.06; addition of 0.005*M* pyrogallol eliminated the aerial fog completely. The effect is probably due to an oxidation product of pyrogallol, not to the agent itself. This is shown by the fact that antifogging action is obtained if the pyrogallol is first oxidized in solution[6] and then added to the hydroquinone solution. It is not surprising, therefore, that no aerial fog is obtained in the oxidation of pyrogallol itself.

In the absence of sodium sulfite, hydroquinone forms little aerial fog. This is probably due to the antifogging action of the quinone itself. The destruction of catalytic centers by quinone at *p*H 8.3 was observed in previous work on development by hydroquinone.[15] A small but definite decrease in aerial fog was obtained by bathing the fogged film prior to development in a freshly prepared solution of quinone, potassium bromide and sodium carbonate. (The quinone decomposes rapidly in this solution.) Almost complete destruction of aerial fog was effected in a neutral quinone-bromide solution.

The first small additions of sodium sulfite to the hydroquinone solution increase the aerial fog, due to removal of quinone. Upon further additions of sulfite, the aerial fog formation passes through a maximum, then rapidly decreases. This second stage is due to the action of the sulfite in decreasing the rate of oxidation of the hydroquinone, and hence the rate of formation of HO_2. The sulfite may also react with the peroxide radical itself, as indicated by the effect upon aerial fog in durohydroquinone solutions.

Finally, the marked increase in aerial fog produced by the addition of small amounts of copper salts to the oxidizing solution must be considered. Aerial fog has been detected when copper salts were added to many solutions (even those of pyrogallol) which normally do not give measurable aerial fog. Copper accelerates the oxidation of hydroquinone and other developers, and it might be supposed that this is the explanation of the enhanced fogging action. However, the increase in fog is out of proportion to the increase in oxidation rate, so far as can be judged from experiments on oxidation rates at lower *p*H. Moreover, the standard fogging hydroquinone test solution showed a *decrease* in fogging action when the oxidation rate was increased by use of a pure atmosphere of oxygen. This effect resulted from accumulation of hydroquinone oxidation products, since it was not present at higher sulfite concentrations.

An explanation of the effect of copper is suggested by the following experiment. Strips of film were partially immersed in an ammoniacal solution of cuprous oxalate. The surface of the solution had free access to air. As soon as slight fog formation became evident on the film portion immersed in the solution, the film was removed, rinsed in 1 percent acetic acid, and washed for 10 minutes. It was then "developed" in a standard elon-hydroquinone developing solution. A heavy collar, similar to that shown in Fig. 1, was obtained. In two typical experiments, the normal fog densities were 0.24 and 0.33; the collar densities were 0.88 and 1.10, respectively. Thus, considerable aerial fog arises from oxidation of cuprous salt.

In a developing solution of normal composition, cupric salts are readily reduced to the cuprous state. The cuprous salt, which is probably adsorbed to the silver bromide, can readily give rise to aerial fog by reaction with oxygen, forming HO_2. The cuprous salt is reoxidized to cupric in the process, but will again be reduced to cuprous by reacting with the developing agent once more. Since these reactions are quite rapid, a small amount of copper salt can and does give rise to heavy aerial fog.

ACKNOWLEDGMENT

The author is indebted to Dr. S. E. Sheppard, Dr. J. A. Leermakers, and Mr. C. E. Ives for valuable discussions and suggestions.

[15] T. H. James, J. Phys. Chem. **44**, 42 (1940).

The Quantum Yield of Diacetyl Fluorescence

G. M. Almy and P. R. Gillette
Physics Department, University of Illinois, Urbana, Illinois

(Received December 12, 1942)

The quantum yield of fluorescence of diacetyl, excited by radiation of λ4047 and λ4358, has been measured and found to be 0.145±0.03. It is approximately independent of pressure. On the other hand, the yield with excitation of λ3650, as first observed by Henriques and Noyes, increases apparently from zero at zero pressure to nearly the value obtained for the longer wave-length excitations at a pressure of 5 cm Hg. This marked difference in pressure effect for different energies of excitation is explained by assuming that predissociation occurs at a level between those reached upon λ3650 and λ4047 excitations. By removing vibrational energy collisions can save for fluorescence a molecule excited by λ3650, but they do not play an important role in the case of molecules with excitation energy below the predissociation limit. The observed phenomena of diacetyl fluorescence can be explained in terms of a model which involves a metastable state just below the state reached on absorption. This model is compared with McMurry's predictions of states for molecules of the type of diacetyl.

INTRODUCTION

EXPERIMENTS on the fluorescence of diacetyl show that the photochemistry of this molecule involves a number of elementary processes.[1–3] Energy absorbed at λλ3650, 4047, 4358 partly reappears as long-lived green fluorescence with maximum intensity at 5120A and partly leads to other processes, including decomposition. It is important for the description of what happens to the excited molecule to know the quantum yield of the fluorescence. Inferences regarding fluorescence and other processes can also be drawn from the effect of temperature and pressure on the fluorescent yield.

A tentative determination of the yield was made in this laboratory[4] with the result that at pressures of 4–5 cm, it was about 0.03 with excitation at λλ3650 and 4358, but much less at λ4047. Henriques and Noyes,[3] using only λ3650 excitation, found that the relative yield increased with increasing pressure. This unusual behavior had not been observed with λ4358 excitation.[1]

To clear up uncertainties in the absolute yield, two new determinations of the yield have been made and the earlier values have been found to be greatly in error. The error was due to the use of filters in the calibration of a photo-cell against a thermopile. The thermopile readings were apparently affected either by infra-red transmitted by the filter or by heating and reradiation of the filters as a consequence of absorption of most of the incident energy. The sensitivity of the photo-cell used to measure the incident energy was thus underestimated, the light absorbed overestimated and the calculated yields came out too low and not even relatively correct for the different wave-lengths. A thermopile is not, unless special precautions are taken, a reliable instrument for measuring the apparently monochromatic energy transmitted by a filter in the visible or ultraviolet spectrum.

Two new determinations of the yield have been made. In the first, the apparatus was unchanged except that a monochromator was used instead of filters in the calibration mentioned above. At diacetyl pressures of 4 to 5 cm the quantum yield with λλ4057 and 4358 excitation was found to agree to within 5 percent with the value obtained in the second determination, described below, under similar conditions.

In the second determination, described in detail in this paper, a new K-O photo-cell replaced the Cs-O photo-cell for measuring the fluorescence intensity and a new thermocouple as well as the pile previously used were employed in the calibrations. The yield at λλ4047 and 4358 was found to be 0.145. At λ3650 the yield at 5 cm pressure was 0.84 of the yield under similar conditions at λλ4047 and 4358. At λ3650 the

[1] Almy, Fuller and Kinzer, J. Chem. Phys. **8**, 37 (1940).
[2] G. M. Almy and S. Anderson, J. Chem. Phys. **8**, 805 (1940).
[3] F. C. Henriques and A. W. Noyes, Jr., J. Am. Chem. Soc. **62**, 1038 (1940).
[4] Fuller, Phillips, and Almy, J. Chem. Phys. **7**, 973 (1939).

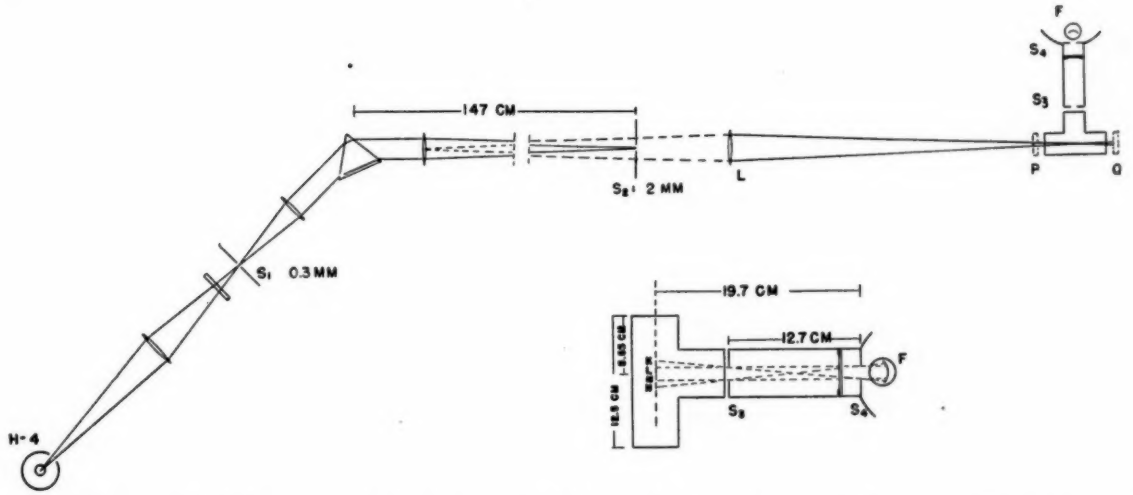

FIG. 1. Diagram of optical apparatus, showing source, H-4; improvised monochromator; fluorescence tube; slit system and photo-cell (S_3, S_4, and F) for measuring fluorescence intensity; photo-cell successively at P and Q to measure incident and transmitted exciting light. Inset shows enlargement of fluorescence tube and photo-cell F with slits.

pressure effect found by Henriques and Noyes was verified. It does not occur at the longer wave-lengths.

The previously proposed model for the energy states and processes of the diacetyl molecule[2] will account for the variation with wave-length of the effect of pressure on yield by the assumption of a simple natural process in the state reached immediately on absorption.

EXPERIMENTAL ARRANGEMENT AND METHOD

Preparation of Diacetyl

The diacetyl was supplied by two firms, the Lucidol Corporation and Eastman Kodak. Each batch used was placed in a blackened bulb on the system, frozen down with liquid air and pumped for hours. After it had melted approximately the first quarter was pumped off. The last quarter was also not used.

Optical System

The optical system is shown in Fig. 1. The fluorescence tube was connected to a suitable vacuum system from which diacetyl could be admitted at pressures measured accurately by a multiplying manometer. The source was a General Electric H-4 mercury lamp. The wave-lengths used were isolated by means of an improvised quartz monochromator which included a large quartz prism from a Steinheil spectrograph. The intensity and purity of visible spectrum were nearly as good as with filters and the uncertainties mentioned in the introduction were avoided.

The beam of fluorescent light striking the photo-cell F was limited by two similar apertures, S_3 and S_4, 1 cm wide by 2 cm high. The solid angle of fluorescence seen by the photo-cell is practically constant for all points between L and M in the exciting beam. For points outside LM the slit S_3 causes the effective solid angle to decrease linearly with the distance from L, or M, to zero at K, or N. The beam of exciting light is about 1 cm in diameter in the region between K and N.

Instruments and Their Calibration

The energy incident upon the tube and the energy transmitted were measured in turn by placing a GM Visitron F 2A photovoltaic cell, connected directly to a shunted wall type galvanometer, at P and Q (Fig. 1). The cell intercepted the whole beam in each case. The fluorescent energy passing through S_4 was measured by a GM 1044 TDV K-O vacuum photoemissive cell. It was placed in a vacuum chamber together with a Western Electric D96475 electrometer tube. The latter was used in a Barth balanced circuit, with an input grid resistance of 11,000 megohms.

The sensitivities of the photo-cells in their associated circuits, at the appropriate wave-lengths, were compared with that of a Moll vacuum thermocouple, which had a lens one cm in diameter for focusing the incident light on the thermojunction. For the photoemissive cell calibration a ribbon filament lamp and a Kipp and Zonen glass two-prism monochromator, followed by a corrected lens placed at its focal length from the exit slit, were used to produce a nearly uniform monochromatic beam. The beam was much larger than the slit S_4. The ratio of thermocouple and photo-cell deflections (d_{th}/d_F) was determined at a series of wave-lengths from 4800A to 6100A. With this arrangement plus a rotating sector disk the linearity of response of the photo-cell circuit and the ratios of the galvanometer Ayrton shunt were also checked.

The ratio of thermocouple and photovoltaic cell deflections (d_{th}/d_V) was obtained by placing them alternately in a nearly uniform but slightly diverging beam produced by removing lens L. A diaphragm with a circular opening of known area A was placed on the photovoltaic cell for the calibration. The ratio of deflections was obtained at λλ3650, 4047, 4358. This calibration was repeated with the use of a Coblentz thermopile in air. The relative sensitivity of the photo-cell at λ4047 and λ4358 was the same with Coblentz and Moll instruments and in agreement with information in a paper by Parker.[5] At λ3650, however, the Moll couple indicated an increase in sensitivity of the photo-cell, due, no doubt, to the absorption of lens and glass envelope in front of the thermojunction. The Coblentz pile gave results in agreement with an extrapolation of Parker's curves. Hence the Coblentz pile was used as the standard in the 3650A–4358A range and the Moll couple, whose greater sensitivity was very helpful in the calibration of the photo-cell behind S_4, was assumed to measure energy, independent of wave-length, in the overlapping range 4047A–6100A.

Method of Measuring Quantum Yield

Since Beer's law was observed to hold, the energy absorbed between two planes, distant x_1 and x_2 from the window of the tube, is given by

$$E_{abs}=E_{inc}e^{-\theta}(e^{-\alpha p x_1}-e^{-\alpha p x_2}),$$

where $e^{-\theta}$ is the fraction of incident energy transmitted by the window, measured for each wave-length. Under the conditions of the experiment, this equation can be replaced by

$$E_{abs}=E_{inc}e^{-\theta}(x_2-x_1)\exp\left[-\alpha p\frac{x_1+x_2}{2}\right],$$

with

$$x_2-x_1=\frac{KL+MN}{2}+LM=1.566\text{ cm}$$

and

$$\frac{x_1+x_2}{2}=5.55\text{ cm}.$$

The total fluorescent energy emitted between x_1 and x_2 is the energy passing through S_4 multiplied by $4\pi/\omega$, where ω is the solid angle subtended at the fluorescence by S_4 and by e^{θ} to correct for absorption in the exit window. This assumes that the long-lived fluorescence of diacetyl has a uniform angular distribution.

Now if the total incident radiation produces a deflection D_v on the photovoltaic cell (aperture of area A removed) the energy absorbed per sec. in the diacetyl is proportional to

$$D_v\left(\frac{d_{th}}{d_v}\right)_\lambda\cdot A\cdot e^{-\theta}\alpha p(x_2-x_1)\exp\left[-\alpha p\frac{x_1+x_2}{2}\right].$$

If the fluorescence passing through S_4 produces a deflection D_F in the photoemissive cell circuit the total energy radiated per sec. is similarly proportional to

$$D_F\cdot\left(\frac{d_{th}}{d_F}\right)_{5120A}\cdot\text{area of }S_4\cdot e^{+\theta}\cdot 4\pi/\omega.$$

The above rates of absorption and emission could be expressed in watts if the thermopile deflection were also obtained in the known radiation field (watts per cm²) of a standard lamp. This is not necessary, however, in order to calculate the absolute quantum yield which is given by

$$Y=\frac{\text{energy radiated}}{\text{energy absorbed}}\frac{\lambda_{flu}}{\lambda_{abs}}.$$

[5] A. E. Parker, Illum. Eng. **35**, 833 (1940).

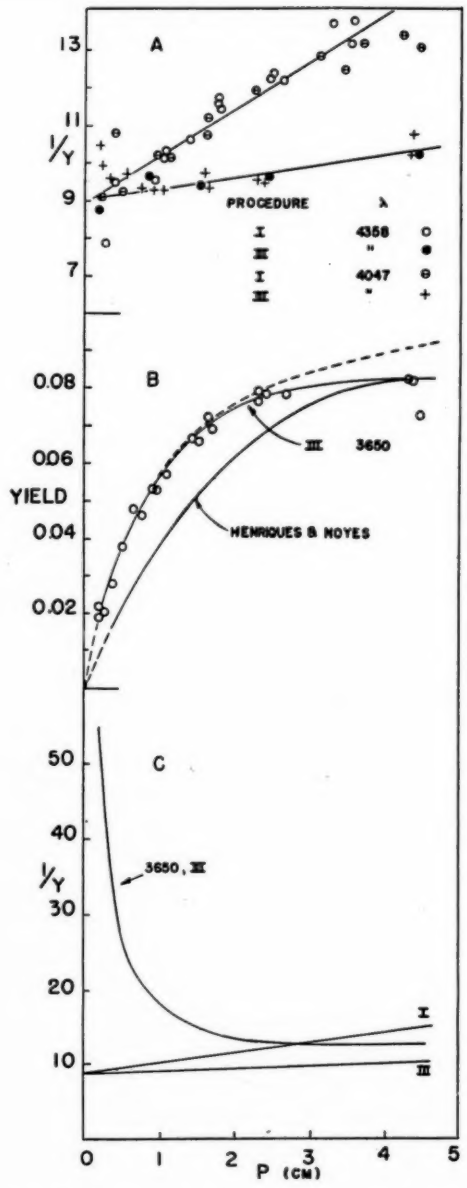

FIG. 2. (A) Reciprocal yield of fluorescence when excited by λλ4358 and 4047, as a function of pressure, for samples with different preliminary treatments (see text). (B) Yield with λ3650 excitation. Dashed curve is Eq. (8a). (C) Reciprocal yields for λ3650 excitation, contrasted with those for λλ4047 and 4358, transcribed from (A).

RESULTS

Readings of both incident energy and energy getting through the fluorescence tube, as well as readings of diacetyl pressure, were taken each time the tube was filled; this gave a large number of data from which the variation of absorption with pressure could be accurately determined. It was found that Beer's law was obeyed. Values of the absorption coefficient obtained from these data are:

λ (H-4 lamp)	α at 27°C per cm Hg per cm path
4358	0.0215±0.0005
4047	0.0193±0.0005
3650	0.0048±0.0005

The intensity of fluorescence was measured at λλ4358, 4047, 3650 in a pressure range of 0.2 cm to 4.5 cm Hg, by the use of three different procedures:

I. The tube was refilled for each pressure.

II. The tube was filled and emptied by steps and readings were taken at each step.

III. The tube was filled to the maximum pressure of the run, radiated strongly with unfiltered light from a glass H-2 mercury lamp for two or three hours, and then readings of intensity of fluorescence taken as the pressure was reduced in steps. The sample also was given 10-min. radiations from the H-2 lamp between steps. This procedure was used because it was found that the variation of yield with pressure depended upon the past radiation of the sample.

In Fig. 2A are plotted in detail the reciprocal of the yield against the pressure for two runs for λ4358 and two for λ4047 by procedure I (tube refilled at each point) and three runs by procedure III (strong preradiation). Within experimental error, (1) identical results are obtained for excitation by λ4047 and by λ4358, (2) the points fall on a line for each run and all lines have the same intercept at $p=0$, although the slopes of the lines vary with the procedure followed. Several additional runs, mostly by procedures I and II all gave results similar to those plotted: straight lines with different slopes but with intercepts within 5 percent of an average value of 9.0.

Upon excitation by λ3650, on the other hand, the yield increases sharply with increasing pressure but becomes nearly constant and nearly as large as the yield at λλ4047 and 4358 for pressures above 3 cm (Fig. 2B). Procedure III was used since the "impurity" pressure effect, discussed in the next paragraph, was then nearly eliminated with the longer wave-length excita-

tion. The variation with pressure at λ3650 is in substantial agreement with the result obtained by Henriques and Noyes. Their Fig. 2 is transcribed to our Fig. 2B adjusted to the new scale of ordinates. The striking contrast between the behavior with λ3650 excitation and with the longer wave-lengths is shown in Fig. 2C. This difference will be discussed in the following section.

The straight lines in Fig. 2A indicate that a Stern-Volmer mechanism is followed. The variation in slope rules out self-quenching but can be understood if we assume that a quenching substance is present in amounts proportional to the pressure of diacetyl and is destroyed by strong radiation. Under these conditions, the yield is given by

$$Y=\frac{k_\nu}{k_\nu+k_d+k_q p},$$

where k_ν, k_d, and $k_q p$ are the probabilities, for an excited molecule, of fluorescence, monomolecular competing processes, and quenching, respectively. The reciprocal yield varies linearly with the pressure and the intercept at $p=0$ is the reciprocal yield in the absence of impurities. The slope depends upon the fraction of impurity present and is reduced as the impurity is destroyed by radiation.

Since O_2 is known to be a strong quencher of diacetyl fluorescence[1] (1 part in 10,000 would account for the observed effect) its presence was suspected. Drastic outgassing procedures which in earlier experiments eliminated entirely the dependence of yield on the pressure, at λ4358 excitation, had no effect here.

At all events, the quantum yield for λλ4047 and 4358 excitation was obtained from the reciprocal of the average value of the intercepts of plots like those in Fig. 2A. This average is 9.0, its reciprocal 0.111, which is the yield if all of the fluorescence were at 5120A. We estimated that the two other bands of fluorescence, with maxima at 5580A and 6100A, are each about one-fourth as intense as the main band. Taking into account the smaller size of the quanta at these wave-lengths and the variation in sensitivity of the photo-cell, we obtained a correction factor of 1.3. The quantum yield for λλ4047 and 4358 thus comes out 0.145 with an uncertainty of about 0.03. This estimate of error contains a large contribution from the uncertainty in the correction factor. It does not include an error which may arise from the assumption that the response of the Moll thermocouple is independent of wave-length in the range from 4047A to 6100A.

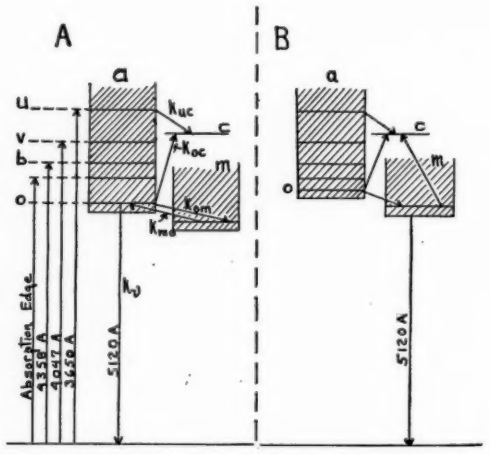

FIG. 3. Schematic energy level diagrams of models of diacetyl molecule. Model A is discussed in detail in text. *a* and *m* are electronic states with many closely spaced vibrational levels. Transition to *c* corresponds to monatomic processes competing with fluorescence, including predissociation. B is an alternative model which probably could also reproduce observed properties of fluorescence.

For λ3650 excitation the yield extrapolated to 5.0 cm pressure, obtained by procedures I and III, was in each case 0.84 of the yield obtained with λ4047 excitation under similar conditions. Earlier results with a Cs-O cell indicated a ratio of about 0.9, at pressures of 4 to 5 cm.

The results can be summarized as follows. When excited by λ4358 or λ4047 diacetyl fluoresces with a quantum yield of 0.145 ± 0.30. In the pure substance this value is nearly independent of pressure in the range 0–5 cm. With excitation of λ3650 the quantum yield rises with pressure, apparently from zero at zero pressure. With increasing pressure it appears to be approaching a yield nearly as great as obtained with the longer wave-length excitation.

Measurements of the variation in yield with temperature, of samples which had received a strong preradiation, gave the result that the yield decreased almost linearly with rising temperature. The yield at 80°C was one-half the yield at 30°C.

DISCUSSION OF RESULTS

The model previously proposed[2] to account for the properties of diacetyl fluorescence can readily be adapted to account for the new experimental results. These are included in the following list:

1. Quantum yield with 4358A- and 4047A-excitation equal to 0.145 at 27°C and independent of pressure.
2. Quantum yield with 3650A-excitation rises apparently from zero at zero pressure to 84 percent of the yield for longer wave-lengths at 5-cm pressure.
3. Y at 25°C/Y at 65°C = 1.65 (4358A excitation).
4. Decay of fluorescence is simply exponential, with a mean lifetime (τ) of 1.40×10^{-3} sec.,[6] independent of pressure, exciting intensity and exciting wave-length.[2]
5. τ at 25°C/τ at 65°C = 2.0 ± 0.4.
6. Lifetime of state reached on absorption is 10^{-5} sec., estimated from integrated absorption coefficient.[2]

The model is shown schematically in Fig. 3A. An alternative appears in Fig. 3B. Assuming model A, consider what happens when a molecule absorbs a quantum of λ4358 or λ4047 and is raised to vibrational state b or v of electronic state a. Redistribution of vibrational energy and collisions bring the molecule to a different and lower vibrational state o, from which it can, (1) fluoresce at the rate k_v, (2) predissociate or dissociate into chemical products (c) by attaining the necessary critical configuration, at the rate k_{oc},[7] or (3) go into the long-lived state m at the rate k_{om}. If it goes into m it can return to a at a slow rate k_{mo} and then has again a chance to radiate. The yield is determined by the competition between k_{oc} and k_v since it is assumed for simplicity that no molecules are lost from m except by return to o. As will be shown below the lifetime depends on several factors, but is made much longer than the reciprocal of k_v+k_{oc} by a large ratio of k_{om} to k_{mo}.

When a quantum of λ3650 is absorbed, the molecule finds itself in state u, above c, which we shall assume is a level at which the molecule can predissociate. In this case, the molecule can (1) be stabilized toward state o by collisions and follow the course outlined for 4358A excitation or (2) predissociate at a high rate directly into c and be lost as a diacetyl molecule. The low fluorescence yield at low pressure is ascribed to the loss of excited molecules to c before sufficient collisions have occurred to save them for a chance at fluorescence.

It may be remarked that the best data for λ4047 (Fig. 2A, procedure III) show the same pressure effect as λ3650 but at much lower pressures, where the error of measurement is nearly as large as the effect. If the departure of the λ4047 plot from a straight line is real it means that collisions also reduce the chance of transition to c with this excitation, but that the chance of this transition is about ten times less than with λ3650 excitation.

These processes can be described more exactly. All molecules excited by λλ4047 and 4358 arrive by collisions at state o. Let n_o be the population of electronic state A, vibrational state o. Let n_m be the population of m. Then

$$dn_o/dt = N_o-(k_{oc}+k_{om}+k_v)n_o+k_{mo}n_m, \quad (1)$$

$$dn_m/dt = k_{om}n_o-k_{mo}n_m, \quad (2)$$

where N_o is the number of molecules excited per sec. At equilibrium each rate is zero. It follows upon adding Eqs. (1) and (2), each set equal to zero, that the quantum yield (Y), which is given by $k_v n_o/N_o$ is

$$Y = k_v/(k_v+k_{oc}). \quad (3)$$

Since, from experiment, $Y=0.145$ and $k_v=10^5$, Eq. (3) leads to $k_{oc}=6\times10^5$, at room temperature. If we assume that $k_{oc}=Z_{oc}\exp[-E_{oc}/RT]$, the observed temperature variation of Y yields the values, $Z_{oc}=8.7\times10^8$ sec.$^{-1}$ and $E_{oc}=4400$ cal./mole.

The transient solution of Eqs. (1) and (2) for n_o is,

$$n_o = c_1\exp(\lambda_1 t)+c_2\exp(\lambda_2 t), \quad (4)$$

where

$$\lambda_1 = -\frac{k_{mo}(k_{oc}+k_v)}{\beta}, \quad \lambda_2 = -\beta+\frac{k_{mo}(k_{oc}+k_v)}{\beta},$$

[6] R. D. Rawcliffe, Rev. Sci. Inst. **13**, 413 (1942).

[7] In place of, or in addition to, this process deactivation to the ground state by "internal conversion" could occur (cf. ref. 8). It is known, however, that diacetyl is decomposed into gases non-condensible in liquid air by radiation of λ4358, as well as by the shorter wave-lengths.

$\beta=k_{oc}+k_\nu+k_{om}+k_{mo}$. In obtaining λ_1 and λ_2, it is assumed that $\{\beta^2-4k_{mo}(k_{oc}+k_\nu)\}^{\frac{1}{2}}$ can be adequately replaced by the first term in its expansion. It appears in the following paragraphs that the rates are such that the approximation is a very good one.

The fluorescent intensity ($=k_\nu n_o$) is observed to decay exponentially at a rate of about 10^3 sec.$^{-1}$. λ_2, however, is of the order of magnitude of 10^6. Hence $c_2 \ll c_1$; otherwise an initial rapid drop, before the observed slow decay, would occur. The fluorescence mean life must, therefore, in this model, be,

$$\tau=-1/\lambda_1=\beta/k_{mo}(k_{oc}+k_\nu). \tag{5}$$

Substituting for β, setting $\tau=1.4\times10^{-3}$, $k_{oc}+k_\nu=7\times10^5$, Eq. (5) becomes

$$1.4\times10^{-3}=\frac{1}{k_{mo}}+\frac{k_{om}}{7\times10^5 k_{mo}}, \tag{5a}$$

in which a term or order 10^{-6} has been dropped. Since both terms on the right are positive, $k_{mo}>7\times10^2$ and $k_{om}/k_{mo}<10^3$.

By applying the boundary conditions at $t=0$, namely, $n_o=c_1+c_2$ and $n_m=n_o k_{om}/k_{mo}$, one finds that

$$\frac{c_2}{c_1}=\frac{k_{oc}+k_\nu}{k_{om}+k_{mo}}. \tag{6}$$

Since from experiment this ratio is small, say less than 0.1, it follows that $k_{om}>7\times10^6$. But $k_{om}/k_{mo}<10^3$ and, therefore, $k_{mo}>7\times10^3$, ten times the lower limit deduced from Eq. (5a). Hence $1/k_{mo}$ can be dropped from Eq. (5a) and it follows that, approximately, $k_{om}/k_{mo}=10^3$.

Thus lower limits and a ratio are fixed for k_{om} and k_{mo}. Since they measure the rates of radiationless transitions in and out of the metastable state they probably depend upon the amount of vibrational energy in the initial state.

For molecules excited by λ3650 the analysis given holds except that N_o in Eq. (1) is the number reaching state o by collision, against the competition of immediate transition to c. If the number reaching u per sec. is N_u the fraction of these reaching o is

$$N_o/N_u=k_s p/(k_{uc}+k_s p), \tag{7}$$

where $k_s p$ is the chance for a stabilizing collision at pressure p. Substituting for N_o in Eq. (1) and solving for the yield as before one finds

$$Y=\frac{k_\nu n_o}{N_u}=\frac{k_\nu}{k_\nu+k_{oc}}\frac{k_s p}{k_{uc}+k_s p}=Y_\infty\frac{k_s p}{k_{uc}+k_s p}. \tag{8}$$

Y_∞ is the limiting yield at high pressure and should be equal to the yield at λλ4047 and 4358, which was 0.11, before correction for distribution in wave-length. From measurements by Anderson[2] on the diffusion of excited diacetyl molecules, kinetic theory gives a cross section of 11.3×10^{-5} cm^2 or a collision diameter of 5.9A. Assuming the same diameter is required for a collision in which enough vibrational energy is transferred to stabilize a molecule in state u, the number of collisions per excited molecule per sec. comes out to be $1.5\times10^8 p$, with p in cm Hg; that is to say, $k_s=1.5\times10^8$.

We can estimate k_{uc} from the experimental curve. The fluorescence yield, after a small correction is made for the type of pressure quenching observed with λλ4047 and 4358, is 0.055 (half of Y_∞) at $p=0.95$ cm. Hence, $k_{uc}=1.4\times10^8$. Equation (8) becomes

$$Y=0.110\frac{1.5p}{1.4+1.5p}. \tag{8a}$$

It is plotted as a dotted line in Fig. 2B. It fits the observed fluorescence curve well if the latter is assumed to be depressed by the "impurity" pressure effect observed under similar conditions with the longer wave-lengths. In fact, Y/Y_∞ calculated from (8a) is, at $p=5.0$ cm, equal to 0.84, which is the ratio found experimentally between the yields at λ3650 and at λλ4047 and 4358, under similar conditions. The experimental curve of Henriques and Noyes can be fitted with the same type of equation if k_{uc} is set equal to 2.5×10^8. These authors find that if the total pressure is raised by adding acetone the curve passes through a maximum, due presumably to the superposition of a weak quenching by acetone on the main pressure effect.

The lifetime for predissociation is $1/k_{uc}$ or 5×10^{-9} sec. Although this is much longer than the vibrational periods of the molecule are likely to be, it is not an unreasonably long time for a polyatomic molecule to get into the critical

configuration which may be necessary for predissociation.

The mechanism shown in Fig. 3B could doubtless also account for the observed properties of the fluorescence. In this case the fluorescence is the transition $m \rightarrow X$, with decomposition or other monatomic process $m \rightarrow c$ competing. The level at which m dissociates into c may or may not be the same as the level into which a dissociates.

In either scheme, A or B, the essential special features are (1) a long-lived state m at about the same energy level as state a, (2) a predissociation limit below vibrational level u to account for the differences observed with λ3650 as against λλ4047 and 4358 excitations, (3) predissociation or other monomolecular decomposition or deactivation processes, competing with the fluorescence, whatever the exciting wave-length, at a rate which depends on the temperature.

Henriques and Noyes have proposed a mechanism which will also account for the effect of pressure on yield with λ3650 excitation. A state B^0 (our a) is reached on absorption which may dissociate or go reversibly into B^1 (our m). B^1 may be transformed *by collisions* into B^2 which may fluoresce. It is similar to our model if B^2 is identified with a low vibrational level o of electronic state a. The essential difference is in the role of collisions. In their model, collisions enhance the transfer to the final fluorescing state ($B^1 \rightarrow B^2$); in ours, collisions prevent immediate predissociation upon excitation by λ3650. It is certainly easier with our model to give a simple and natural explanation of the qualitative difference in the effect of pressure with λ3650 excitation as compared with excitations by longer wave-lengths.

The state m may correspond to a tautomeric form of excited diacetyl, of the kind suggested by Franck and Livingston[8] to explain certain properties of dyes. It may, however, be a state which is metastable against electronic transition in the usual sense. The electronic states of conjugated ketones have been discussed by McMurry[9] and it appears that in molecules containing two conjugated

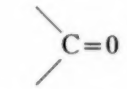

groups, such as diacetyl, the first excited states come in pairs (called E' and E'' states) which are nearly degenerate. Transition to only one of a pair is allowed by the electronic selection rules. McMurry states, however, that both transitions probably do occur and that both owe most of their intensities to perturbation due to electronic-vibrational coupling. But if we identify states a and m in our model with the two states of a pair (E_1' and E_1'') and suppose that on account of the electronic selection rules the transition $a \rightarrow X$ is more than one hundred times as probable as $m \rightarrow X$, the model proposed fits qualitatively with the theoretical picture.

---

[8] J. Franck and R. Livingston, J. Chem. Phys. 9, 184 (1941).

[9] H. L. McMurry, J. Chem. Phys. 9, 241 (1941).

The Electrical Conductivity of Lead Chromate*

THEODORE WILLIAM LASHOF
University of Pennsylvania, Philadelphia, Pennsylvania
(Received November 18, 1942)

The conductivity of sintered pellets of lead chromate varies with the temperature in accordance with the Boltzmann-type law $\sigma \propto \exp(-1.48\ \text{ev}/kT)$ in the temperature range 700°C to 350°C and with the law $\sigma \propto \exp(-0.60\ \text{ev}/kT)$ at lower temperatures. At constant temperature the conductivity increases with decreasing oxygen pressure, $\sigma \propto P_{O_2}^{-1/3.1}$, which indicates that lead chromate probably dissociates in accordance with the equations: $2PbCrO_4 \rightarrow Pb(CrO_2)_2 + Pb^0 + 2O_2$ and $Pb^0 \rightarrow Pb^+ + e$. The energies of these reactions are 5.28 and 1.20 electronvolts, respectively. These same reactions would explain optical and thermal darkening as well as the conductivity, and they indicate along with transport measurements and Seebeck effect measurements that lead chromate is an excess electronic semiconductor.

I. INTRODUCTION

CHROME yellow pigments, which consist essentially of lead chromate, have the unfortunate property of darkening on exposure to light. It was expected that lead chromate is one of that interesting group of photo-sensitive materials, which includes the silver halides and zinc sulfide, that decompose photolytically. With this possibility in view the work of the present paper on the electrical properties of pure lead chromate was undertaken. It was hoped that from this work would come an understanding of the fundamental chemical reactions that produce darkening. In addition to the present paper, studies of the optical and electrical properties of variously treated lead chromate pigments are being carried out at this laboratory, and the results will be published in other papers.

Lead chromate belongs to that group of solids known as semiconductors. The solids classified as semiconductors are those which have "a small electronic conductivity that is negligible at very low temperatures and increases with increasing temperature."[1] The electrical conductivity of a semiconductor is very much a property of the method of measurement. In determining the conductivity of a semiconductor, therefore, certain problems must be considered: the contact with the semiconductor; the effect of impurities and of the mechanical and thermal history on the conductivity; the dependence of the conductivity on voltage, temperature and oxygen pressure; and the determination of the type of conduction. These problems are discussed in the order given in the section on results.

II. PREPARATION OF SAMPLES

Pure lead chromate pigments were prepared for this work by the Krebs Pigment Department of E. I. du Pont de Nemours and Company. They started with C.P. sodium chromate and C.P. lead nitrate and obtained by carefully controlled fractional crystallization very pure salts from which the lead chromate was obtained by precipitation. A spectroscopic analysis made at the du Pont experimental station showed that the samples contained possibly "several parts in 10,000 of Si, Na, and Ca; traces perhaps picked up in analysis of Mg and Ba; and no other metallic impurities." In all of the work carried out here the structure of the material used was restricted to the monoclinic phase which is stable from room temperature to 707°C.

The pigment was pressed into pellets about one-half inch in diameter and one-quarter inch thick with the use of a press made from an eight-ton hydraulic truck jack. Although a die made of hardened tool steel and equipped with two hardened plungers was found satisfactory for making the pellets used in rough measurements, considerable difficulty was encountered because the pigment stuck to the die. In order to reduce this and to eliminate the strains produced when

* A dissertation in physics presented to the Faculty of the Graduate School in partial fulfillment of the requirements for the degree of doctor of philosophy.

[1] F. Seitz, *The Modern Theory of Solids* (McGraw-Hill Book Company, Inc., New York, 1940).

removing the pellet from the die a special divided die was constructed of extremely hard material. About 2 grams of the pigment were used to make each pellet, and the optimum forming pressure employed was 9000 lb./in.^{2}. The density of the pellets thus formed was about 50 percent of the single crystal value. It may be added that natural single crystals from Siberia and Tasmania have a density of 5.92 and 6.00 grams/cm^3, respectively, whereas artificial crystals have a density between 6.1 and 6.3 g/cm^3.[2]

On exposure to the atmosphere the lead chromate pellets were found to absorb up to 0.1 percent of their weight in moisture. This amount of moisture increased the conductivity a hundred-fold. If, however, a current was allowed to pass through the sample for several hours, the conductivity dropped below the value for a carefully dried specimen. Subsequent examination of the sample showed dark areas at the contacts. The conduction increased when these areas were removed. For standardization, all of the pellets used in the final measurements were dried at 105°C for approximately 24 hours.

Contact was made to the sample either with platinum disks which were held against the pellet with a strong spring, or with gold films that were vacuum-evaporated onto the parallel surfaces of the pellet. Platinum disks were usually pressed against the gold layer.

In order to measure the contact resistance some of the samples were formed with probes. Two small flat spirals of 1-mil Nichrome wire were imbedded between three 1-gram sections which were formed into a single pellet. The pellet was pressed in stages, each section being pressed to 2000 lb./in.^{2} before the spiral and next section were placed on it. The entire unit was completed at a pressure of 9000 lb./in.^{2}.

For lead chromate heated 18 hours at 400°C in air the density becomes 5.8 grams/cm^3 or 93 percent of single crystal density. Pellets thus sintered possess the advantage that many of their properties are nearly those of a single crystal. For some measurements the temperature and oxygen pressure during sintering were varied and the sample was quenched to room temperature.

[2] B. Grossner and F. Mussgnug, Zeits. f. Krist. **75**, 410 (1930).

III. APPARATUS AND CIRCUITS

Most of the measurements were made with the current-voltage circuit shown in Fig. 1(a). To prevent puncturing of the sample as a result of Joule heating and the consequent runaway conduction, the ballast tube 6D6 was used as a series resistor with its grid bias adjusted so as to hold the current below 5 milliamperes.

In order to measure the contact resistance, the potentiometer circuit of Fig. 1(b) was added to that of Fig. 1(a). The tube 6F5 is operated as an impedance changer, and was selected because of its large grid resistance and large transconductance. The unknown potential difference appears across the 1 megohm cathode resistor, and is measured with a vacuum tube voltmeter (VV).

Two furnaces were used to determine the temperature and oxygen dependence. The high temperature furnace (Fig. 2) is a modification of that described in the thesis of M. Earle.[3] The Alundum tubes (A), Glowbar heating elements (G), and quartz tube (Q) for the vacuum

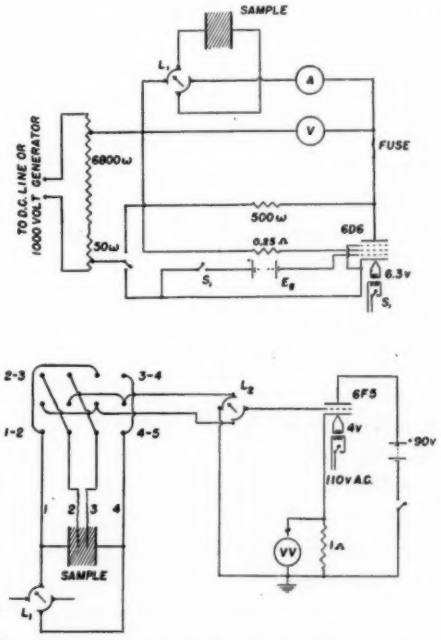

FIG. 1. (a) Upper, circuit for measuring current-voltage characteristics. (b) Lower, circuit for measuring contact potential drop. L_1 and L_2 are two lucite commutator switches coupled so as to keep the grid of the tube 6F5 positive when reversing the current through the sample. Note: ω=ohm, Ω=megohm.

[3] M. D. Earle, Phys. Rev. **61**, 56 (1942).

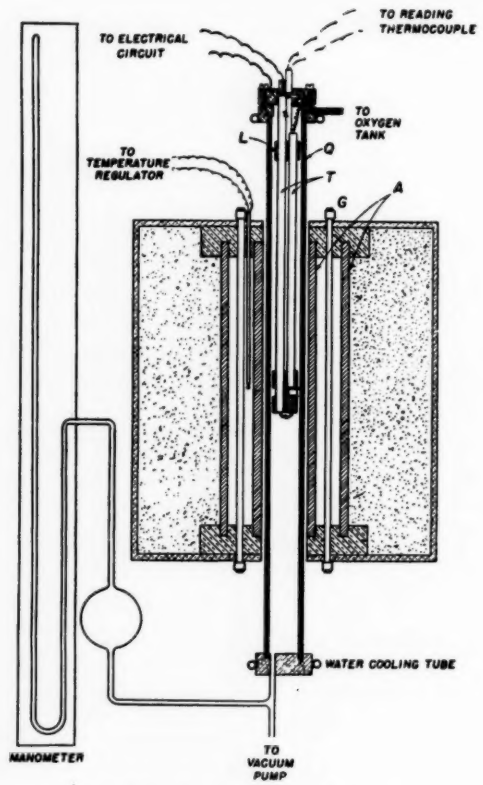

FIG. 2. High temperature furnace.

or oxygen chamber are the same as in his design. Only the reading thermocouple and sample holder are changed. These are inserted through the top end of the quartz tube. A $\frac{3}{8}$-inch diameter thermocouple tube 18 inches long (T) is waxed into a tightly fitting hole in the 1-inch thick brass cap. Two lavite blocks (L) are sealed to the thermocouple tube with Alundum cement. A third lavite block is sealed to the lower end of a 12 inch tube of the same diameter. This second tube can be moved up and down parallel to the first, during which motion the lavite blocks serve as guides. They also serve as supports for the platinum electrodes. The weight of the 12-inch tube is sufficient to give the mechanical contact. The leads from the sample are taken through the thermocouple tubes. The resistance of both lavite and thermocouple tubing (Alundum) was found to be very high compared with the resistance of the sample at any given temperature.

The second furnace is useful in the temperature range from room temperature to 220°C. Nichrome wire replaces the Glowbar heating element and a Pyrex tube replaces the quartz tube of the foregoing furnace. The electrodes are brass, supported by a stainless steel tube and insulated by Pyrex rods.

IV. RESULTS

A. The Electrical Contacts

As already mentioned, a moist sample through which current is flowing develops on its surface a layer possessing high resistance. The probe method indicates that vacuum-evaporated gold electrodes show no contact resistance when placed on a thoroughly dried sample, whereas vacuum-evaporated aluminum electrodes show a contact resistance. For example, at 105°C the resistance varied from a value equal to three times the volume resistance of the sample at 5 volts to about 5 percent of the volume resistance at 50 volts. On the other hand, at 105°C a contact made mechanically with a platinum electrode has a contact resistance which is independent of the voltage and is 5 times that of the volume resistance of the sample. Mechanical electrodes of lead foil show the same high contact resistance as platinum. The method is not too accurate since the exact position of the probes is difficult to ascertain. Also in these porous unsintered samples the evaporated gold possibly penetrated the surface of the sample. See Table I.

For sintered pellets at 105°C platinum and Nicrome mechanical contacts have about twice the resistance of evaporated gold or lead foil contacts. Aquadag contacts, on the other hand, seem to have half this resistance, perhaps because Aquadag introduces moisture into the

TABLE I. Voltage drop across sections of unsintered sample at 105°C.

	1–2	2–3	3–4	1–4
Pt-Pt	5.5	0.7	3.8	10.0
mechanical	33	3.8	23.1	59.2
	3.7	0.6	3.0	7.0
Au-Au	3.2	3.8	2.9	9.8
evaporated	16.1	18.2	13.8	47.6
Pt-Au				
mech. evap.	44.5	2.8	1.7	49.1
Al-Al	2.45	0.40	2.40	5.25
evaporated	17.2	14.6	17.1	49.1

sample. The probe method, which for the set-up used becomes accurate only at higher temperatures (150°C) when the resistance of the sample is sufficiently low, shows that evapoated gold electrodes have no contact resistance. Platinum mechanical electrodes, however, have a high resistance until about 500°C when they become as good as gold electrodes.

B. The Effect of Impurities on the Conductivity

Moisture increases the conductivity, the electrolysis of the water contributing the added conduction.

A series of samples were measured at several temperatures below 200°C. The material from which the samples were made contained metal oxides added after precipitation of the lead chromate. The conductivity of the treated material was found to decrease by as much as a factor of 10,000 and depended directly on the amount and type of oxide added. This behavior

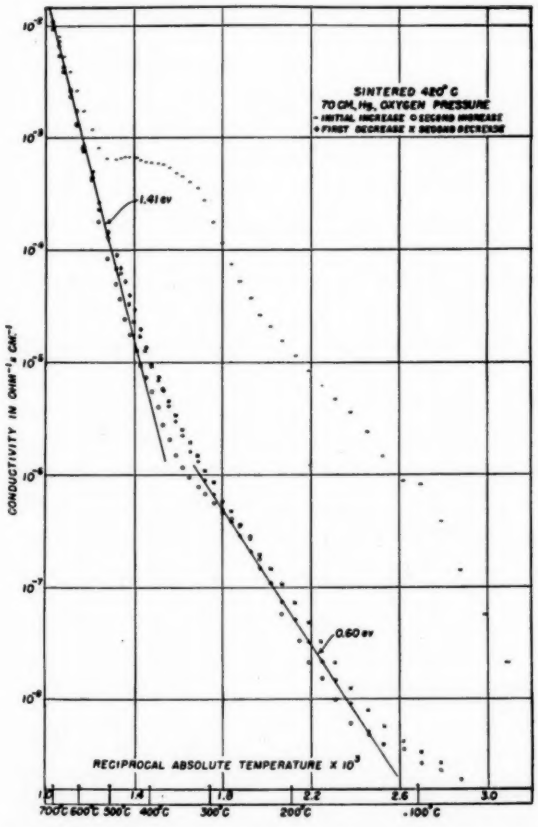
SINTERED 480° C
70 CM. Hg. OXYGEN PRESSURE
1.41 ev
0.60 ev
RECIPROCAL ABSOLUTE TEMPERATURE X 10³
700°C 600°C 500°C 400°C 300°C 200°C 100°C

FIG. 3. Conductivity as a function of temperature. The run either up or down took 80 minutes in each case.

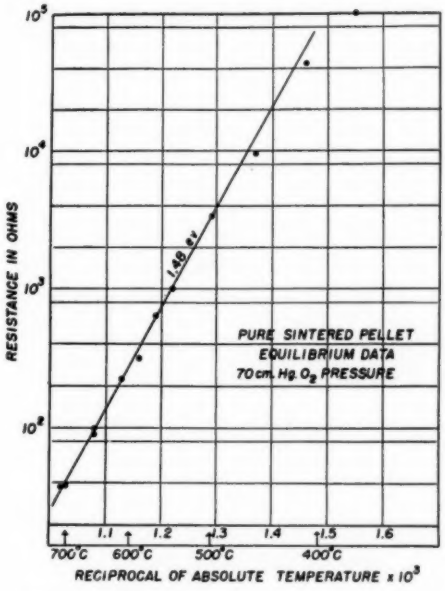

FIG. 4. Resistance-temperature curve for oxygen equilibrium.

is readily explained by assuming that the oxides form layers or coatings of high resistance on the particles of lead chromate. It was found that the light-fastness of these materials in general increased with decreasing conductivity, showing that there is probably a connection between the two properties.

C. The Effect of the Thermal History on the Conductivity

An unsintered sample has a conductivity of 1.2×10^{-5} ohm^{-1} cm^{-1} at 105°C. The conductivity of a sintered pellet, on the other hand, also at 105°C, varies with the sintering temperature and oxygen pressure. In fact values that range from 10^{-9} to 10^{-6} ohm^{-1} cm^{-1} have been obtained. The value of 5×10^{-9} ohm^{-1} cm^{-1} found by Kapp[4] for a natural single crystal lies within this range.

D. The Conductivity as a Function of Voltage

The dependence of the conductivity of an unsintered sample on the voltage is related to the contacts, the temperature, and the impurities. Gold electrodes extend the range of Ohm's law

[4] G. Kapp, Ann. d. Physik 22, 257 (1935).

to lower voltages and the temperature and impurities have a marked effect on the high voltage end of the range. On the other hand, a carefully prepared sintered pellet shows none of the foregoing behavior, and is closely ohmic over a large range of voltage.

E. The Conductivity as a Function of Temperature

The dependence of the conductivity σ on the absolute temperature T is given for certain temperature ranges by the Boltzmann-type equation

$$\sigma = Ae^{-\epsilon/kT}$$

where k is the Boltzmann constant, ϵ a constant called the activation energy, and A is relatively independent of T. The name "activation energy" will be restricted to k times the slope of the log σ *versus* $1/T$ curve. The significance of the activation energy will be discussed in the next section.

The most significant data concerning temperature dependence have been taken on samples sintered at 700°C. In this case the activation energy is 1.48 ev, as shown in Figs. 3 and 4, in the temperature range from 700°C to about 350°C when the rate of temperature change is sufficiently slow so that oxygen equilibrium is maintained. At lower temperatures the activation energy fluctuates widely about the value 0.60 ev. During very quick runs in which the specimen is taken from 700°C to 375°C in about 4 minutes, the activation energy is 0.65 ev below 20 cm of Hg oxygen pressure and is 0.96 ev in some samples at higher pressures.

As already mentioned, the conductivity at low temperatures depends very much on the temperature and oxygen pressure at sintering. These factors affect the log σ *versus* $1/T$ curves on the initial heating of a quenched specimen from room temperature in the manner shown in Fig. 3. It may be seen that there is a dip, or at least a plateau, in the curve at about 300°C. The precise character of this dip depends upon both the temperature and oxygen pressure at sintering. The low temperature conductivity, despite variations, is in all cases lower after heating than before.

F. The Conductivity as a Function of Oxygen Pressure

There are a few semiconductors in which at higher temperatures there is observed an intrinsic electronic conductivity.[5] It frequently happens, however, that at least part of the conductivity depends on the surrounding gas atmosphere.[6] In such cases the conductivity is related to the presence of a stoichiometric excess of one of the constituent atoms. This concentration of stoichiometric-excess atoms in the semiconductor is proportional to some power of the partial pressure of one of the constituents of the semiconductor in the surrounding atmosphere. In excess semiconductors in which there is conduction by electrons this is a negative power, whereas in defect semiconductors in which holes conduct it is a positive power. The particular law which applies in a given case gives a hint concerning the chemical reaction which produces the conducting units in the semiconductor. In zinc oxide, for example, the conductivity varies inversely as the fourth root of the oxygen pressure. This indicates that zinc atoms are formed and oxygen molecules released. In the case of zinc oxide, however, it is not possible to tell immediately whether nearly all or only a few of the zinc atoms lose their electrons to the conduction band, since both possibilities lead to the one-fourth law.[7]

The case of lead chromate is more complicated than the usual case of the metallic oxide, because a chromate radical replaces the simpler oxygen ion. However, the steps used to compute the oxygen dependence associated with an assumed reaction are the same as in the simpler cases. As we shall see, there is reason for assuming that a small number of lead chromate molecules dissociate according to the reaction:

$$2PbCrO_4 \rightarrow Pb(CrO_2)_2 + Pb^0 + 2O_2$$

or

$$Pb^{++} + 2CrO_4^{--} \rightarrow 2CrO_2^{-} + Pb^0 + 2O_2.$$

There are formed in this way n_b neutral lead

[5] H. Dünwald, H. H. von Baumbach, and C. Wagner, Zeits. f. physik. Chemie **B22**, 226 (1933).
[6] K. Baedacker, Ann. d. Physik **22**, 749 (1907); **29**, 566 (1909); Baedacker, Physik. Zeits. **9**, 431 (1908); **13**, 1080 (1912); C. Wagner, Physik. Zeits. **36**, 721 (1935); B. Gudden, Ergeb. d. exact. Naturwiss. **13**, 223 (1934).
[7] P. H. Miller, Phys. Rev. **60**, 890 (1941).

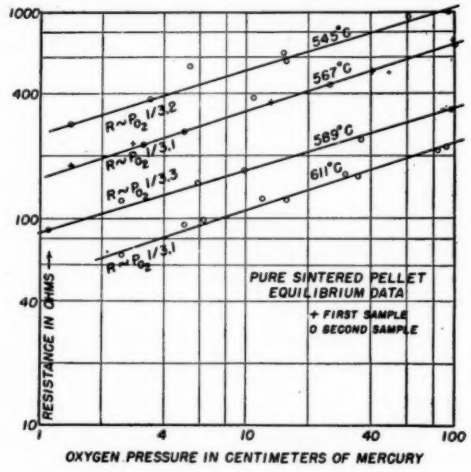

FIG. 5. Resistance-pressure curves.

atoms which probably occupy interstitial positions. n_b may be calculated as follows.

We make the assumption that the crystal is in thermodynamic equilibrium at the temperature T. This requires that the free energy shall be a minimum. The free energy A is made up of the following terms: (1) the energy required to produce the above reaction; (2) the free energy of the vacancies in the positive ion lattice; (3) the free energy associated with the chromite, CrO_2^-, ions; and (4) the free energy of the oxygen molecules. Thus

$$A=n_b\epsilon_b+kTn_b \ln (n_b/N)+2kTn_b \ln (2n_b/N) +kT(N_0+2n_b) \ln N_0+2n_b/C,$$

where ϵ_b is the energy of the foregoing chemical reaction, N is the number of molecules of lead chromate composing the lattice, N_0 is the number of molecules of oxygen in the gas surrounding the crystal, and C is a constant.[8] It follows that for the free energy to be a minimum n_b must satisfy the following condition

$$n_b \propto N_0^{-\frac{1}{3}} \exp (-\epsilon_b/3kT) \propto P_0^{-\frac{1}{6}} \exp (\epsilon_b/3kT)$$

since N_0 is proportional to the partial pressure of the oxygen and provided that $n_b \ll N_0$.

At a particular temperature, n_f of these n_b lead atoms will be ionized:

$$Pb^0 \rightarrow Pb^+ + e.$$

The number n_f of free electrons thus produced may be calculated with the assumption of thermodynamic equilibrium following the procedure outlined above. This leads to the condition

$$n_f \propto n_b^{\frac{1}{2}} \exp (-\epsilon_f/2kT)$$

provided $n_f \ll n_b$. Therefore, since the conductivity σ is proportional to n_f,

$$\sigma \propto P_0^{-\frac{1}{12}} e^{-\epsilon/kT}$$

where $\epsilon=\epsilon_f/2+\epsilon_b/6$.

We now see the significance of the activation energies of the previous section. They consist of two terms. One arises from the energy necessary to produce the chemical reaction and the other comes from the energy necessary to produce the ionization reaction. Both of these terms enter when the rate of temperature change is such as to maintain oxygen equilibrium, so that we must set $\epsilon_f/2+\epsilon_b/6$ equal to 1.48 ev. When the temperature is changed very rapidly, however, the slower chemical reaction is suppressed to a great extent, so that the activation energy depends mainly on the ionization reaction. Therefore $\frac{1}{2}\epsilon_f$ lies between 0.96 and 0.65 ev. In the opinion of the writer the lower value is the most reliable. This is indicated by the fact that at low temperatures where the chemical reaction is almost completely suppressed the activation energy is about 0.60 ev (Fig. 3). Using 0.60 ev for $\frac{1}{2}\epsilon_f$ it follows that ϵ_f is 1.20 ev and ϵ_b is 5.28 ev.

If the assumption that lead chromate dissociates according to the equations given above is valid, we should expect lead chromate to be an excess electronic conductor and should therefore expect that the conductivity would decrease with increasing oxygen pressure. This in fact is found to be the case. Measurements of the oxygen dependence of the conductivity were made around 600°C. The results are shown in Fig. 5. It is found that the conductivity obeys the law:

$$\sigma \propto P_0^{-1/3.1}$$

which is very close to the foregoing theoretical law, namely:

$$\sigma \propto P_0^{-\frac{1}{6}}.$$

The reaction which leads to this theoretical law was chosen from a number of possible reactions as being the most likely. It should be noted that

[8] C is approximated by $(2\pi mkT)^{\frac{1}{2}}V/h^3$ where m, k, T, and h have the usual meaning and V is the volume of the containing vessel; see F. Seitz, reference 1, p. 462.

lead chromate becomes green on being heated in the absence of oxygen. This color must be assumed to come from trivalent chromium, which supports the preceding reaction.

It is of interest to note that if most of the interstitial lead atoms are ionized, thermodynamic considerations would predict

$$\sigma \propto P_0^{-\frac{1}{4}}.$$

G. The Ionic or Electronic Nature of the Conducting Carriers

The foregoing discussion indicates that lead chromate is a normal electronic conductor. Transport measurements of the type employed by Tubandt[9] have been made to test this directly. The results indicate that the ionic conduction must be less than 1 percent of the total conduction. It must be admitted that there is a slight possibility that blocking layers between the pellets or between the individual grains prevented the ions from migrating to the electrodes. This seems very unlikely, however, since Tubandt's methods have proved successful in so many cases.[10]

Hall effect measurements have also been attempted. However, the results to date have not been reliable because of the high resistance of the samples.

Seebeck effect measurements, on the other hand, indicate clearly that lead chromate is an excess semiconductor. From qualitative measurements the Seebeck e.m.f. per degree is in the neighborhood of 3 millivolts at 50°C. The hotter electrode was positive, so that the conductors are electrons. As a check, the effect was measured in Cu_2O, which is known to be a hole conductor, and it was found that the hotter electrode was negative as it should be. It is interesting to note that the free electron model predicts that the Seebeck e.m.f. should be equal to $\frac{1}{2}\epsilon_f/T$. This gives for the Seebeck e.m.f. at 50°C the value $\frac{1}{2}(1.20/325)$ or about 2 millivolts which is in rough agreement with the measured value.

H. Summary of Results

In the measurement of the electrical conductivity of lead chromate the best results have been obtained with the use of sintered pellets possessing gold electrodes that were evaporated on in vacuum. (1) Such samples have a negligible contact resistance and obey Ohm's law over a large range of voltage and temperature. (2) The conductivity has been found to vary with the temperature in the range from 700°C to 350°C in accordance with the Boltzmann-type law $\sigma \propto \exp(-1.48ev/kT)$, whereas the conductivity obeys the law $\sigma \propto \exp(-0.60ev/kT)$ at lower temperatures. (3) At constant temperature the conductivity increases with decreasing oxygen pressure in accordance with the relation $\sigma \propto P_0^{-1/3.1}$. This relation indicates that lead chromate dissociates in accordance with the equations:

$$2PbCrO_4 \rightarrow Pb(CrO_2)_2 + Pb^0 + 2O_2$$
$$Pb^0 \rightarrow Pb^+ + e.$$

The activation energies for these reactions are probably 5.28 and 1.20 electron volts, respectively. These same reactions may explain the optical darkening process with the optical excitation replacing thermal excitation in producing the darkening substance. (4) Hall effect measurements on sintered pellets have not been reliable; however, transport measurements show that ionic conduction is probably less than 1 percent and Seebeck effect measurements indicate conduction by electrons with a Seebeck e.m.f. of about 3 millivolts per degree. (5) It is concluded that lead chromate is an excess electronic semiconductor.

In conclusion I wish to thank Professor F. Seitz, Dr. P. H. Miller, and Dr. A. W. Lawson for suggesting this problem and for their helpful advice and criticism. I am also indebted to W. Feldman and members of Works Progress Administration Project 25792 for assistance in observation and the Krebs Pigment Department of E. I. du Pont de Nemours and Company for financial assistance.

[9] C. Tubandt, *Handbuch der Experimentalphysik* (1932), Vol. 12, p. 396.

[10] In support of the conclusions drawn here is the recently published article by Selma B. Brody in J. Chem. Phys. **10**, 650 (1942) in which it is concluded from x-ray investigations that lead chromate has a close packed structure and therefore ionic migration is unlikely.

Distance Correlations and Bose-Einstein Condensation

F. LONDON
Department of Chemistry, Duke University, Durham, North Carolina
(Received December 3, 1942)

The correlation effect on the molecular distance distribution in a Bose-Einstein gas is calculated as a function of volume and temperature, particularly for the case of degeneracy (condensation) of the gas. It is shown that, under certain conditions in the condensed state, the density as seen from any one molecule appears, over a rather extended region around it, to be considerably larger than the true density. This result seems to have direct relation to the fact that the low temperature modification of liquid helium has a negative coefficient of thermal expansion.

1. INTRODUCTION

UHLENBECK AND GROPPER[1] have shown that the symmetry properties of the wave functions of an ideal Bose-Einstein and Fermi-Dirac gas involve peculiar distance correlations between the respective force-free gas molecules. In the limiting case of high temperatures they found that the probability of finding a particle within the distance interval $(r, r+dr)$ of a chosen particle is given by:

$$(N/V)\{1\pm\exp(-2\pi r^2/\lambda^2)\}4\pi r^2 dr.$$

Here the plus sign refers to the Bose-Einstein case, the minus sign to the Fermi-Dirac case and λ is the de Broglie wave-length corresponding to the temperature T, $\lambda=h[2\pi mkT]^{-\frac{1}{2}}$.

The formulas above are valid only for high temperatures or small densities, namely, for $V\gg N\lambda^3$. For the Fermi-Dirac gas, Wigner and Seitz[2] have given the distribution function for the opposite limiting case $V\ll N\lambda^3$ (strong degeneracy), where the distribution becomes independent of temperature:

$$\frac{N}{V}\left\{1-9\left[\frac{2\pi k_0 r\cos 2\pi k_0 r-\sin 2\pi k_0 r}{2\pi k_0 r}\right]^2\right\}4\pi r^2 dr.$$

Here k_0 is the wave number per cm at the top of the Fermi distribution i.e. $(4\pi/3)k_0^3 V=N$.

A general scheme of the statistical thermodynamics of the density matrix has recently been given by Kofink.[3]

In this paper we will explicitly calculate this correlation effect for a Bose-Einstein gas at *all* temperatures. One may expect that the peculiar condensation phenomenon, by which the degeneracy of the B. E. gas is distinguished, will have some characteristic consequence on the distance correlations. We shall show that, under certain conditions in the condensed state, the density as seen from any one molecule appears, over a rather extended region around it, to be larger than the true density. This peculiar phenomenon seems to have direct relation to the singular fact that liquid helium has a negative coefficient of thermal expansion below the so-called λ-point (2.186°K).[4] While there are still other indications which support the view that the λ transition of liquid helium corresponds in some way to the condensation phenomenon of a Bose-Einstein gas,[5,5a] we will not, in this paper, attempt to substantiate this idea in greater detail and shall restrict ourselves to only qualitatively discussing the possible connection between the condensation phenomenon of the B.E. statistics and the anomalous sign of the coefficient of thermal expansion of liquid He.

[1] G. E. Uhlenbeck and L. Gropper, Phys. Rev. **41**, 79 (1932).
[2] E. Wigner and F. Seitz, Phys. Rev. **43**, 804 (1933).
[3] W. Kofink, Ann. d. Physik **28**, 264 (1937).
[4] W. H. and A. P. Keesom, Physica **1**, 128 (1933).
[5] F. London, Nature **141**, 643 (1938); Phys. Rev. **54**, 947 (1938).
[5a] L. Tisza, Nature **141**, 913 (1938); Comptes Rendus **207**, 1187 (1938).

2. DISTANCE DISTRIBUTION IN AN IDEAL BOSE-EINSTEIN GAS

The symmetric eigenfunction Ψ of N identical B.E. particles, of which n_ρ are assumed to be in the quantum state ρ with the single particle eigenfunction, ψ_ρ, can be written in the form

$$\Psi_{n_0,\, n_1 \cdots n_\rho \cdots}^{(\mathbf{r}_1, \mathbf{r}_2 \cdots \mathbf{r}_N)} = [1/(N! n_0! n_1! n_2! \cdots n_\rho! \cdots)^{\frac{1}{2}}] \sum_Q \psi_0(\mathbf{r}_1)\psi_0(\mathbf{r}_2)\cdots\psi_0(\mathbf{r}_{n_0})\psi_1(\mathbf{r}_{n_0+1})\cdots\psi_1(\mathbf{r}_{n_0+n_1})\cdots. \quad (1)$$

Here $\sum_Q$ means the sum over all $N!$ permutations of the particle numbers. The factor outside is chosen so that the eigenfunction Ψ is normalized to the value 1 if the single particle eigenfunctions ψ_ρ are normalized to the same value.

Now let the ψ_ρ be the eigenfunction of a free particle of the momentum $\mathbf{k}_\rho h$ in a box of volume V with periodic boundary conditions

$$\psi_\rho = V^{-\frac{1}{2}} e^{2\pi i \mathbf{k}_\rho \cdot \mathbf{r}} \quad (2)$$

and let us calculate the probability $P(\mathbf{r}_1, \mathbf{r}_2)$ of the configuration $(\mathbf{r}_1, \mathbf{r}_2)$ of the two particles 1 and 2. Because of the symmetry of Ψ it is immaterial which ones are chosen:

$$P(\mathbf{r}_1, \mathbf{r}_2) = \int \cdots \int \left| \Psi_{n_0,\, n_1,\, \cdots n_\rho \cdots}^{(\mathbf{r}_1, \mathbf{r}_2 \cdots \mathbf{r}_N)} \right|^2 d\tau_3 d\tau_4 \cdots d\tau_N.$$

One obtains:

$$P(\mathbf{r}_1, \mathbf{r}_2) = \frac{1}{V^2}\left\{1 + \frac{2}{N(N-1)} \sum_{\rho<\sigma} n_\rho n_\sigma \cos 2\pi(\mathbf{k}_\rho - \mathbf{k}_\sigma)\cdot(\mathbf{r}_1 - \mathbf{r}_2)\right\}. \quad (3)$$

Here it must be observed that the $\sum_{\rho<\sigma}$ has to be taken so as to contain each pair of states $\rho \neq \sigma$ just *once*.

Let us now calculate the mean value of $P(\mathbf{r}_1, \mathbf{r}_2)$ at the temperature T. It is well known[6] that $\langle n_\rho n_\sigma \rangle_{Av} = \bar{n}_\rho \bar{n}_\sigma$ for $\rho \neq \sigma$. It would further be convenient if we could sum over ρ and σ independently. We are allowed to do so in Eq. (3) if we subsequently subtract the terms $\rho = \sigma$ and divide by 2 for $\rho \neq \sigma$. Thus we may write

$$\langle P(\mathbf{r}_1, \mathbf{r}_2)\rangle_{Av} = \frac{1}{V^2}\left\{1 + \frac{1}{N(N-1)}\left[\sum_{\rho,\sigma} \bar{n}_\rho \bar{n}_\sigma \cos 2\pi(\mathbf{k}_\rho - \mathbf{k}_\sigma)\cdot(\mathbf{r}_1 - \mathbf{r}_2) - \sum_\rho \bar{n}_\rho{}^2\right]\right\}.$$

Since the distribution in temperature equilibrium is isotropic we may first take the average over the orientation of $\mathbf{k}_\rho$ and $\mathbf{k}_\sigma$ for fixed values of $\mathbf{k}_\rho = |\mathbf{k}_\rho|$ and $\mathbf{k}_\sigma = |\mathbf{k}_\sigma|$ separately. In this way the mean value over the angles:

$$\langle \cos 2\pi(\mathbf{k}_\rho - \mathbf{k}_\sigma)\cdot(\mathbf{r}_1 - \mathbf{r}_2)\rangle_{Av} = \frac{\sin 2\pi k_\rho |\mathbf{r}_1 - \mathbf{r}_2|}{2\pi k_\rho |\mathbf{r}_1 - \mathbf{r}_2|} \cdot \frac{\sin 2\pi k_\sigma |\mathbf{r}_1 - \mathbf{r}_2|}{2\pi k_\sigma |\mathbf{r}_1 - \mathbf{r}_2|}$$

is easily calculated and one obtains:

$$\langle P(\mathbf{r}_1, \mathbf{r}_2)\rangle_{Av} = \frac{1}{V^2}\left\{1 + \frac{1}{N(N-1)}\left[\left(\sum_\rho \bar{n}_\rho \frac{\sin 2\pi k_\rho r}{2\pi k_\rho r}\right)^2 - \sum_\rho \bar{n}_\rho{}^2\right]\right\}.$$

This expression depends only on the relative distance $r = |\mathbf{r}_1 - \mathbf{r}_2|$ of the two particles, not on their center of gravity. Integrating over the latter, we obtain a factor V. Finally, since everything is symmetric in all particles, we may multiply by $N-1$ (or as well by N, since we assume $N \gg 1$) in order to obtain the mean number of particles per volume unit or the particle density $D(r)$ at the distance r of any given particle:

$$D(r) = \frac{N}{V}\left\{1 + \frac{1}{N^2}\left[\left(\sum_\rho \bar{n}_\rho \frac{\sin 2\pi k_\rho r}{2\pi k_\rho r}\right)^2 - \sum_\rho \bar{n}_\rho{}^2\right]\right\}. \quad (4)$$

[6] E. Schrödinger, Physik. Zeits. **27**, 95 (1926).

We will now calculate the density $D(r)$ by assuming for $\bar{n}_\rho$ the B.E. distribution

$$\bar{n}_\rho=[\exp(\beta\epsilon_\rho+\alpha)-1]^{-1}=[\exp(\pi\lambda^2k_\rho^2+\alpha)-1]^{-1} \tag{5}$$

where $\beta=(kT)^{-1}=2\pi m\lambda^2/h^2$ and $\epsilon_\rho=k_\rho^2h^2/2m$. The quantity α is defined by the condition:

$$N=\sum_\rho \bar{n}_\rho=\sum_\rho [\exp(\pi\lambda^2k_\rho^2+\alpha)-1]^{-1}. \tag{6}$$

In this relation (6) we may replace the sum over ρ by the integral $\int_0^\infty \cdots 4\pi Vk^2dk$. However, care must be taken as to the term referring to the ground state $k_0=0$, as this has to be considered separately. This state would obtain the incorrect statistical weight 0 instead of 1, if it were regarded as included in the integral.[5] For the other low states the discrepancy between the true value and the asymptotic formula, $4\pi Vk^2dk$, for the number of quantum states in the wave number interval $(k, k+dk)$ is of no consequence. Thus we may write for (6)

$$\begin{aligned} N&=[e^\alpha-1]^{-1}+\int_0^\infty [\exp(\pi\lambda^2k^2+\alpha)-1]^{-1}4\pi Vk^2dk \\ &=[e^\alpha-1]^{-1}+V/\lambda^3\sum_{l=1}^\infty l^{-\frac{3}{2}}e^{-l\alpha}. \end{aligned} \tag{6'}$$

The term $[e^\alpha-1]^{-1}$ refers to the contribution $\bar{n}_0$ of the particles in the ground state $k_0=0$.

Similarly, by separately taking account of the ground state, we may now calculate the sum

$$\begin{aligned} \sum_\rho \bar{n}_\rho\frac{\sin 2\pi k_\rho r}{2\pi k_\rho r}&=\bar{n}_0+\int_0^\infty [\exp(\pi\lambda^2k^2+\alpha)-1]^{-1}\frac{\sin 2\pi kr}{2\pi kr}4\pi Vk^2dk \\ &=\bar{n}_0+\frac{2V}{r}\sum_{l=1}^\infty e^{-l\alpha}\int_0^\infty \exp(-\pi l\lambda^2k^2)\sin(2\pi kr)kdk \\ &=\bar{n}_0+V/\lambda^3\sum_{l=1}^\infty l^{-\frac{1}{2}}\exp(-l\alpha-\pi r^2/l\lambda^2) \end{aligned} \tag{7}$$

and the sum:

$$\begin{aligned} \sum_\rho \bar{n}_\rho{}^2&=\bar{n}_0{}^2+\int_0^\infty [\exp(\pi\lambda^2k^2+\alpha)-1]^{-2}4\pi Vk^2dk \\ &=\bar{n}_0{}^2+V/\lambda^3\sum_{l=1}^\infty (l^{-\frac{1}{2}}-l^{-\frac{3}{2}})e^{-l\alpha} \end{aligned} \tag{8}$$

or, because of (6′),

$$=\bar{n}_0{}^2+V/\lambda^3\sum_{l=1}^\infty l^{-\frac{3}{2}}e^{-l\alpha}-(N-\bar{n}_0).$$

We introduce into (4) the values given by (8) and (7) and obtain, with $D_\infty=N/V$ and $x=\pi r^2/\lambda^2$,

$$D(x)=D_\infty\left\{1+\frac{1}{N^2}\left[\left(\bar{n}_0{}^2+V/\lambda^3\sum_{l=1}^\infty l^{-\frac{3}{2}}e^{-l\alpha-x/l}\right)^2-\bar{n}_0{}^2-\bar{n}_0+N-V/\lambda^3\sum_{l=1}^\infty l^{-\frac{3}{2}}e^{-l\alpha}\right]\right\}. \tag{9}$$

When determining α (or $\bar{n}_0=[e^\alpha-1]^{-1}$) by Eq. (6′) we have to distinguish between two essentially different cases, depending on whether

$$N\lambda^3/V<\sum_{l=1}^\infty l^{-\frac{3}{2}}=2.612$$

or $N\lambda^3/V>2.612$. In terms of the "condensation temperature" T_0,

$$T_0=\frac{h^2}{2\pi mk}\left(\frac{N}{2.612\,V}\right)^{\frac{2}{3}} \tag{10}$$

the two cases correspond to the alternative $T>T_0$ and $T<T_0$, respectively.

(a) If $T>T_0$, then Eq. (6′) is satisfied by α of the order 1. In this case the term $[e^{\alpha}-1]^{-1}=\bar{n}_0$ in (6′) is also of the order of 1, i.e., very small compared with N and may be neglected and we may write the Eq. (6) simply:

$$N=V/\lambda^3\sum_{l=1}^{\infty} l^{-\frac{3}{2}}e^{-l\alpha}$$

or, because of (10)

$$(T_0/T)^{\frac{3}{2}}=\frac{1}{2.612}\sum l^{-\frac{3}{2}}e^{-l\alpha} \text{ for } T\geqslant T_0. \tag{6a}$$

Accordingly in (9) the quantity $\bar{n}_0$ may, for $T\geqslant T_0$, be completely ignored.

(b) If, however, $T<T_0$, then (6) requires α to be extremely small, *viz.*, of the order $1/N$. In this case the sum of (6′) can be replaced by its value for $\alpha=0$, *viz.*,

$$\sum_{l=1}^{\infty} l^{-\frac{3}{2}}=2.612,$$

and $\bar{n}_0=(e^{\alpha}-1)^{-1}$ may be replaced by $1/\alpha$. One obtains for (6′)

$$N=1/\alpha+2.612\,V/\lambda^3$$

or, because of (10),

$$1/\alpha=\bar{n}_0=N[1-(T/T_0)^{\frac{3}{2}}] \text{ for } T\leqslant T_0, \tag{6b}$$

i.e., for $T<T_0$, a finite fraction of all particles is in the single state $k_0=0$.

Considering (9) we notice that the series

$$\sum_{l=1}^{\infty} l^{-\frac{3}{2}}e^{-l\alpha}$$

diverges for $\alpha=0$. However, we need the series rather for very small $\alpha(\sim 1/N)$, not for $\alpha=0$. For such small values of α we may replace the $\sum_l$ by an integral over $(l\alpha)$ and calculate its asymptotic value:

$$\sum_{l=1}^{\infty} l^{-\frac{3}{2}}e^{-l\alpha}\sim\alpha^{-\frac{3}{2}}\int_0^{\infty}(l\alpha)^{-\frac{3}{2}}e^{-(l\alpha)}d(l\alpha)=(\pi/\alpha)^{\frac{1}{2}} \text{ (for } \alpha\ll 1).$$

Taking α from (6b) we obtain:

$$\sum_{l=1}^{\infty} l^{-\frac{3}{2}}e^{-l\alpha}=(\pi N)^{\frac{1}{2}}[1-(T/T_0)^{\frac{3}{2}}]^{\frac{1}{2}} \text{ for } T<T_0. \tag{11}$$

For temperatures $T>T_0$ the quantity α is of the order of one and consequently the value of the series $\sum l^{-\frac{3}{2}}e^{-l\alpha}$ itself is of the order of one.

The term

$$(V/N^2\lambda^3)\sum_{l=1}^{\infty} l^{-\frac{3}{2}}e^{-l\alpha}$$

in (9) will, therefore, be of the order $N^{-\frac{1}{2}}$ for $T<T_0$ and even of the order N^{-1} for $T>T_0$; in each case it is negligible compared to 1 and may be omitted in (8) and in (9).

Let us finally define the function

$$\varphi(V,T)=\frac{2.612\,V}{N\lambda^3}=(T/T_0)^{\frac{3}{2}}=V/V_0 \tag{12}$$

where $V_0=(N/2.612)(h^2/2\pi mkT)^{\frac{3}{2}}$ is the volume at which, at the temperature T, Bose-Einstein condensation appears; further put

$$Q(\alpha, x)=\frac{1}{2.612}\sum_{l=1}^{\infty} l^{-\frac{3}{2}}e^{-l\alpha-x/l}. \tag{13}$$

Omitting in Eq. (9) the terms found to be negligible we now summarize the foregoing remarks and obtain for $D(r)$:

$$D(r)=\begin{cases} D_\infty[1+\varphi^2 Q^2(\alpha, \pi r^2/\lambda^2)] & \text{for } \varphi \geqslant 1 \\ D_\infty[1+(1-\varphi+\varphi Q(0, \pi r^2/\lambda^2))^2-(1-\varphi)^2] & \text{for } \varphi \leqslant 1. \end{cases} \tag{14}$$

In Fig. 1 the function $D(r)/D_\infty$ is drawn for different temperatures and for a fixed value of V. The unit of length chosen is $\lambda(T_0)=h[2\pi mkT_0]^{-\frac{1}{2}}=(2.612V/N)^{\frac{1}{3}}$. Conceived as a function of φ and λ (i.e., of V and T) for fixed r the function $D(r, \varphi, \lambda)$ and its first derivatives are continuous everywhere, but the second derivatives of D are discontinuous at the transition curve ($\varphi=1$) for any value of r.

The asymptotic behavior of $D(r)$ for $r\gg\lambda$ is very different in the cases $T>T_0$ and $T<T_0$. In either case we may obtain asymptotic formulas if we notice that, for $x\gg 1$, the lowest terms of the series for $Q(\alpha, x)$ (Eq. (13)) with an index $l\ll x$ are smaller than $e^{-x/l}$ and may be neglected. Further, the subsequent terms with an index $l\sim x$ and $l>x$ vary so smoothly with l that we may replace

$$\sum_{l=1}^{\infty} \quad \text{by} \quad \int_0^{\infty}\cdots dl.$$

In this way we obtain, for $x\gg 1$:

$$Q(\alpha, x\gg 1)\approx\frac{1}{2.612}\int_0^{\infty} l^{-\frac{3}{2}}e^{-l\alpha-x/l}dl=\frac{1}{2.612}(\pi/x)^{\frac{1}{2}}\exp\left[-2(\alpha x)^{\frac{1}{2}}\right]. \tag{15}$$

For $\alpha>0$ or $T>T_0$, therefore, $D(r)-D_\infty$ disappears exponentially for large r/λ namely like $1/r\exp\left[-4r/\lambda(\pi\alpha)^{\frac{1}{2}}\right]$. For $T=T_0$, however, $D(r)-D_\infty$ behaves asymptotically like $1/r^2$; finally, for $T<T_0$, $D(r)-D_\infty$ behaves like $1/r$.

In the case $T>T_0$, the excess of particles around a chosen one is finite, i.e., independent of the total number N. The number of these excess particles is easily calculated to be

$$\varphi/2.612\sqrt{8} \text{ for } T\gg T_0,$$
$$2\pi\varphi^2/2.612^2(\varphi-1)-1 \text{ for } 0<T-T_0/T_0\ll 1.$$

In the case $T=T_0$ this excess is of the order $N^{\frac{1}{3}}$ and for $T<T_0$ it is of the order $N^{\frac{2}{3}}$.

3. VAN DER WAALS EXCHANGE INTERACTION

The distance correlations which we discussed in the preceding paragraph and the departure of the ideal B.E. gas from the behavior of an ordinary ideal gas are both only different sides of the same matter and thus far our present investigation can, of course, not add anything new to the thermodynamics of an ideal B.E. gas. These correlations may, however, make themselves felt if there is an intermolecular force field insofar as they may give a distinguished weight to those distances where the Van der Waals field is noticeable. This will affect the resultant interaction in a very different way in the cases of the degenerate and of the non-degenerate state.

L. I. Schiff[7] has made a very general investigation of the degeneracy of a non-ideal B.E. gas in which he develops the grand partition function of the system in subsequent steps by considering, in close analogy to the method of Ursell, the consecutive multiple clusters of particles separately.

[7] L. I. Schiff, Phys. Rev. **59**, 751, 758, 927 (1941); *ibid.* **60**, 362 (1941); see also W. E. Lamb jr. and A. Nordsiek, *ibid.* **59**, 927 (1941).

This method is entirely rigorous and should, at least in principle, contain the answer to every thing that could be asked about the influence of interaction forces on the B. E. condensation. However, it is scarcely possible actually to calculate a higher approximation than that which corresponds to the second virial coefficient (binary clusters). It is obvious, however, that cooperative phenomena, like a condensation, cannot satisfactorily be discussed on the basis of a consideration of binary clusters only. Their investigation certainly requires the consideration of the whole of *all* virial coefficients and their convergence properties similar to that which has been developed in the theory of condensation by Mayer and others.[8]

Since we must probably forego any hope, for the present at least, of finding a higher approximation of the Ursell-Schiff development we might try to choose an approach which, though less rigorous, allows one to account more directly for the simultaneous interaction of many neighboring particles. There is the method, which has been applied by Heisenberg and more specifically by Bloch[9] in the theory of ferromagnetism, which offers itself rather immediately to the present problem. While there is no question about the fact that this method is quite crude and, still worse, that it is rather difficult to say in which sense it can be considered as an approximation, it has, in the case of ferromagnetism at least, served to sketch a very simple picture of what certainly is the essential mechanism for the establishment of that cooperative phenomenon. This method consists in taking, as a basis, the first step of the quantum mechanical perturbation development in the following sense: any state of the ensemble is represented by an eigenfunction of "zero order," built up, like our function $\Psi^{(r_1, r_2, \cdots r_N)}_{n_0, n_1, \cdots n_\rho \cdots}$ in Eq. (1), by the eigenfunctions of isolated single particles. This eigenfunction Ψ itself does not account for the interaction forces except implicitly insofar as it has been given the "right symmetry" so that it might be thought of as continuously deforming into the true eigenfunction if the interaction were continuously introduced. Thus the state of the ensemble can still be described by the numbers n_ρ giving the distribution of particles in the single particle state ρ and by the symmetry character of Ψ. The presence of interaction forces is, however, explicitly considered by the *energy* attributed to this state, in that for this energy is taken the quantum mechanical mean value of the total energy H (including the interaction energy) in the configuration $\Psi_{n_0, n_1, n_2 \cdots n_\rho \cdots}$. This mean value is given by

$$E(n_0, n_1, n_2 \cdots n_\rho \cdots) = \int \Psi^*_{n_0, n_1 \cdots n_\rho \cdots} [H, \Psi_{n_0, n_1 \cdots n_\rho}] d\tau_1, d\tau_2 \cdots d\tau_N \tag{16}$$

which is, in fact, the so-called first-order approximation for the energy. One may now develop the statistics for the $n_0, n_1 \cdots n_\rho \cdots$ in the usual way by utilizing the above approximation for the energy.

Let us assume as Hamilton function

$$H = \frac{1}{2m} \sum_k p_k^2 + \sum_{i<k} W(r_{ik}) \tag{17}$$

where $W(r_{ik})$ is the potential of the intermolecular forces, assumed as additive central forces, between the particles i and k. The approximate energy value (16) of a state characterized by the distribution $n_0, n_1 \cdots n_\rho \cdots$, i.e., by the Ψ-function (1), is given by

$$E(n_0, n_1, \cdots n_\rho \cdots) = \sum n_\rho \epsilon_\rho + U(n_0, n_1, \cdots n_\rho, \cdots)$$

where $\epsilon_\rho = k_\rho^2 h^2/2m$ and

$$U(n_0, n_1 \cdots n_\rho \cdots) = \sum_{i<k} \int W(r_{ik}) \, |\Psi^{(r_1, r_2 \cdots r_N)}_{n_0, n_1 \cdots n_\rho \cdots}|^2 d\tau_1 d\tau_2 \cdots d\tau_N.$$

Because of the symmetry of H and Ψ in all particles all $\frac{1}{2}N(N-1)$ terms of the sum $\sum_{i<k}$ have the

[8] J. E. Mayer, and S. F. Harrison, J. Chem. Phys. **6**, 87, 101 (1938); M. Born and K. Fuchs, Proc. Roy. Soc. **A166**, 391 (1938); B. Kahn and G. E. Uhlenbeck, Physica **5**, 399 (1938).

[9] F. Bloch, Zeits. F. Physik **57**, 546 (1929).

same value. By using (2) and (3) we obtain:

$$U(n_0, n_1 \cdots n_\rho \cdots) = \frac{1}{2}N(N-1)\frac{1}{V^2}\int W(r_{12})\left\{1+\frac{2}{N(N-1)}\sum_{\rho<\sigma} n_\rho n_\sigma \cos 2\pi(\mathbf{k}_\rho-\mathbf{k}_\sigma)\cdot(\mathbf{r}_1-\mathbf{r}_2)\right\}d\tau_1 d\tau_2.$$

Therefore we may write:

$$E(n_0, n_1, \cdots n_\rho \cdots) = \sum_\rho n_\rho \epsilon_\rho + \frac{N(N-1)}{2}W_0 + \tfrac{1}{2}\sum_{\rho\neq\sigma} n_\rho n_\sigma W_{\rho\sigma} \tag{18}$$

where

$$W_0 = \frac{4\pi}{V}\int_0^\infty W(r) r^2 dr \tag{19}$$

is the "classical" mean value of the van der Waals energy per pair, whereas the quantities

$$\begin{aligned} W_{\rho\sigma} &= \frac{1}{2}\int W(r_{12})[\psi_\rho(r_1)\psi_\sigma^*(r_1)\psi_\rho^*(r_2)\psi_\sigma(r_2)+\psi_\rho^*(r_1)\psi_\sigma(r_1)\psi_\rho(r_2)\psi_\sigma^*(r_2)]d\tau_1 d\tau_2 \\ &= \frac{1}{V}\int W(r)\cos 2\pi(\mathbf{k}_\rho-\mathbf{k}_\sigma)\cdot\mathbf{r}\,d\tau \end{aligned} \tag{20}$$

are the "exchange integrals" which account for the correlations of the B.E. statistics. In the Fermi-Dirac case they would appear in the energy expression with negative sign or, if there is a spin, with both signs depending on the relative spin-orientation, and would give rise, eventually, to ferromagnetism.

Since we assume the molecular forces to be central forces, we may integrate, in (20), over all orientations and obtain:

$$W_{\rho\sigma} = \frac{4\pi}{V}\int_0^\infty W(r)\frac{\sin 2\pi|k_\rho-k_\sigma|r}{2\pi|k_\rho-k_\sigma|r}r^2 dr. \tag{20'}$$

4. PRELIMINARY DISCUSSION OF THE EQUILIBRIUM DISTRIBUTION

Let us now consider the distribution for thermal equilibrium taking the energy (18) as a basis. The condition for the most probable distribution, $\hat{n}_0, \hat{n}_1, \cdots \hat{n}_\rho \cdots$, leads to the following system of simultaneous equations:

$$\ln\frac{\hat{n}_\rho+1}{\hat{n}_\rho} = \beta\partial E/\partial n_\rho + \alpha$$

or with (18):

$$kT\ln\frac{\hat{n}_\rho+1}{\hat{n}_\rho} = \epsilon_\rho + \sum_{\sigma\neq\rho}\hat{n}_\sigma W_{\sigma\rho} + \alpha kT. \tag{21}$$

It seems rather difficult to solve the system of Eqs. (21) in full generality. We may, however, gather some information from a discussion of their solution at $T=0°\mathrm{K}$, which solution can be found easily. We may presume that the $W_{\sigma\rho}$ which, in this case, come in question belong to very small momenta k_ρ and k_σ so that $|k_\rho-k_\sigma|r$ will be very small compared with 1 for all values of r for which $W(r)$ is noticeably different from zero. Indeed we may verify this assumption once we have found the solution. Then we may replace the sin in (20′) by its argument and obtain $W_{\rho\sigma}\sim W_0$ for all ρ and σ which come in question. Further it appears reasonable to presume that W_0 is negative, $W_0=-|W_0|$, since it is an average taken over an, in general, attractive field. Thus we may write, for sufficiently low temperature, instead of (21) simply

$$\begin{aligned} kT\ln\frac{\hat{n}_\rho+1}{\hat{n}_\rho} &= \epsilon_\rho - |W_0|\sum_{\sigma\neq\rho}\hat{n}_\sigma + \alpha kT \\ &= \epsilon_\rho - |W_0|(N-\hat{n}_\rho) + \alpha kT \end{aligned}$$

or with the notation $\mu = -\alpha kT + N|W_0|$

$$kT\ln\frac{\hat{n}_\rho+1}{\hat{n}_\rho} = \epsilon_\rho - \mu + \hat{n}_\rho|W_0| \tag{21'}$$

from which equations, in the limit $T\to 0$, the quantities $\hat{n}_\rho\to n_\rho^0$ and $\mu\to\mu^0$ are easily determined:

$$n_\rho^0 = \begin{cases} \dfrac{(\mu^0-\epsilon_\rho)}{|W_0|} & \text{for } \epsilon_\rho < \mu^0 \\ 0 & \text{for } \epsilon_\rho \geqslant \mu^0. \end{cases} \tag{22}$$

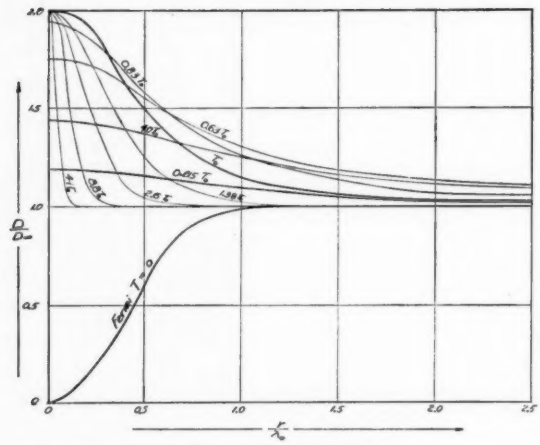

FIG. 1. Density of an ideal Bose-Einstein gas around a given molecule for different temperatures and for fixed volume.

The condition $\sum_\rho n_\rho{}^0 = N$ determines the quantity μ^0:

$$\mu^0 = \left(\frac{h^2}{2m}\right)^{3/5}\left(\frac{15}{8\pi}\frac{N|W_0|}{V}\right)^{2/5}. \tag{23}$$

The energy at absolute zero of the distribution (22), (23) can be evaluated easily:

$$E_{\text{kin}} = \sum n_\rho{}^0 \epsilon_\rho = (3/7)N\mu^0, \tag{24a}$$

$$\begin{aligned} E_{\text{exch}} &= -\tfrac{1}{2}|W_0| \sum_{\rho\neq\sigma} n_\rho{}^0 n_\sigma{}^0 \\ &= -\tfrac{1}{2}|W_0| \sum_\rho n_\rho{}^0 (N - n_\rho{}^0) \\ &= -\tfrac{1}{2}|W_0| (N^2 - \sum_\rho (n_\rho{}^0)^2) \\ &= -\tfrac{1}{2}|W_0| N^2 + (2/7)N\mu^0 \end{aligned} \tag{24b}$$

$$E_{\text{class}} = -\frac{1}{2}N^2|W_0|. \tag{24c}$$

In total we obtain for the energy (18) of the distribution (22) (23):

$$E = -\frac{1}{2}N^2|W_0| + (5/7)N\mu^0. \tag{24}$$

The distribution (22) appears very different from that of the ideal B.E. gas: Instead of being concentrated in a single quantum state the molecules are spread, somewhat similarly to a Fermi distribution, over many quantum states according to the condition $\epsilon_\rho < \mu^0$, which condition together with (23), yields the value k_m for the wave number of the highest occupied state, namely,

$$k_m = \frac{1}{h}(2m\mu^0)^{\frac{1}{2}} = \left(\frac{2m|W_0|}{h^2}\frac{15N}{8\pi V}\right)^{1/5}. \tag{25}$$

However, this spreading over many states is of sub-microscopic extension so to speak, and has no noticeable effect, for example, on the kinetic energy. In order to obtain an estimate of the orders of magnitude in question let us notice that $N(h^2/2m)(15N/8\pi V)^{\frac{1}{2}}$ is of the order of the thermal energy per mole at the transition temperature, say $R\Theta_1$, and that $N^2|W_0|$ also can be presumed to be of the order of a small thermal energy per mole, say $R\Theta_2$, since it corresponds to the contribution of the van der Waals cohesion to the evaporation heat. With these notations the increase of kinetic energy (24a) due to the spreading over the states $k_\rho < k_m$ can be written in the form

$$E_{\text{kin}} = (3/7)N^{-2/5}R\Theta_1{}^{3/5}\Theta_2{}^{2/5}.$$

This shows the kinetic energy is of the order $N^{-2/5}$ times a measurable thermal energy, i.e., negligible.

The number of occupied states can be estimated easily in the same way. It is given by

$$\frac{4\pi}{3}k_m{}^3 V = \frac{5}{2}N^{2/5}\left(\frac{\Theta_2}{\Theta_1}\right)^{3/5} \sim N^{2/5}.$$

The number of molecules in one of the occupied states must accordingly be of the order $N^{3/5}$. For example, from (21) and (22) we obtain for the number of molecules in the lowest state:

$$n_0{}^0 = N^{3/5}(\Theta_1/\Theta_2)^{3/5}. \tag{26}$$

While, with respect to the kinetic energy, the transition to the new distribution (22) involves no noticeable change, it has a considerable effect on the exchange energy. If all molecules were in a single state the exchange energy would be zero, whereas the apparently minute spread over the $N^{2/5}$ states represents a considerably more stable arrangement, since it has an exchange energy of about $-(N^2/2)|W_0|$.

For a temperature $T>0$ the exchange integrals of the excited states, $W_{\rho\sigma}$, will appear in (18), which quantities then can no longer be replaced by W_0. Since $|W_{\rho\sigma}| < |W_0|$, the exchange interaction will have the tendency to favor the B.E.

condensation once the latter is initiated and this might lead to a more pronounced discontinuity at the condensation point than that of an ideal B.E. gas.

5. DISTANCE CORRELATIONS IN THE CASE OF WEAK EXCHANGE INTERACTION

We will now calculate the distance correlations for the modified distribution (22), which may be written in the form

$$n_\rho^0=\begin{cases} n_0^0(1-k_\rho^2/k_m^2) & \text{for } k_\rho \leqslant k_m \\ 0 & \text{for } k_\rho > k_m \end{cases} \qquad (22')$$

where k_m and n_0^0 are given by (25) and (26). If we introduce this distribution into (4), we may easily calculate the summations in question and obtain

$$D(r)=D_\infty\left\{1+\frac{225}{(2\pi k_m r)^{10}}[(3-(2\pi k_m r)^2)\sin(2\pi k_m r) -3(2\pi k_m r)\cos(2\pi k_m r)]^2-\frac{4}{7}\frac{n_0^0}{N}\right\}. \qquad (27)$$

The term $-(4/7)n_0^0/N$, which corresponds to the term $(1/N^2)\sum_\rho n_\rho^2$ in Eq. (4), is negligible compared with 1 since it is of the order $N^{-2/5}$ (see Eq. (26)). For $2\pi k_m r \ll 1$ we may develop the sin and cos in (27) and obtain:

$$D(r)\sim D_\infty\left\{2-\frac{(2\pi k_m r)^2}{7}+\frac{4}{441}(2\pi k_m r)^4-\cdots\right\} \quad \text{for } r\ll(2\pi k_m)^{-1}.$$

Seen from a given molecule it appears as if in the neighborhood within the radius $r\sim(2\pi k_m)^{-1}=N^{1/5}(V/N)^{1/3}(\Theta_1/\Theta_2)^{2/9}$, i.e., of the order of $N^{1/5}$ mean molecular distances, the density of the gas has just the double of its true value. The number of the excess molecules amounts to $(4/7)n_0^0\sim N^{3/5}$. Outside of this region of anomalous density the excess must be, of course, compensated by a corresponding decrease in density below its normal value. This decrease is accounted for by the small term $-(4/7)n_0^0/N$ in (27), which, in this balance, therefore must not be ignored.

It is a characteristic feature of the distribution (22) that its $\sum_\rho n_\rho^2$ is of a smaller order than N^2 (namely $N^{8/5}$ see Eq. (24b)) whereas for the ideal B.E. distribution in the case of degeneracy this sum is of the order N^2 (Eq. (8)). For higher temperatures the distribution will certainly not be more concentrated; hence the $\sum_\rho n_\rho^2$ can only be smaller than its value at 0°K. Thus, it is safe to conclude that $\sum_\rho n_\rho^2$ is *always* to be considered as small compared with N^2 as soon as there is a however feeble interaction with a negative exchange integral.

Accordingly, when we now consider the distance distribution for $T>0$°K, the term in Eq. (4) containing $(1/N^2)\sum_\rho n_\rho^2$ can certainly be regarded as negligibly small and may be omitted. On the other side the sum (7) will have to be recalculated. The integral over the states with an energy of the order of a thermal excitation will be about the same as before. The term $\bar{n}_0$ in (7), however, will now have to be replaced by a sum (or integral) over the states of a "submicroscopic" energy interval containing sin factors with various wave numbers of the order $\sim k_m$ (Eq. (25)). For distances $r\ll k_m^{-1}$ these sin factors can again be replaced by their arguments and in this case, the sum (7) yields the same value as before, again with a finite fraction of N, corresponding to $\bar{n}_0$ in (7), set apart from the integral. For $r\gg k_m^{-1}$, however, these sin terms will cancel each other by interference as in (27), i.e., for $r\gg k_m^{-1}$ the term corresponding to $\bar{n}_0$ in (7) is to be omitted. Observing the preceding remarks we obtain, instead of (14), for $\varphi\leqq 1$:

$$D(r)=\begin{cases} D_\infty[1+(1-\varphi+\varphi Q(0,\pi r^2/\lambda^2))^2] & \\ \qquad\qquad \text{for } r\ll k_m^{-1} & (28a) \\ D_\infty[1+(1-\varphi)^2] \quad \text{for } \lambda\ll r\ll k_m^{-1} & (28b) \\ D_\infty \qquad\qquad \text{for } r\gg k_m^{-1}. & (28c) \end{cases}$$

For $\varphi\geqq 1$ i.e. for the uncondensed state, the distribution is the same as before:

$$D(r)=D_\infty[1+\varphi^2 Q^2(\alpha,\pi r^2/\lambda^2)]. \qquad (28d)$$

In Fig. 2 the distribution (28) has been drawn for different values of T. We see that, in the condensed state, apart from a small region within a radius λ, an observer fixed on a given molecule has the impression of being in a medium, not of the "true" density D_∞, but rather of an "apparent" density $D_\infty[1+(1-\varphi)^2]$. Only in a distance of the order $k_m^{-1}\sim N^{1/5}(V/N)^{1/3}$ does this apparent density decrease to the true value

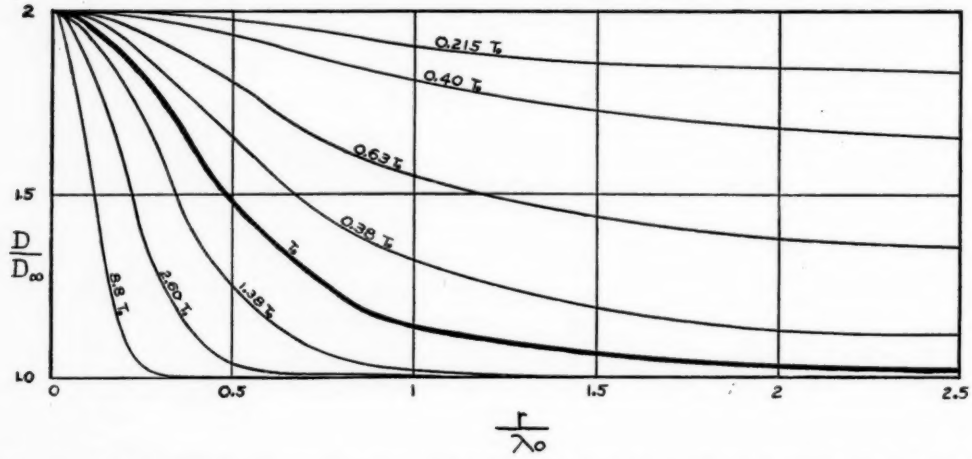

FIG. 2. Density of a Bose-Einstein gas around a given molecule for the limit of a weak van der Waals exchange interaction.

D_∞ (or rather to the slightly smaller value $D_\infty[1-(1/N^2)\sum n_\rho{}^2]$).

The dualism of an "apparent" and a "true" density is not so difficult to picture as it might appear on first view. A simple model which shows distance correlations of the kind in question is represented by the molecular distribution in a piece of Swiss cheese full of holes. In such a cheese infinitely many more molecules are located in the interior of the massive substance, than are found on the surface of a hole. Accordingly the *mean* density around an average molecule is the density of a piece of hole-free cheese. This, however, holds only within a range which is given by the mean distance of a molecule from the next hole. Beyond this distance the mean density relative to a central molecule decreases to the "true value," as it is given by averaging over the holes and the massive substance indiscriminately.

It is significant that in our case the increase in density of the hole-free region, $D_\infty(1-\varphi)^2$, is independent of the strength of the intermolecular energy, but rather determined by the degree of degeneracy, as a pure statistical effect. Only the number and the size of the holes depend on the strength of the van der Waals field, which, therefore, at least in the limit of very weak interaction, is reduced to the role of essentially a surface effect.

CONCLUSION

Comparing the two distribution functions, Fig. 1 and Fig. 2, we notice that there is, in the condensed state, a peculiar instability. Figure 2 represents the limiting case of a very small *negative* exchange integral. It can further be shown that Fig. 1, which we calculated to be the distance distribution of an ideal B.E. gas, moreover represents also the limiting case of a very small *positive* exchange integral. At the transition curve ($\varphi=1$), the discontinuities of D, conceived as a function of φ, are of the same character for the two cases, $W\gtrless 0$ and $W<0$: D and $\partial D/\partial\varphi$ are continuous, but $\partial^2 D/\partial\varphi^2$ is discontinuous for $\varphi=1$ for any value of r (except for $r=0$ and $W_0<0$ where $D=2$ independently of φ).

The increase of $D(r)$ (Eq. (28)) to the value 2 with $r\to 0$ is only a mathematical formality without any physical significance. Actually the intermolecular repulsive forces prevent the molecules from coming nearer than a certain minimum distance, within which $D(r)$ will in reality be practically zero. These repulsive forces are, of course, supposed to be included in the interaction potential $W(r)$; however, they do not obtain explicit expression in the first-order approximation (18) which has been considered exclusively so far. The higher approximations of the perturbation method will, of course, account for the actual impenetrability of the molecules.

On the other hand it is quite clear that our results, which are based on the assumption of wave functions of force free molecules, can certainly not be trusted as valid in distances beyond the mean molecular free path.

In view of these two limitations—with respect

to large as well as small distances—it might appear that our results cannot have much relation to reality. There is, however, some chance that, notwithstanding these limitations, some residue of the distance correlations may be realized by helium—the only substance which is at least liquid for the temperature and density for which B.E. condensation should occur. Tisza[5a] has directed attention to the peculiarity of normal liquid helium (above the λ-point) having a positive temperature coefficient of viscosity ($\partial\eta/\partial T>0$); this is distinctly different from the behavior of the viscosity of any other liquid (which all have a $\partial\eta/\partial T<0$), but quite analogous to the viscosity of a gas. The above fact as well as the relatively very open structure of liquid helium as indicated by its x-ray analysis[10] have been taken to support the view[5] that it might be justified to consider liquid helium (below and above the λ-point) somewhat more similar to a gas than one would be inclined to believe reasonable for liquids in general; thus one might try to interpret the viscosity above the λ-point as due to a typical gas viscosity mechanism with momentum transfer over a *mean free path* rather than of the liquid-viscosity type (with momentum transfer over potential barriers) and, in particular, interpret the peculiar state of He below the λ-point as corresponding to the condensed phase of an ideal B.E. gas.

If then it appears reasonable to speak, with all due reserve, of a mean free path of the molecules in liquid helium it might be worth while to discuss, at least qualitatively, what implications would follow from assuming that there actually exists, within the range of the mean free path around every single molecule, a tendency toward such an increase of density as it is described by our formula (28b) for a degenerating B.E. gas in medium distances from a given molecule.

It is true, the repulsion between the neighbors of the central molecule will actually exert a resistance to such an enormous increase of density and, in addition, the repulsion due to the zero-point energy coming from the quantization of the mean free path[11] will also act in the same direction.

However, this opposition will not necessarily have a prohibitive character. It can rather be expected that a compromise between the two tendencies will be reached: For a fixed volume, the crowding around each central molecule will not be of quite as large an amount and of as wide a range as given by (28b); but there will be at least some crowding. On the other hand, in this somewhat crowded condition the repulsion between the neighbors and the action of the zero-point motion will have an increased effectiveness and this will be felt as an additional pressure necessary for maintaining the volume. This pressure will increase with decreasing temperature, namely with progressing degeneracy. Thus $(\partial p/\partial T)_V$ will be negative for $T<T_0$.

Or to say it differently inasmuch as it is the density *relative to any one molecule* which is essentially significant for the operation of the intermolecular forces, the system will tend to keep the "apparent" density about constant at a value near that realized above the condensation point; to accomplish this the true density correspondingly has to decrease. For constant external pressure, therefore, the system will, with progressing degeneracy, expand to a greater volume. Thus also $(\partial V/\partial T)_p$ will be negative for $T<T_0$.

It is certainly very unusual if a substance shows a negative coefficient of thermal expansion. Since $(\partial V/\partial T)_p=-(\partial S/\partial p)_T$, this property implies that by isothermally compressing the substance in question, entropy can be increased or disorder generated. On first view one should think that by compressing a system of spherically symmetrical molecules it could only be brought into an arrangement of higher order. In fact liquid He below the λ-point is one of the few examples where the anomalous (negative) sign of $(\partial V/\partial T)_p$ and $(\partial p/\partial T)_V$ actually has been found. It seems hardly possible to think that any mechanism, other than the one we have discussed above, could be made responsible for this singular behavior of liquid helium.

[10] W. H. Keesom and K. W. Taconis, Physica **5**, 270 (1938); F. London, J. Phys. Chem. **43**, 49 (1939).

[11] F. London, Proc. Roy. Soc. **A155**, 576 (1936).

Letter to the Editor

PROMPT publication of brief reports of important discoveries in physics may be secured by addressing them to this department. The closing date for this department is the third of the month. Because of the late closing date for the section no proof can be shown to authors. The Board of Editors does not hold itself responsible for the opinions expressed by the correspondents. Communications should not in general exceed 600 words in length.

On the Structure of $Mo(CN)_8^{-4}$

GIULIO RACAH
The Hebrew University, Jerusalem, Palestine
January 27, 1943

IT was shown by Hultgreen[1] that no more than six equivalent cylindrical bond functions may be constructed by $s-p-d$ hybridization, and it was generally assumed[2,3] that f eigenfunctions are needed to construct eight equivalent bonds. Since the restriction to cylindrical bond functions was only based on the feeling that other bond functions would have a considerably smaller strength, it seemed worth while to us to show that eight equivalent non-cylindrical bond functions may be constructed by $s-p-d$ hybridization, and to calculate the strength that may be reached by them.

It is easy to see with the help of the group-theory methods used by Mulliken[4] and Van Vleck[2] that this construction is possible only if the symmetry group of the bonds is the point group D_4, and that the bond functions are

$$(p_z+d_{x+y}+d_{xy}+s\cos\beta+d_z\sin\beta)/8^{\frac{1}{2}} + [(p_x+d_{xz})\cos\alpha+(p_y+d_{yz})\sin\alpha]/2$$

and the seven others which are obtained from it by the symmetry operations of D_4. The parameters α and β are arbitrary; if we fix them by the condition of giving the maximal strength to the bonds, we obtain $\alpha=22°30'$ and $\beta=18°$; the bonds are then directed to the corners of a square antiprism, make an angle of 60°54′ with the tetragonal axis and have the strength 2.9886, while the best $s-p-d$ bond has the strength 3. The restriction to cylindrical bond functions on ground of strength considerations is therefore not justified.

The obtained structure, however, does not agree with the experimental results of Hoard and Nordsieck,[5] which found that the eight bonds of $Mo(CN)_8^{-4}$ are not equivalent, but split into two sets, each consisting of four approximately equivalent bonds and having very nearly the symmetry D_{2d}; the bonds of the first set make angles of about 34° with the z axis, those of the second set angles of about 73°.

This structure also may be obtained by $s-p-d$ hybridization, assuming for the first set the bond function

$$(s\sin\alpha+d_z\cos\alpha+d_{x+y}\sin\beta+p_z\cos\beta)/2 + (p_x\sin\gamma+d_{xz}\cos\gamma)/2^{\frac{1}{2}}$$

and the three others which are obtained from it by the symmetry operations of D_{2d}, and assuming for the second set the same expressions with the parameters α, β, and γ increased by 90°. The sum of the strengths reaches its maximum when $\alpha=40°13'$, $\beta=19°35'$, $\gamma=30°57'$; for these values of the parameters the bonds of the first set make an angle of 34°33′ with the z axis and have the strength 2.9954, those of the second set make an angle of 72°47′ and have the strength 2.9676.

The strengths are also in this case very satisfactory and the angles agree with the experimental results.

[1] R. Hultgreen, Phys. Rev. **40**, 891 (1932).
[2] J. H. Van Vleck, J. Chem. Phys. **3**, 803 (1935).
[3] W. G. Penney and J. S. Anderson, Trans. Faraday Soc. **33**, 1363 (1937).
[4] R. S. Mulliken, Phys. Rev. **43**, 765 (1933).
[5] J. L. Hoard and H. H. Nordsieck, J. Am. Chem. Soc. **61**, 2853 (1939).

The Inhibitory Effect of Iodine on the Photolysis of Gaseous Hydrogen Iodide

RICHARD A. OGG, JR. AND RUSSELL R. WILLIAMS, JR.
Department of Chemistry, Stanford University, Stanford University, California
March 1, 1943

WHILE seeking a precision actinometric method for study of another photochemical reaction, we have reinvestigated the supposedly classical photolysis of gaseous hydrogen iodide. Monochromatic light of λ2537A was used, and the reaction was followed by measurement of the quantity of hydrogen produced. The partial pressure of hydrogen iodide was varied from some 50–150 mm Hg, and that of iodine from 0–20 mm Hg. Twelve separate experiments at 108°C are in excellent agreement with the widely accepted mechanism (analogous to that for photolysis of hydrogen bromide):

$$\begin{aligned} &HI+h\nu \rightarrow H+I, \\ &H+HI \rightarrow H_2+I, && k_2 \\ &H+I_2 \rightarrow HI+I, && k_3 \\ &2I+M \rightarrow I_2+M. \end{aligned}$$

The ratio of rate constants k_3/k_2 was found to have the value (at 108°C) of 4.9 ± 0.3. Over a temperature range of some 50°C there appeared to be no appreciable change in this ratio.

The only previous quantitative investigation of this iodine inhibition appears to be that of Bonhoeffer and Farkas,[1] who estimated the ratio k_3/k_2 to be about 100—these authors claiming that 15 percent of iodine "completely" inhibits the photolysis of hydrogen iodide. This figure of 100 has been rather widely used in interpretation of related reaction rate experiments.[2] However, the experiments of Bonhoeffer and Farkas were conducted at extremely small gas pressures, and there seems little doubt that the secondary reactions occurred principally on the walls of the vessel. The value of k_3/k_2 reported here certainly corresponds to the true homogeneous reactions.

The ratio k_3/k_2 for the analogous reactions of Cl_2 and HCl is known qualitatively to be rather large—at least 100.[2] For the analogous reactions of Br_2 and HBr the ratio is accurately known to be 8.4.[3] The above value of 4.9 for the reactions of I_2 and HI thus falls into a logical sequence, whereas the previously estimated value seemed highly anomalous.

The practical independence of the ratio k_3/k_2 on temperature indicates that the above reactions 2 and 3 have practically identical activation energies. However, the previous estimate[2] of zero for the activation energy of reaction 3 was based upon the erroneous estimate of k_3/k_2 as 100. It seems probable that reaction 3 must have a finite, although undoubtedly small, activation energy.

[1] K. F. Bonhoeffer and L. Farkas, Zeits. f. physik. Chemie **132**, 235 (1928).
[2] J. C. Morris and R. N. Pease, J. Chem. Phys. **3**, 796 (1935).
[3] M. Bodenstein and G. Jung, Zeits. f. physik. Chemie **121**, 127 (1926).

Energy Relations in Film Penetration

JACK SCHUBERT AND G. E. BOYD
George Herbert Jones Laboratory, University of Chicago, Chicago, Illinois
March 10, 1943

SINCE the energy relations in film penetration[1,2] are largely unknown it has appeared worth while to investigate these relations for an insoluble film of cetyl alcohol penetrated by sodium cetyl sulfate.

Information on the composition of a mixed film in equilibrium with a cetyl alcohol crystal may be obtained by use of the Gibbs equation:

$$d\gamma_e = -\Gamma_1 d\mu_1 - \Gamma_2 d\mu_2 - \Gamma_3 d\mu_3, \tag{1}$$

where the subscripts designate the species water, sodium cetyl sulfate, and cetyl alcohol, respectively; Γ and μ the surface concentrations and chemical potentials; and γ_e the surface tension of the equilibrium film.

The position of the Gibbs plane may be chosen in a manner such that the surface concentration of water, Γ_1, is zero. Equation (1) thus becomes:

$$d\gamma_e = -\Gamma_2^{(1)} d\mu_2 - \Gamma_3^{(1)} d\mu_3. \tag{2}$$

Additionally, if the underlying solution is saturated with cetyl alcohol, as is likely to be the case when spreading results from excess crystals, the quantity μ_3 may be assumed constant, resulting in the further specialization of (1):

$$(\partial\gamma_e/\partial m_2)_{\mu_3} = -\Gamma_2^{(1)}(\partial\mu_2/\partial m_2)_{\mu_3}, \tag{3}$$

where m_2 is the concentration of the sodium alkyl sulfate in the bulk phase.

Since

$$d\mu_2 = RTd \ln m_2 f_2,$$

where f_2 is the activity coefficient, Eq. (3) becomes:

$$\left(\frac{\partial\gamma_e}{\partial m_2}\right)_{\mu_3} = -RT\Gamma_2^{(1)}\left[\frac{1}{m_2} + \left(\frac{d \ln f_2}{dm_2}\right)_{\mu_3}\right]. \tag{4}$$

If it be assumed for highly dilute solutions that

$$(\partial \ln f_1/\partial m_2)_{\mu_3} = 0,$$

(4) changes to a convenient equation for the determination of the adsorption of sodium cetyl sulfate in the film:

$$\Gamma_2^{(1)} = -(m_2/RT)(\partial\gamma_e/\partial m_2)_{\mu_3}. \tag{5}$$

Thus, a method of determining the surface concentration of alkyl sulfate is made possible. The information necessary is the variation of the surface tension of the mixed film with m_2, the concentration of the alkyl sulfate.

The free energy change in the penetration process appears to be comprised of two parts in the main: (1) the reversible work of adsorption of the sodium cetyl sulfate from the body of the solution, and (2) the mechanical work necessary to compress the cetyl alcohol monolayer sufficiently to make room for the penetrating molecules. Thus,

$$\Delta F = RT \ln (c^\sigma/c^\alpha) + \int \pi_e d\sigma, \tag{6}$$

where c^σ and c^α are the surface and bulk concentrations of sodium cetyl sulfate, π_e the equilibrium film pressure,[3] and σ the molar area of alkyl sulfate in the mixed film resulting from penetration.

The free energy may be obtained also from the equation

$$(\Delta F_m) = (\Delta H_m)_s - (Q_m)_s, \tag{7}$$

where the molar latent heat $(Q_m)_s$ is given by an application of the Clapeyron equation

$$(Q_m)_s = T(\partial\pi_e/\partial T)_{\sigma_f}(\sigma_m - \sigma_s) \tag{8}$$

and the enthalpy by[4]

$$(\Delta H_m)_s = -\int_{\sigma_s}^{\sigma_m}\left[\frac{\partial(\pi_e/T)}{\partial(1/T)}\right]_{\sigma_f, \Sigma} d\sigma. \tag{9}$$

Experiments have been completed on the variation of the surface tension with temperature and with composition of a system consisting of excess cetyl alcohol crystals in contact with the surface of a solution of sodium cetyl sulfate. It is planned to publish details and calculations when time permits.

[1] (a) J. H. Schulman and A. H. Hughes, Biochem. J. **29**, 1236, 1243 (1935); (b) J. H. Schulman and E. Stenhagen, Proc. Roy. Soc. **B126**, 356 (1938); (c) J. H. Schulman and E. K. Rideal, Proc. Roy. Soc. **B122**, 29, 46 (1937); (d) F. Sebba and E. K. Rideal, Trans. Faraday Soc. **27**, 273 (1941).
[2] (a) N. K. Adam, F. A. Askew, and K. G. A. Pankhurst, Proc. Roy. Soc. **A170**, 485 (1939); (b) K. G. A. Pankhurst, *ibid.* **A179**, 393 (1942).
[3] The equilibrium spreading pressure π_e is defined by $\pi_e = \gamma_0 - \gamma_e$, where γ_0 may be either the surface tension of the solution or of the clean water at the temperature in question and γ_e is the surface tension of the aqueous or solution surface covered by the insoluble monolayer in equilibrium with the crystal.
[4] W. D. Harkins, T. F. Young, and G. E. Boyd, J. Chem. Phys. **8**, 954 (1940).

THE AMERICAN INSTITUTE OF PHYSICS

INCORPORATED

ADMINISTRATIVE STAFF

HENRY A. BARTON, *Director*

MADELINE M. MITCHELL, *Publications Manager*

JOHN T. TATE, *Adviser on Publications*

Office: 175 Fifth Avenue, New York, New York

JOURNALS

THE PHYSICAL REVIEW

REVIEWS OF MODERN PHYSICS
JOHN T. TATE, *Editor (on leave)*
J. W. BUCHTA, *Acting Editor*

JOURNAL OF THE OPTICAL SOCIETY OF AMERICA
GEORGE R. HARRISON, *Editor*

THE JOURNAL OF THE ACOUSTICAL SOCIETY OF AMERICA
FLOYD A. FIRESTONE, *Editor*

AMERICAN JOURNAL OF PHYSICS
DUANE ROLLER, *Editor*

THE REVIEW OF SCIENTIFIC INSTRUMENTS
GAYLORD P. HARNWELL, *Editor*

THE JOURNAL OF CHEMICAL PHYSICS
JOSEPH E. MAYER, *Editor*

JOURNAL OF APPLIED PHYSICS
ELMER HUTCHISSON, *Editor*

GOVERNING BOARD

PAUL E. KLOPSTEG, *Chairman*
Central Scientific Company

GEORGE B. PEGRAM, *Secretary*
Columbia University

For the American Physical Society:

JOHN T. TATE
University of Minnesota

L. A. DUBRIDGE
University of Rochester

GEORGE B. PEGRAM
Columbia University

For the Optical Society:

A. C. HARDY
Massachusetts Institute of Technology

K. S. GIBSON
National Bureau of Standards

R. C. GIBBS
Cornell University

For the Acoustical Society of America:

HARVEY FLETCHER
Bell Telephone Laboratories

FLOYD A. FIRESTONE
University of Michigan

WALLACE WATERFALL
The Celotex Corporation

For the Society of Rheology:

R. B. DOW
Aberdeen Proving Ground

HERMANN MARK
Brooklyn Polytechnic Institute

N. W. TAYLOR
The Pennsylvania State College

For the American Association of Physics Teachers:

A. G. WORTHING
University of Pittsburgh

PAUL E. KLOPSTEG
Central Scientific Company

T. D. COPE
University of Pennsylvania

The American Institute of Physics is a membership corporation of which five societies are the founding members. These five societies are the principal national societies devoted to pure and applied physics in America. Their names, and those of their representatives who form the Governing Board of the Institute, are given above. The principal work of the Institute is the publication of journals sponsored by the societies or by itself. The names and the editors of the journals are also listed above.

The broad purpose of the Institute is to represent, in all matters of wide or common interest, the five thousand or more members and subscribers associated with the Founder Societies and the journals. It aims to advance the science and profession of physics, and to promote cooperation between pure research, the applied sciences and the industries. To achieve these aims, it is greatly in need of an endowment and is empowered by law to administer grants and funds of any kind.

CONTENTS

THE JOURNAL OF CHEMICAL PHYSICS VOL. 11, NO. 4 APRIL, 1943

Average H–H₂ Repulsive Potential from Collision Cross Section Measurements . . I. AMDUR 157

Vibration-Rotation Energies of the Linear X-Y-Z Type Molecule . . . . ALVIN H. NIELSEN 160

Quenching of Cadmium Resonance Radiation (3261A) by Hydrocarbons and Other Gases . . . . . E. W. R. STEACIE AND D. J. LEROY 164

Transference Numbers of Potassium Bromide in Aqueous Solution at 25°C . . . . . A. G. KRENAM AND A. R. GORDON 172

Influence of Hindered Molecular Rotation on the Dielectric Constants of Water, Alcohols, and Other Polar Liquids . . . . . GERALD OSTER AND JOHN G. KIRKWOOD 175

Diffraction of X-Rays by Sodium Stearate at Room Temperature . . . . . JAMES W. MCBAIN, ALEXANDER DE BRETTEVILLE, JR., AND SIDNEY ROSS 179

Determination of the Intermediate Step in the Accumulation of Hydroquinone. Axial Fogging of Photographic Emulsions . . . . . T. H. JAMES 183

Quantum Yield of Diacetyl Fluorescence . . . . . G. H. ALMY AND P. R. GILLETTE 188

Electrical Conductivity of Lead Chromate . . . . . THEODORE WILLIAM LASHOF 196

Dielectric Constants and Rotary Diffusion . . . . . F. LONDON 203

Letters to the Editor:

On the Structure of $H_3O^+(H_2O)_n$ . . . . . GIULIO RAZZI 214

Inhibitory Effect of Iodine on the Photolysis of Gaseous Hydrogen Iodide . . . . . RICHARD A. OGG, JR. AND RUSSELL R. WILLIAMS, JR. 214

Energy Relations in Film Formation . . . . . JACK SHUBERT AND G. E. BOYD 215

LANCASTER PRESS, INC., LANCASTER, PA.